RAPID PYROLYSIS

OF

POLYMERIC SOLID PROPELLANT BINDERS

A THESIS
Presented to
The Faculty of the Division of Graduate Studies

By

Robert John Powers

In Partial Fulfillment
of the Requirements for the Degree of
Doctor of Philosophy
in the School of Aerospace Engineering

Georgia Institute of Technology
June, 1986

RAPID PYROLYSIS

OF

POLYMERIC SOLID PROPELLANT BINDERS

Approved

Edward W. Price, Chairman

Gary A. Flandro

Jechiel J. Jagoda

Robert K. Sigman

Date Approved by Chairman 5/22/86

To my wife Virginia,
my daughter Erin, and my son Ryan . . .

ACKNOWLEDGEMENTS

I wish to express my sincerest gratitude to my Professor, Edward W. Price, without whom my graduate career would not have been possible; his guidance, his experience, his insight have been invaluable throughout the course of this work. To the members of my committee, Drs. I. A. Jagoda, F. L. Cook, G. A. Flandro, R. K. Sigman, I am indebted for their many hours of discussion and their suggestions. Special thanks to my friend William Meyer whose skill with the microcomputer is second to none, and upon whose expertise the graphics in this work depends. To my friend Robert S. Albright, whose advice and assistance on micro-computers and electronics was indispensable, again my thanks. In addition, I would like extend my appreciation to Christos Markou, for his interest and help with the experimental portion of the work; the advice of my fellow graduate students is gratefully acknowledged. My special thanks the Office of Naval Research and to Dr. R. Miller for their support of this work; this research was carried out under contract N00014-79-C0764.

To my wife Virginia, for her patience, her encouragement, and for her devotion . . . my gratitude and my love.

TABLE OF CONTENTS

Appendices

LIST OF TABLES

LIST OF ILLUSTRATIONS

NOMENCLATURE

a	Area, (cm^2)
A	Pre-exponential Term in Arrhenius Rate Law
c	Specific Heat (cal/g-°K)
E	Youngs Modulus, (dynes/cm^2)
e	Napierian Constant
Ea	Energy of Activation, (cal/mole)
f	Conversion Function
h	Specific Enthalpy (cal/g)
H	Magnetic Field Intensity
I.D.	Inside Diameter of Probe, (mm)
I	Area Moment of Inertia, (cm^4)
k	Reaction Rate Constant
K	Kinetic Constant, Lumped Coefficient
L	Probe length, (mm)
m	Mass, (g)
M	Molecular Weight, (g/mole)
n	Reaction Order, (dimensionless)
$\underline{n}$	Generic Product
O.D.	Outside Probe Diameter, (cm)
P	Generic Reactant
Q	Heat of Reaction, (cal)
R_o	Specific Gas Constant, (cal/g-°K)
r	Surface Regression Rate, Burning Rate, (cm/s)
S	Entropy, (cal/°K)

t	Time, (s)
T	Temperature, (°K)
u	Dummy Variable, (Dimensionless)
V	Velocity of Species with Respect to Surface,(cm/s)
w	Weight (mass), (g)
x	x-direction
y	y-direction
z	z-direction

Greek Symbols

α	Reaction Coordinate (Fraction Reacted), (dimensionless)
β	Heating Rate, (°K/s)
τ	Reaction Coordinate (Fraction Remaining), (dimensionless)
δ	Skin Depth, (μm)
$\underline{\delta}$	Constant, (dimensionless)
μ	Linear Tube Density, (g/cm)
μ_r	Relative Magnetic Permeability, (dimensionless)
μ_o	Magnetic Permeability of Free Space
λ	Thermal Conductivity, cal/cm-s-°K
ρ	Density, (g/cc)
ϕ	Resistivity of Heating Element (micro-Ohms-cm)
Φ	Euler's Integral, (Dimensionless)
Θ	Frequency, (Hertz)
ω	Rate of Production of Species, (g/s-cc)
Ω	Dimensionless Heating Rate

Subscripts

i	i-th Species
c	condensed phase
f	final
g	vapor phase
v	vapor phase or vaporization
o	initial
s	condensed phase

ABBREVIATIONS

AE	Avrami-Erofeyev Equation
AP	Ammonium Perchlorate
AR	As Required
BW	Bandwidth
CC	Contracting-Cube Formula
CPP	Curie Point Pyrolyzer
CR	"Coats and Redfern" Kinetic Analysis [35]
CTPB	Carboxy-Terminated Poly(butadiene)
DC	Direct Current
DCO	DC-Offset
DSC	Differential Scanning Calorimetry
DSM	"Direct Solution Method" [53]
DTA	Differential Thermal Analysis
FVC	Frequency-to-Voltage Converter
HTPB	Hydroxy-Terminated Poly(butadiene)
LP	Linear Pyrolysis
PBAN	Poly(butadiene-co-acrylonitrile)
PGC	Pyrolysis Gas Chromatography
PMMA	Poly(methyl-methacrylate)
RMS	Root Mean Square
RF	Radio Frequency
RHBP	Rapid-Heating Bulk Pyrolysis
SHBP	Slow-Heating Bulk Pyrolysis

Page missing from thesis

SUMMARY

An investigation into the rapid pyrolysis of polymers has been conducted; this investigation focuses on experimental methods to measure global Arrhenius parameters of polymers under conditions approaching those found in combustion. Prior work in the field of rapid pyrolysis is reviewed.

From theoretical considerations, it is concluded that using Arrhenius parameters, determined at low pressures and low-heating-rates, to extrapolate reaction rates to regions far outside of this domain is unwarranted, and often incorrect. Global kinetic parameters of complex substances are not necessarily constants, and must be measured in the domain of interest, wherein "effective" energies of activation and pre-exponential terms can be interpolated based upon the local conditions.

A novel "Vibrational Thermogravimetric Analyzer" (VTGA) has been constructed which uses a vibrating quartz tube to make continuous mass measurements during sample pyrolysis at heating rates up to 60 °C/s. The samples, thin films coated on a metal substrate, are rapidly heated using a non-contact radio frequency induction heater; these samples are in contact with a thermocouple throughout the course of the

pyrolysis. Global Arrhenius parameters are calculated for the thermal decomposition of Hydroxy-terminated poly(butadiene) (HTPB), Poly(butadiene-co-acrylonitrile) (PBAN), and Ammonium Perchlorate (AP); low-heating-rate results from the VTGA compare favorably with data obtained under similar conditions using a conventional TGA. A limited number of kinetic measurements have been made on these materials at heating rates between 20 and 60 °C/s - rates which would be relevant to the low pressure combustion of polymers.

The work demonstrates that vibration is a suitable technique to make rapid and continuous mass measurements of samples undergoing pyrolysis at moderate heating rates. Modifications to the VTGA are suggested which should permit operation at heating rates in excess of 100 °C/s.

S/N	Signal-to-Noise
TGA	Thermogravimetric Analysis
TVA	Thermal Volatilization Analysis
VDC	Volts DC

CHAPTER I

INTRODUCTION

1.1 Background

Recent years have seen the ever increasing use of synthetic polymers in virtually all aspects of aerospace engineering. Polymers are the essential ingredient in light-weight composite structural materials, as well as in modern heat resistant fabrics. They are used in very low temperature environments, such as space-storable systems, and in very high temperature environments where they are required to retain their desirable mechanical properties for substantial periods of time. In addition, synthetic polymers have important applications in high temperature ablative systems, and currently, are finding wide spread use in advanced solid propellants. New classes of energetic polymers are emerging which will revolutionize solid propellant technology. Consequently, polymers are exposed to a wide range of thermal environments. Continued effective use of these materials necessitates a complete mechanistic understanding of the details of their degradation, pyrolysis, and combustion. A thorough understanding of these details would figure prominently in analytically predicting the behavior of solid propellants; quantifying the burning

characteristics of polymers, synthetic structural materials, and fabrics; and predicting performance of ablation systems, etc.

The capability of analytically predicting the behavior of burning solid materials, and in particular polymers, over a broad spectrum of conditions has long been the goal of combustion researchers. However, due to the physical and chemical complexity often encountered in the combustion environment, no such general capability currently exists. The inner details of the combustion zone are ordinarily extremely difficult to measure, primarily due to the microscopic, transient, and hostile nature of the combustion wave. Prediction and control of the burning characteristics of solid materials continues to be an important and completely unresolved problem.

A number of workers [1-9] have developed combustion models which hold over a limited range of conditions. Recognizing that the chemistry of the combustion zone presents an insurmountable mathematical and experimental dilemma, recourse is taken to global kinetics to describe the chemical rate processes. For these models to hold over a broad range of conditions, it is necessary to include constitutive relations of appropriate functional form, and to have an accurate knowledge of the associated physical and chemical parameters for the entire domain over which the model is to remain valid. These parameters include: the

thermal conductivity and diffusivity of the condensed and gas phase species; coefficients of viscosity and mass diffusivity; reaction rate constants, orders, Arrhenius parameters; etc.

The chemical kinetic parameters, especially activation energy, have the greatest impact upon the problem; it is readily apparent from Table 1-1 that small errors in estimating the activation energy produce serious errors in predicted rates.

Table 1-1. Error Estimate in Arrhenius Parameters.

Arrhenius Parameters for
a Theoretical Polymer

E_a = 45000.00 cal/mole
A = 1.82 x 10^{13} s^{-1} ≈ RT/Nh
T = 600 °C

Presumed E_a cal/mole	k s^{-1}	Error in E_a %	Error in k %
36000.	17722.	- 20	+ 17622
40500.	1325.	- 10	+ 1225
42750.	362.	- 5	+ 262
45000.	100.	0	0
47250.	27.	+ 5	- 73
49500.	7.	+ 10	- 93
54000.	.6	+ 20	- 99

It is unfortunately not possible to calculate these kinetic values for such complex systems. Furthermore, currently available analytical equipment does not permit the measurement of many these quantities at the temperatures, pressures, and heating rates commonly encountered in combustion. As the global kinetic parameters can be strong functions of the system state variables, it is also in general not possible to extrapolate this data from the more manageable low temperature, low heat flux, and low pressure test environments used in contemporary thermal analysis equipment [10]. As a result there is clearly a need for analytical and empirical methods which address these difficult test conditions. It is the purpose of this work to investigate such methods and apply them to study of selected polymeric materials.

1.2 Statement of the Problem

The combustion zone in the vicinity of a polymer can be loosely envisioned as composed of two parts: a gas phase reaction zone - the flame, and a condensed phase zone encompassing a region at and slightly below the deflagrating surface. Heat fed back to the surface via conduction, radiation, and convection, produces: condensed phase reactions, phase changes, and decomposition in the condensed materials. The degree of decomposition is of course dependent upon the temperature and the heat flux to the surface

- this is especially true of polymeric materials. The products of the decomposition vaporize, and provide new reactant species to the gas phase reaction zone.

In a typical propellant, burning at 34 atm., the gas phase combustion wave has a thickness of 10^3 μm, thermal gradients as large as 30 °C/μm, and temperatures on the order of 10^3 °C [11]. Polymeric binders in the condensed phase exhibit surface temperatures of about 600 °C (the exact figure is unknown), and sub-surface thermal gradients of about 15 °C/μm [11]. Overall burning rates are around 10 mm per sec. This translates into average heating rates of the condensed phase material of the order of 10^5 °C/s!

In contrast, a polymer burning at pressures of around 1 atm, has a much more expanded gas phase combustion wave with thermal gradients at the surface of about 0.25 °C/μm [12]; this greatly reduces the heat-flux to the surface, and therefore, reduces linear regression rates to about 10^{-2} mm./s. The surface temperatures are still approximately 600 °C, however, with the result that average heating rates are on the order of 10^1 °C/s.

Polymers used as ablatives in high temperature erosive environments have linear regression rates which fall in between these two extremes typically 10^{-1} mm/s [7]. Assuming a similar surface temperatures and sub-surface gradients this gives average heating rates on the order of 10^3 °C/s. Table 1-2 summarizes these order of magnitude estimates.

Table 1-2. Order of Magnitude Estimates of Various Combustion Zones.

Combustion Zone	Low Pressure Combustion	Ablation	Propellant Combustion
GAS PHASE			
Thickness, μm	10^4	-	10^3
Temperature, °C	10^3	-	10^3
Thermal Gradients, °C/μm	0.25	Convection	30
CONDENSED PHASE			
Thickness, μm	40	-	40
Surface Temperature, °C	≈600	≈600	≈600
Sub-Surface Gradients, °C/μm	15	15	15
Burning Rates, mm/s	10^{-2}	10^{-1}	10
Average Heating Rates, °C/s	10^1	10^3	10^5

When analytically modeling such complex combustion processes, the modeler is faced with the task of solving the appropriate conservation equations of mass, species, momentum, and energy for both the gas and condensed phases. Generally simplifying assumptions are made to render the problem tractable, but nevertheless the task is still formidable. Of particular importance and difficulty are the associated rate processes of species and energy conversion in the condensed phase, which enter the analysis through the conservation of species and energy equations. For the one dimensional, steady case, and in a coordinate system which

is fixed with respect to the regressing surface, these are [7]:

$$\frac{r\, d\rho_i}{dy} = -\frac{d[\rho_i V_i]}{dy} + \dot{\omega}_i \qquad (1\text{-}1)$$

$$\frac{dT}{dy} \sum_i \rho_i c_i [\, r + V_i \,] = \frac{d[\, \lambda\, dT/dy \,]}{dy} - \sum_i h_i \dot{\omega}_i \qquad (1\text{-}2)$$

where the last terms in these equations are the rate of species generation per unit volume and the rate of enthalpy production due to chemical reactions per unit volume, respectively. In practical situations the overall rate is normally defined in terms of global zero-order kinetics [13] and an assumed Arrhenius-type temperature dependence, Eqn. 1-3.

$$\omega = A\, e^{-Ea/RT} \qquad (1\text{-}3)$$

To use this relation in connection with Eqns. 1-1 and 1-2, it is absolutely essential to accurately know Ea, "the energy of activation" and A, the "pre-exponential term," as

a function of the temperatures and pressures over which the model is to be used. This is particularly true of Ea upon which the burning rate is exponentially dependent. Again, it is not possible to calculate these quantities; and the modeler is forced to rely on their empirical determination - generally from thermal analysis/decomposition experiments.

Experimental difficulties and equipment limitations have largely limited thermal analysis to temperatures, heating rates, and pressures that are well below those found in combustion. There is no reason to assume that data from decomposition studies at conventional conditions are relevant to combustion situations, although, they are often used for lack of better information. DSC, DTA, TGA, TVA, etc., with heating rates on the order of 0.5 °C/s, have been used to estimate Arrhenius parameters of a number of propellant related materials. However, Bouck, Baer, et al. [14] note that "Several important questions concerning the applicability of these laboratory tests to . . . combustion conditions have never been adequately answered." The most serious question concerns validity of extrapolating data obtained at heating rates of 1 °C/s to combustion situations, wherein the rates may range from 10^1 °C/s. in one-atmosphere flames, to as high as 10^5 °C/s in propellant combustion. While these low rate techniques are very suitable for material characterization, for example, propellant ingredient aging studies and polymer degradation, they

are not necessarily relevant to combustion and other high rate phenomenon! F. Farre-Ruis and G. Guiochon [15] have shown that heating rate and heat flux to the sample are the controlling factors in polymer decomposition. It has also been shown [14] that various crosslinked polymers gave high-rate pyrolysis results that were quite different than those in low temperature DSC studies. In addition, high temperature exotherms were observed in high-heating-rate experiments (conducted in air) that were not observed in DSC.

> Presumably, when temperature-sensitive materials are heated at low rates to high temperatures, slow low-temperature reactions are permitted to proceed, extensively modifying the virgin material before high temperatures are reached; thus the same high temperature pyrolysis mechanisms are not observed. [14]

Indeed, at conventional heating rates, the sample is usually completely decomposed long before reaching the temperatures at which most of the decomposition occurs in combustion. The relevance of typical decomposition studies to combustion is therefore necessarily suspect.

This situation dictates that new experimental methods must be developed with a strategy for applicability to higher temperatures, elevated heating rates, and high pressure environments. The experimental designs should be predicated on: the objectives of the study, the nature of the material under investigation, and most importantly, the

conditions of the process to be emulated.

1.3 Present Work in Perspective

1.3.1 Thermal Decomposition of Polymers

Polymers are a unique class of materials. Unlike low molecular weight substances, their physical and chemical properties, such as, molecular weight, density, melting point, boiling point, thermal conductivity, decomposition temperature, vapor pressure, solubility, and reactivity are not well defined. These properties often vary from sample to sample or even within a sample; polymers have been shown to be non-isotropic with respect to thermal, mechanical, and even chemical behavior. These unique properties are engendered by variations in: molecular weight distribution, the degree of crosslinking, crystallinity, methods of preparation, additives, as well as the ratios of constituents in co-polymers. Indeed polymers may be viewed as composite materials in their own right.

This complexity underscores the need to interpret experimental results with some reserve. These results can depend heavily on the physical and chemical makeup of the sample, with the result that inter-laboratory agreement is often poor. Thorough characterization of samples is the only way to mitigate this problem.

Mass loss which occurs during polymer pyrolysis is

essentially a degradative-vaporization process; polymer molecules are too large for vaporization to occur without substantial "cracking" [16]. Kinetically, pyrolysis can be divided into three categories: rate proportional to surface area - the rate limited by molecular vaporization; rate proportional to surface area and inversely proportional to sample thickness - diffusion controlled vaporization; and rate proportional to current weight of sample - kinetically limited.

In kinetically limited pyrolysis, the rate of mass loss, and hence vaporization, is controlled by the rate of bond rupture, which would of course be directly proportional to the weight of the decomposing polymer. Bond rupture is normally the rate determining step in polymers having no low molecular weight constituent, however, under certain conditions the rate of vaporization can be the rate controlling factor.

The maximum theoretical rate of vaporization of a material at a given temperature will occur in a vacuum, this represents the greatest upper bound on the mass loss rate due to vaporization. As long as the rate of conversion to products remains less than this rate, the process will be kinetically limited.

Diffusion controlled vaporization is primarily of importance in cases where the sample size is large, and decomposition takes place throughout the bulk of the sample.

Due to the poor thermal conductivity of polymers, temperature gradients in combustion are large and thermal waves in the solid are thin. Therefore, diffusion should prove unimportant, although, it may be a factor in the low heating rate pyrolysis of bulk samples. (See TGA results Figs. 5-1a and 5-1b.)

Several broadly defined mechanisms are recognized in the non-oxidative thermal decomposition of polymers: a number of polymers "unzip" from the chain ends to yield almost one-hundred percent monomer, while on the other extreme, many polymers exhibit a "random" chain scission mechanism, yielding varying amounts of monomer along with smaller and larger fragments. The behavior of other polymers falls somewhere in between these two extremes. In addition, some polymers, Poly(vinylchloride) for example, decompose through the elimination of small stable molecules. This can occur with simultaneous or subsequent main chain breakup. A given polymer can transition among these mechanisms depending upon the physical conditions controlling the pyrolysis at the time.

"Unzipping" to monomer is highly favored in polymers with tertiary carbon atoms such as PMMA and poly(α-methylstyrene). This mechanism is characterized by the easy volatilization of pyrolysis products with little or no change in the molecular weight of the sample, at least in the early stages of the decomposition. Monomer yield is

also favored in structures and reaction environments where the formation of free radicals is favored. Large amounts of available hydrogen and chlorine (not fluorine), which scavenge free radicals, discourage their formation, and promotes the generation of random fragments. Teflon, for example, completely devoid of hydrogen, yields 100% monomer at moderate temperatures.

Even so-called random chain scission is not entirely random; it has been demonstrated that many of these type of polymers decompose through a "backbiting" mechanism, at least at low temperatures. Chain ends loop back to form ring structures with the main chain, and chain scission occurs at the point of loop-back, followed by ring opening. The number of carbons per ring is influenced by such factors as ring-strain, steric hindrance, and stereo-chemical factors. The most probable number of carbon atoms in the fragment are six or seven depending upon temperature. Random chain scission is characterized by a rapid reduction in molecular weight of the sample during the early stages of decomposition.

These mechanisms hold below about 500 °C depending upon the thermal stability of the polymer. At temperatures in excess of this value, the amounts of monomer are significantly reduced, and products contain more fundamental fragments. Table 1-3 gives the yield of monomer for various polymers undergoing pyrolysis in vacuum (the large mean-

free-path eliminates obscuring secondary reactions); the decreased monomer yield with temperature is apparent.

The pyrolysis products of a particular polymer are, therefore, not necessarily unique. The product yield can depend upon temperature, heat flux, and pressure. Variation in product distribution, which implies variation in the overall mechanism, could also affect vaporization rates; both could certainly influence the magnitude of measured of global kinetic values.

Table 1-3. Monomer Yield of Polymers with Temperature. [17]

Polymer	Percent yield of monomer based upon total volatiles		
	At 500 °C	At 800 °C	At 1200 °C
Polyethylene	0.03	5.5	26.4
Polypropylene	0.4	17.9	15.8
Polyisobutylene	36.5	69.0	13.0
Polystyrene	51.0	10.5	0.6
Poly(methylmethacrylate)	94.2	81.8	12.9
Poly(tetrafluoroethylene)	96.6	91.2	78.1
Poly(α-methylstyrene)	100	88.5	37.7

1.3.2 Global Arrhenius Parameters

Virtually all combustion models to date [1-7] assume an Arrhenius type dependence to describe the binder decomposition on the propellant surface, and, for the most part, these parameters have been taken as constants - independent of

temperature, heat-flux, and pressure. Only recently have attempts been made to measure these quantities under conditions similar to combustion. [18-30] In the past, values obtained at low heating rates and temperatures, were often used to extrapolate reaction rate constants to regions far outside of the domain of applicability; implicit in this approach is the assumption is that the pyrolysis proceeds through a one-step reaction whose rate is a function of temperature and is independent of other physical processes. More realistically these "global" values should be measured throughout the domain interest, where "effective" Ea's and A's could be interpolated based upon the "local" conditions. Without a priori knowledge of the details of the pyrolysis process (which is often unavailable), Arrhenius parameters must be assumed to be "global". In order to examine how these global parameters depend upon the details of the system, it is helpful to recall some of the fundamental aspects of chemical kinetics.

Energies of activation and frequency factors are familiar and fairly well understood concepts of chemical kinetics. They are usually explained in terms of elementary gas phase reactions. In this context, the energy of activation can be loosely envisioned as an energy barrier between reactants and products, while frequency factors can be related to the molecular collision or vibration frequency, and the reactant concentration. For the reaction to proceed

to completion at an appreciable rate, there must be a sufficient number of reactants or activated complexes possessing energies in excess of this barrier potential.

This simple description can be extended to species in solution or even to reactions in the solid state, particularly if the reaction is a simple, one-step processes, which occurs at modest rates. The literature is replete with analytical and numerical methods to determine Arrhenius parameters which are based upon this simple model. When an attempt is made to apply these analytical methods to "complex processes", where species can undergo a variety of chemical and physical changes as function of the state variables, serious questions arise as to the validity of the calculated Ea's and A's.

Gontkovskaya, _et al._ [31,33], have recently investigated the thermal decomposition of a material, subjected to a linear temperature rise, decomposing _via_ two parallel exothermic reactions, Eqn. 1-4.

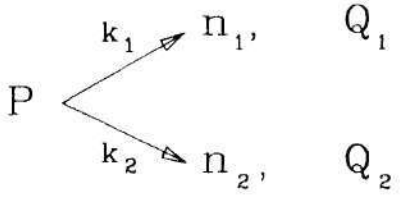

(1-4)

Here P is the reactant and n_1 and n_2 are the respective products. Their theoretical investigation involved the

solution of the following equations:

$$\beta \frac{d\eta_1}{dT_s} = A_1 e^{-E_1/RT} (1 - \eta_1 - \eta_2) \qquad (1\text{-}5a)$$

$$\beta \frac{d\eta_2}{dT_s} = A_2 e^{-E_2/RT} (1 - \eta_1 - \eta_2) \qquad (1\text{-}5b)$$

$$c\rho\beta \frac{dT}{dT_s} = \sum_i Q_i A_i e^{-E_i/RT} (1 - \eta_1 - \eta_2) - \alpha \frac{S}{V} (T - T_s) \qquad (1\text{-}5c)$$

$$T = T_s = T_i \qquad \eta_1 = \eta_2 = 0 \qquad (1\text{-}5d)$$

where Eqns. 1-5a and b are the rates of generation of the products, $\underline{n}_1$ and $\underline{n}_2$ respectively, and Eqn. 1-5c represents the energy balance for the material in an environment (subscript $\underline{s}$) heated at a constant rate, β. Eqns. 1-5d, state the initial conditions. In the numerical solution of the non-dimensional form of these equations, Q_1 and Q_2, the heats of reaction, were taken as equal and E_1 was always

less than E_2. Calculations for various ratios of the pre-exponentials, and for ratios of the activation energies show that, from the thermograms (decomposition curves) alone, it is impossible to determine whether one or several reactions are taking place! In any case, the first reaction to start is always the one with lowest activation energy, however, the question of how rapidly the second reaction starts and by what path the bulk of the conversion takes place, depends upon the ratio of the rate constants and the heating rate. The higher heating rates promote the course of the reaction with the higher activation energy, indeed, for $A_2/A_1 \approx 10^4$ and $E_1/E_2 \approx 0.8$, over 90% of the reaction proceeded via the path with the largest activation energy! It is further shown that, in principal, it is possible to describe the net rate of conversion of P decomposing by several parallel reactions through an effective rate expression Eqn. 1-6., where η represents the fraction of P remaining at any temperature.

$$\Omega \frac{d\eta}{d\Theta} = \gamma A_{eff} e^{[-\sigma_{eff}\Theta/(1 - \epsilon\Theta)]} (1 - \eta) \qquad (1-6)$$

In this expression, σ_{eff}, is the effective nondimensional activation energy where, $E_{eff} = \sigma_{eff} \cdot E_2$.

$$E_{eff} = \sum_i \underline{\delta}_i E_i \qquad (1\text{-}7)$$

where $\underline{\delta}_i$ is the relative rate of the i-th reaction. This implies that the effective activation represents linear combination of the activation energies of all parallel reactions which are in progress. These $\underline{\delta}$'s and consequently the E_{eff} depend upon heating rate. Since most traditional methods of analysis presume that the kinetics are described by Eqn. 1-6, it is not surprising that results found in traditional TGA experiments and high-heating rate work often differ substantially.

The situation is further complicated if one considers vaporization in the overall rate of mass loss. Chaiken [28] observed a decrease in Ea at high temperatures to levels which could not be accounted for on the basis of molecular structure. (In principal, the lower limit of the activation energy should be the bond energy of the weakest bond in the molecule.) He postulated that an apparent activation energy of 11 kcal/mole from the linear pyrolysis of PMMA at temperatures above 600 °C, corresponded to the heat of vaporization of PMMA monomer - the mass loss is limited by the rate of vaporization. The overall process can be represented by

Eqn. 1-8.

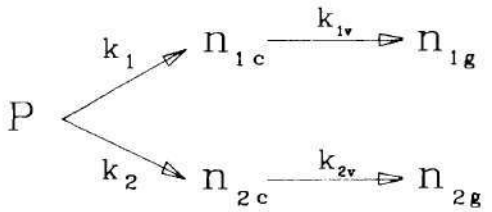

(1-8)

The upper molecular limit for the vaporization of large organic structures has been investigated by Wall [16]. Contrary to statements made in [9], it has been shown that the rate of mass loss, in grams/s, due to evaporation can be represented by an Arrhenius type expression, Eqn. 1-9,

$$\frac{dw}{dt} = \left[6.25 \left\{ \frac{M}{T} \right\}^{\frac{1}{2}} a e^{-\Delta S_v / R} \right] e^{-\Delta E_v / RT} \qquad (1\text{-}9)$$

from which may be derived a temperature dependent activation energy, Eqn. 1-10.

$$E_v = \Delta E_v + RT/2 = \Delta H_v + 3RT/2 \qquad (1\text{-}10)$$

Vaporization is therefore a result of the fraction of

molecules which have sufficient energy (Ea in the previous equation) to overcome their cohesive forces of the medium. Since both kinetics and vaporization have the same functional form, both effects may contribute to the σ_{eff} in Eqn. 1-6. In addition, Since heating rate can influence the overall kinetics of sequential reactions [32,33], under appropriate conditions it is possible that either $k_{1,v}$ or $k_{2,v}$ may dominate in Eqn. 1-8. Therefore, the assumption of constant Arrhenius parameters, implicit in virtually all traditional data analysis schemes, is not necessarily correct in the case of complex processes.

A global Ea is not an Energy of Activation in the strict sense - a col point on a reaction-coordinate vs. potential-energy surface. It is a lumped parameter which must be empirically determined. It is "constant" only in so far as the relative contribution of the participating reactions and physical processes do not greatly change during the course of the decomposition. Therefore constancy in these parameters can be safely assumed only if the decomposition is steady, and takes place over a relatively narrow range in temperature, heat-flux, and pressure.

In connection with polymer pyrolysis, the Arrhenius equation should be used as a heuristic relation based upon notions from statistical mechanics and collisional gas dynamic theory. The Arrhenius parameters should be taken as representing some sort of weighted average of the individual

parameters for the of instantaneous reaction set. These parameters should be viewed as merely numbers used to fit the Arrhenius equation to the experimental data. However the importance of the numbers should not be underestimated. These numbers, if experimentally known, over the conditions for which the model is used, represent the definitive description of the processes occurring in the domain of interest.

1.3.3 Rapid Pyrolysis - State of the Art

In recent years, a number of scientists [18-30] have been designing experiments which try to more nearly approximate conditions found in combustion. Experiments of this type can be divided into two groups: "rapid uniform heating or bulk-pyrolysis" (RHBP) experiments, and the so-called "surface or linear" pyrolysis (LP) experiments.

The bulk pyrolysis experiments attempt to rapidly heat samples, sufficiently uniformly, such that thermal gradients are reduced to a minimum and may be neglected in the analysis. Some workers [18] assume that samples can be heated to a known temperature without substantial loss of material, in which case, an "isothermal" analysis is applied at the various final temperatures. Other methods provided for a non-isothermal analysis on samples subjected to a rapid "uniform" temperature rise. In general, both methods require extremely thin samples coupled with very powerful heating techniques.

Linear pyrolysis experiments are designed so as to replicate details of the combustion as much as possible. They attempt to reproduce the high heating rates, surface temperatures, and high thermal gradients, found in combustion. However, this is often coupled with some uncertainty in these values; as these experiments become more "combustion-like", the same difficulties are encountered in measuring these quantities as are encountered in actual combustion situations. The benefits of this type of approach over conventional TGA normally out weigh these uncertainties. The highlights of this work appear in a review by McAlevy and Blazowski [24].

Surface pyrolysis measurements include surface regression rates and temperature; estimates of thermal gradients are made where possible. "Surface kinetic" parameters are extracted from this data using Arrhenius plots[28] . More elaborately, Houser [9] determines these quantities from "measured" surface temperatures, and estimated thermal profiles at several mass regression rates. The HRBP experiments rely on the more traditional methods of analysis of Arrhenius plots and modification of techniques used in the slow heating rate methods [10].

Linear Pyrolysis. Experiments to investigate the pyrolysis of materials in environments somewhat similar to combustion began in the mid-nineteen-fifties. This work was in part motivated by the proposal of Wilfong, Penner, and

Daniels [8], that the burning rate of a solid material should be equal to the decomposition rate of the solid at a temperature equal to the steady-state temperature of the burning surface, T_s. They further proposed that the rate-determining step would be the unimolecular decomposition of molecules at the burning surface. This all implied that the rate of linear regression could be described using the an Arrhenius expression and zero order kinetics, Eqn. 1-11

$$r = A\, e^{-E/RT_s} \qquad (1-11)$$

(Zero order, since, the concentration of surface reactant/area is constant (in a homogeneous material) - surface molecules are continually being renewed by the formation of fresh surface.)

Among the first linear pyrolysis experiments were the so-called "hot-plate" experiments originally devised by Shultz and Dekker [26] and later improved by Barsh[27]. In these experiments, a sample is pressed with constant force against a hot-plate of known temperature, and the linear regression rate is measured. Temperatures are either determined by a thermocouple in the hot plate or a thermocouple sandwiched between the hot-plate and the sample. Arrhenius

type plots of the mass regression rate vs. 1/T allow for the calculation of apparent energies of activation. Shultz and Dekker [26], using a "hot-wire" pyrolysis technique, measured the Arrhenius parameters of PMMA and found Ea = 27.5 kcal/mole, A = 1.88 x 10^{6}, at temperatures between 450 and 503 °C. They conclude that the rate controlling mechanism is probably the same as that in low-heating-rate bulk pyrolysis - the depolymerization of the condensed polymer on the surface. In subsequent work by Coates on AP [23], the solid hot-plate is replace by a porous plate, thus reducing the build-up of pyrolysis gas in the vicinity of the surface - the principal cause for ambiguity in surface temperature in earlier work. Pyrolysis gases are removed from the back side of the porous plate through the application of a vacuum. Coats work focused mainly on solid oxidizers. Chaiken, et al. [28] applied the hot-plate method to the pyrolysis of PMMA, using an apparatus that permitted much higher temperatures than could be obtained by Shultz and Dekker, but, without the benefit of the porous plate. (Presumably, polymers would clog the porous plate). Investigations on both linear and crosslinked PMMA revealed two distinct energies of activation: ≈26 kcal/mole at temperatures less than 400 °C, in close agreement with that of Shultz and Dekker and a value of 11.2±0.06 kcal/mole at temperatures between 636 and 400 °C. The effect of crosslinking was to increase rates across the entire temperature range but not

affect the Ea's. It is pointed out that this unusually low value for Ea cannot be reconciled on the basis of bond rupture as the rate controlling step, but, is more consistent with surface desorption of the monomer whose heat of vaporization is reported to be 9.2 kcal/mole at 100 °C. The experimental data suggests that the polymer decomposes by a "first-order" surface-depolymerization to monomer which at low temperature is kinetically limited. Whereas at high temperature, the surface becomes saturated with monomer and the vaporization is the rate controlling step!

The principal criticisms leveled at the "hot-plate" experiments are largely aimed at the interferences of the pyrolysis products with experimental measurements/conditions. The actual surface temperature of the sample and hot-plate may differ due to the interposed pyrolysis gas layer. Moreover, the regression rate may be influenced by the accumulation of gases at the interface; these emerging pyrolysis gases flowing radially across the surface may produce erosive conditions not found in combustion. As far as is known to the author, no report of this technique being used at pressure has been published. Whether this is an oversight, or that experimental difficulties preclude this, is not clear. Notwithstanding these limitations, the hot plate technique, especially the porous plate experiments, provides the most clear cut approximation to combustion to date which permit a definitive estimation of the important

variables.

In a attempt to overcome some of the uncertainties associated with the hot-plate experiments, McAlevy et al. [22], performed experiments using a "self-heating diffusion-flame" technique. In this work, an oxidant gas is directed at the surface of a PMMA sample and a diffusion flame is established above the surface. The sample, the lower portion of which is water cooled, automatically advances, thereby keeping the sample surface stationary. The "apparent surface brightness temperature" is measured optically using an infrared radiometer which "looks" through the pyrolysis gases, and also by a 15μm bead thermocouple embedded in the polymer. Using this apparatus, the authors were able to determine "surface energies of activation" for a number of polymers, (but not pre-exponentials), at heat fluxes around 10 cal/cm²-s, surface temperatures around 500 °C, surface regression rates of .32 - .08 mm/s, and pressures of one atm. Accurate measurement of pre-exponentials requires precise measurement of the emissivity of the polymer surface. Temperature data obtained from thermocouple measurements showed considerable scatter as was the case in earlier studies [11]. McAlevy found an Ea for PMMA of 37 kcal/mole over a temperature range of 530 - 490 °C. A liquid layer was observed on the surface of the PMMA. It was concluded that in the hot plate technique, the temperature measured is that of the solid-liquid interface, whereas the optical tech-

nique measures the temperature of the liquid-vapor interface. Values of E, reported for linear PMMA are between 47 and 62 kcal/mole while the values for the crosslinked material are 39-47; it is not clear over what "apparent surface brightness temperature" the PMMA data was collected although it appears to be in the range 500 - 600 °C. The spread in these values is interpreted as a temperature dependence of the activation energy, nevertheless, these values are substantially higher than those obtained by Chaiken. No explanation is given for this discrepancy. It is concluded that there is not a single temperature independent mechanism which controls the decomposition mechanism in the case of PMMA. Experiments were performed on PBAN and CTPB, but surface charring prevented meaningful temperature measurements: apparently, radiometric temperature measurements are unsuitable for the temperature measurement of some important propellant binders.

Cohen, et al. [25], in an important paper, examined a number of propellant related polymers in a linear pyrolysis experiment which used radiative heating to pyrolyze samples at heat fluxes up to 200 cal/cm²-s and pressures up to 1000 psi. Mass loss was again measured by discontinuous weighing of the sample on an analytical balance after an exposure to various heat-fluxes for arbitrary periods of time. Surface temperatures were measured using an infrared radiometer "looking" through the pyrolysis products of the samples;

these samples contained carbon to permit the assumption of black-body conditions. Kinetic and heat of decomposition data were determined for the various polymers, the results of which are given in Table 1-4.

Table 1-4. Kinetic Constants from Ref. [25].

	HTPB	CTPB	PBAN
Ea, kcal/mole	16.9	10.5	16.7
A, g/cm²	299	12.8	270
Q, cal/g	433	381	564

As with the work of Chaiken, the striking feature of this data is the unusually low values of the Ea's; these results cannot be correlated with polymer structure since, for example, the bond energies of the C-C bond are of the order of 80 kcal/mole and C-H bond is about 108 kcal/mole in HTPB. Without the presence of AP all polymers exhibited molten surface layers. Evolved gas analysis was performed using a mass spectrometer (low pressure tests). The major species to appear were heavy hydrocarbons with the greatest variety in the HTPB tests (mass numbers 82 and 84 predominate - a value consistent with a backbiting mechanism); results indicate that heavy hydrocarbons are more representative of

fuel species in the AP-binder diffusion flame than the previously assumed methane fuel. The authors also measure heats of decomposition for the polymers which are an order of magnitude greater than previously assumed. Calculations performed by Cohen [25], using these newly measured values in the so-called Derr, Beckstead, Price combustion model [4], suggest that: the flame temperature and primary flame kinetics are the most important factors influencing the burning rate, the heat of decomposition has only a secondary effect on the rate and, the magnitude pre-exponential term for the pyrolysis has only a minor effect. In addition, they arrive at the surprising conclusion that the kinetics of polymer pyrolysis are independent of heat flux and pressure. The various binders exhibit a range of kinetic constants, but the activation energies do not exceed 17 kcal/mole, they believe that bond rupture is not the rate determining factor. The magnitude of the forgoing kinetic parameters, coupled with the mass spectrometer tests, appear to support the work of Chaiken. The forgoing tends to lend support to the argument of Chaiken that the rate determining step is the vaporization of large hydrocarbon fragments from the surface - at least under conditions of high-heat-flux and high temperature. If, however, vaporization is the rate controlling mechanism, the rate, contrary to the findings in [25], would certainly be a function of pressure. Considerable controversy exists in the literature as to whether the

rate limiting step for the surface pyrolysis is a chemical or physical process.

While all these linear-pyrolysis techniques have made significant strides toward making meaningful kinetic measurements, all possess certain limitations which impede the accuracy of the data. Hot-plate experiments, which permit the determination of excellent mass regression rates, suffer from uncertainty in the temperature and possible erosive effects. On the other hand the diffusion flame approach of McAlevy also suffers from ambiguity in temperature measurement due to the lack of information of on the emissivity of the polymer surface as a function of temperature. This is partially overcome in Cohen's work by the addition of carbon black to the specimen, but here mass regression estimates are made by discontinuous weighing which introduces some uncertainty in the result. Nevertheless, this method permits samples to be pyrolyzed at heating rates more meaningful to combustion than do most other approaches.

Rapid Heating Bulk Pyrolysis. In 1961, S. Kohn [19], in connection with work on high temperature ablation of polymers, recognized the importance of elevated heating rates, and designed a "rapid" TGA and DSC. The "rapid" TGA suffered from several shortcomings. Samples were heated by rapid introduction into a furnace to effect heating; heating rates were on the order of 20 °C per second. Mass measurements

were made discontinuously - the experiment was interrupted after a given time and the sample removed and weighed. Time required to cool the sample prior to weighing was as much as eighty seconds! This, the author points out, was a major drawback of the apparatus which makes it difficult to interpret results. Sample sizes are relatively large, 100 mg, and due to the poor thermal conductivity of polymer, thermal gradients across the sample are large. Temperature time relationships could not be determined during the tests. Given these facts, determination of kinetic parameters proved impossible; "at most, it may be expected that some information about the endo- or exothermal nature of the degradation may be. . ." ascertained.

Somewhat later, Shannon and Erickson [21], studied the thermal decomposition of some polymers used as binders in solid propellants. The methods used included DSC (80 °C/min.), radiation furnace (4 - 10 cal/cm²-sec), and flash-heating techniques (no estimate given); the three techniques being used to provide three levels of heat flux. In the radiation furnace method, samples were rapidly inserted into a furnace for certain periods of time, and weight-loss was intermittently recorded as a function of total energy absorbed. In the flash-heating experiments, samples were suspended from a micro-balance and mass continuously recorded as a function of total energy absorbed. Results in all cases were largely qualitative in nature. No

effort was made to estimate sample temperature, nor was any attempt made to determine kinetics.

Some of the best work in rapid-heating bulk-Pyrolysis and in high speed decomposition has been done by A. D. Baer et al. [10,14,18,20]. In 1973 [14] Bear reported work on a high speed thermal decomposition technique which produced data very similar to that of a DTA. In this work, "unsupported", 100μm thick, polymer films were heated by radiation from a 1200W projection lamp; heating rates were measured using an infrared radiometer at about 300 °C/s. Since the sample is not in contact with an "infinite" energy reservoir as in DTA, heat evolved due to reaction produces a permanent temperature change in the sample. The data is reported in the form of ΔT vs. T. The ΔT is derived from the difference in the measured sample temperature and a calculated temperature of an inert sample exposed to an equivalent heat flux. Estimates of temperature differences across the sample were not more than 10 °C. The principal advantages of the arrangement are: low thermal inertia, small sample size, may be operated at pressure, and is suitable for crosslinked polymers. The principal disadvantages are that low heating rates are not possible in this technique, therefore data cannot be compared with classical methods; data is insufficient to estimate kinetic parameters; and that ΔT estimates rely in part on calculated values. The most significant result of this work is that polymers exhibited high tempera-

ture "exotherms" which were not observed in low temperature thermal analysis! The authors suggest, that at the even higher temperatures and heating rates characteristic of propellant processes, yet other reactions may be observed. In addition, polymers investigated remained intact to temperatures as high as 700 °K. In 1977, Baer, Hedges, Seader, et al., in a singular paper [20], reported another fast heating approach, which was used to characterize materials used as ablative insulators. The instrument, a form of TGA, heated 25 - 125μm polymer films at rates of 70 °C/sec in a N_2 atmosphere. Samples were coated on an electrically heated 25μm metal strip; the temperature of the strip was determined using an infrared radiometer on the side opposite to the sample coating. Pre-weighed samples were heated at a constant rate to a predetermined temperature. Samples were then quickly cooled, by a blast of cold nitrogen, at rates estimated to be 830 °C/s and subsequently weighed. Repetition of this procedure produced a non-continuous set of data in the form of residual-weight as a function of temperature for constant heating rates. Samples were evaluated on this apparatus at variety of heating rates, and on a conventional TGA at low heating rates. In addition, the authors determine kinetic parameters for the samples - three Neoprene/acrylonitrile butadiene composites. The finding of major significance in this work, is that decomposition curves predicted by extrapolation of the

conventional TGA data are greatly different than observed under the rapid pyrolysis experiment. As far as is known this is the first example of kinetic data from a rapid bulk pyrolysis experiment, unfortunately, no data is provided on common polymers. Some uncertainty is implicit in these results, since mass measurements are made discontinuously, and there is no way to determine the effectiveness of the "rapid" quench procedure. Some decomposition may occur in the time between max-temperature and sample weighing. In subsequent work in 1978 [20] and a related paper of 1981 [18], ignition and degradation test were conducted on several neat-polymers, however, these tests were performed in air which makes comparison with the N_2 tests impossible. It would be fortunate if these tests could be repeated in an nitrogen atmosphere and analyzed according to the methods of [14]. The purpose of the work presented in [18] was to investigate polymer ignition under approximated fire conditions, and to determine polymer decomposition kinetics at high heating rates. The instrument used in the ignition tests was similar to that used in the 1977 study; it heated 25 - 125μm polymer films at 200 °C/s; this experiment measured ignition temperature as function of heating rate. In the decomposition work, unlike the 1973 study, samples were heated in air at 1000 °C/s to a constant pre-defined temperature, where the material was allowed to decompose "isothermally". The implicit assumption of course is that

no decomposition takes place during heating. The rapid decomposition experiments produced mass loss vs. temperature data. Somewhat arbitrary, mechanisms were proposed for the isothermal decomposition of mylar and polyethylene; global kinetic parameters were calculated.

The rapid heating bulk-pyrolysis methods permit pyrolysis to be performed under more definable conditions than is apparently possible with linear pyrolysis. Rapid heating of thin films, in contact with metal surfaces (heat sinks), provides for uniform sample heating, and permits accurate measurement of temperatures. Emissivities of the metal supports can be determined as a function of temperature, and therefore permit more accurate optical temperature measurements. These methods are also amenable to high pressure operation. Besides the assumption of no mass loss during sample heating, the principal drawback of this type of experiment appears to be discontinuous mass measurement.

1.4 Objectives

Mindful of the foregoing, an investigation into rapid pyrolysis was undertaken. This investigation focused on the construction of a TGA which would operate at heating rates beyond those obtainable with conventional instruments. Samples were limited to pure materials, thereby avoiding the complexity of ingredient interaction.

The long term objectives of the research are to

underscore the need for experimental methods which address the combustion environment, and to explore theoretical and experimental techniques which can provide the needed data.

The short term objectives of this work were: firstly, to review previous theoretical and experimental developments in rapid pyrolysis. Secondly, build an apparatus capable of measuring, at elevated heating rates, the extent of sample decomposition as a function of temperature. Thirdly, to extract Arrhenius parameters from this data, and lastly, to apply the foregoing techniques to kinetically analyze HTPB and PBAN during high rate pyrolysis.

CHAPTER II

APPROACH

2.1 Overview

The determination kinetic parameters during rapid pyrolysis, requires techniques which can rapidly heat samples, while simultaneously making the necessary high speed mass and temperature measurements. As indicated in the last chapter, the performance of any of these tasks independently is a relatively straight forward matter; however, designing an instrument to make the concerted measurements is much more difficult. An investigation into rapid heating and mass measurement techniques was therefore conducted; this investigation resulted in the design and construction of new type of thermogravimetric analyzer. A sketch of this instrument is shown in Fig. 2-1. The device relies on vibration to perform rapid mass measurements. The sample ($\leq$ 1 mg.), a polymer dissolved in a solvent, is "painted" on a small metal strip which has been cemented in the free end of a quartz tube. It is surrounded and pyrolyzed by a non-contact heating device, such as a furnace or an RF induction-heater.

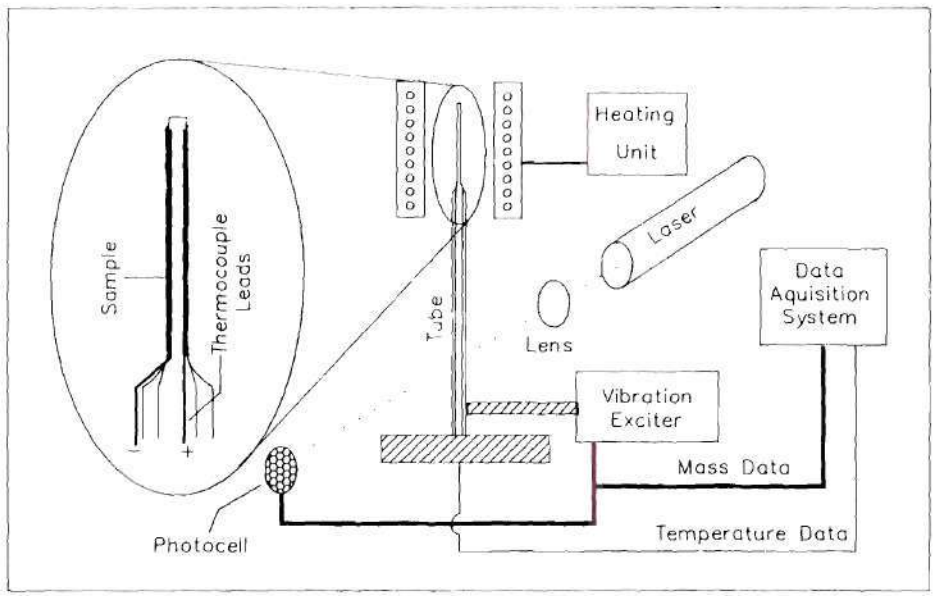

Fig. 2-1 Sketch of the Vibration-based-TGA. (VTGA)

If the tube is excited in transverse oscillation, the period of oscillation is directly proportional to the instantaneous sample mass. As the material pyrolyzes, the resonant vibration frequency of the tube (really the system) increases. Monitoring the change in frequency or period provides a means of estimating the instantaneous sample mass. The frequency is determined using a laser-photodiode pair. The laser (1.0 mWatts) "looks" across the tube at the photodiode, the output from which is a sinusoidal signal whose frequency is identical to the frequency of the vibrating tube. This signal is fed-back into the vibration exciter which excites the tube at the current resonant frequency of the system. This electrodynamic feedback-loop

causes the tube to be continuously excited at the instantaneous resonant frequency, thereby making a continuous mass measurement possible. The system can be calibrated by application of known masses. The actual amplitude of oscillation is less than a millimeter. Sample temperatures are measured by a fine wire thermocouple "embedded" in the metal strip upon which the sample is coated. This, unlike conventional TGA's, places the sample in good thermal contact with the thermocouple and permits the measurement of the actual sample temperature rather than the furnace temperature. The functional parts of the system are enclosed in an chamber so that tests may be performed in an inert atmosphere. Frequency and temperature data are acquired on a two-channel, 2 MHertz digital oscilloscope interfaced to a microcomputer, to which data is transferred for subsequent analysis. (See Appendix A.) A typical output is illustrated in the oscillograph shown in Fig. 2-2; this figure shows the output of the mass and temperature data lines during the low-heating-rate decomposition of HTPB. The top curve in this figure is the amplified thermocouple output, while the lower curve is generated by passing the feedback loop signal through a frequency to voltage converter (FVC). This last curve, is proportional to the instantaneous resonance frequency of the system, and therefore inversely proportional to the instantaneous mass loading, represents the fraction of material vaporized. In

Table 2-1, the parameters associated with the data of Fig. 2-2 may be found. In essence, the system depicted in Fig 2-1 is a Vibrational-TGA (VTGA).

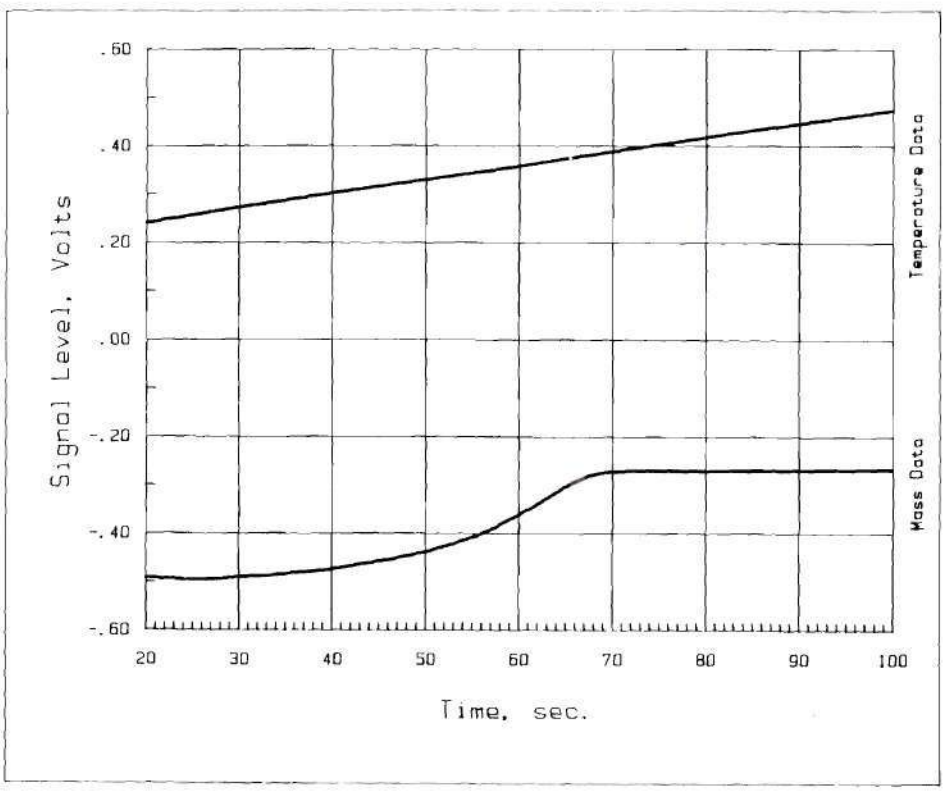

Fig. 2-2. Oscillograph - Typical Output of VTGA.

In order to demonstrate the functionality of the instrument several tasks were accomplished. Firstly, selected polymers were kinetically analyzed on a conventional thermogravimetric analyzer.

Table 2-1. Parameters for Curves in Fig. 2-2.

Apparatus:	VTGA
Material:	HTPB
Heating Rate:	3.3 °C/s
Sample Size:	≈ 1.0 mg
Quartz Tube Geometry:	See Fig. 3-1

Secondly, Arrhenius parameters were then extracted from this data using a modified form of a classical data reduction scheme from the literature. These values serve as baseline data. Thirdly, these polymers were re-evaluated on the new VTGA under comparable conditions. This was to demonstrate that the new instrument is indeed a functional thermogravimetric analyzer. Lastly, these polymers were again evaluated on the VTGA at increased heating rates to assess the capabilities of the new instrument; results are examined in terms of the scant elevated heating-rate data in the literature.

2.2 Pressure Dependence

No high pressure tests were performed in this work, although, the functional parts of this prototype instrument were selected such they would be suitable for implementation at high pressure. Unlike combustion, results from the proposed experiment should be a weak functions of pressure, particularly if the rate controlling step for the mass loss

is the surface decomposition kinetics. Strictly speaking, rates of condensed phase reactions are independent of pressure. In combustion situations, however, pressure controls the position of the gas phase combustion wave relative to the deflagrating surface, this in turn influences the heat flux to the surface. In the present experiment heat flux is controlled by the power input by the heating unit; a gas phase combustion wave does not exist. Therefore, pressure is expected to have a minimal effect on the overall results. If, however, the rate controlling process is vaporization, pressure would certainly influence the results. It is interesting to point out that in experiments such as the diffusion flame work of McAlevy [22], and in most combustion type experiments, the effects of pressure and heat flux are coupled. In most RHBP, which includes the present experiment, heat-flux and pressure are decoupled and can be varied independently. Subsequent work should examine the dependence of the results on the systematic variation of these parameters. This also re-emphasizes the importance of performing experiments under conditions where the heat-flux matches that of the "real world" process being emulated.

2.3 Data Analysis

As is usually the case in TGA analyses, reactions of the form:

$$a\ A(s) \xrightarrow{\Delta} b\ B(s) + \ldots + c\ C(g) + \ldots$$

$$b = 0, \text{ or } b \neq 0$$

are considered. In general it is possible that several such reactions may take place concurrently or consecutively in the course of the decomposition, especially when dealing with complex substances such as polymers. The calculation of global Arrhenius parameters requires, in the isothermal case [34], an accurate measurement of the fraction of sample decomposed as a function of time, $\alpha(t)$, and in the non-isothermal case [35], a measure of the fraction decomposed as a function of temperature $\alpha(T(t))$. The ratio of the change in mass to the total change in mass provides a convenient measure of α, a non-dimensional representation of which is given by Eqn. (2-1).

$$\alpha = 1 - \gamma = \frac{m_o - m}{m_o - m_f} \qquad (2\text{-}1)$$

In this expression, α represents the "fraction reacted"; γ is the "fraction remaining", m_o is the initial mass of the sample, m_f is the final mass of the sample, and m is the instantaneous sample mass. The rate of disappearance of the sample can be described in terms of the so-called conversion function, $f(\gamma)$ in Eqn. 2-2. This equation asserts that the

rate of mass loss is proportional to a constant, k, the rate constant, times some function of the remaining mass.

$$\frac{d\gamma}{dt} = -k\, f(\gamma) \qquad (2\text{-}2)$$

Since γ is by definition equal to $1-\alpha$, Eqn. (2-2) becomes:

$$\frac{d\alpha}{dt} = k\, f(1-\alpha) \qquad (2\text{-}3)$$

Implicit in the foregoing is the assumption used in most TGA analyses that the sample is thermally thin - uniform temperature throughout. That is, the measured reaction rates must be independent of the sample thickness; this is especially important in rapid heating experiments [25] and must be verified on a case-by-case examination.

The principal difficulty in the determination of Arrhenius parameters from thermal analysis experiments is that there is basically one equation - the rate equation, and three unknowns - E, A, and n. The general approach is to integrate the rate expression and linearize the result, such that a plot of the data in some reduced coordinate system yields a straight line, where the slope is some

function of Ea and the intercept is some function of A; n is determined parametrically.

In general, two main approaches are normally considered: isothermal and non-isothermal methods. If the experimental method can ballistically heat samples to some high constant uniform temperature before substantial decomposition occurs, the balance of the decomposition will occur at constant temperature and an isothermal treatment of the data may be used. This is preferable since the functional form of $f(\gamma)$ can be empirically determined in this type of analysis, and a greater understanding of the decomposition mechanism is possible [36]. If, however, a large weight loss occurs during heat-up, recourse must be taken to a non-isothermal analysis; this is always accompanied by some ambiguity in result, due to the uncertainty in the functional form of $f(\gamma)$. Farre-Ruis, and Guiochon [15] point out that substantial decomposition occurs in thermally stable polymers even at the highest heating rates. It is due to this and other compelling practical considerations that a non-isothermal analysis has been selected in this work.

There are many techniques in the literature [37] which permit the calculation of Arrhenius parameters using non-isothermal data if one assumes a general functional form for $f(\gamma)$. Indeed, polymer decomposition in a combustion wave is a non-isothermal process, and in the final analysis one would like to program the heating rate such that the sample

would experience the same "thermal history" as a small volume element in the burning solid.

2.3.1 Non-Isothermal Data Analysis.

In the past 30 years, a number of techniques have been proposed to estimate Arrhenius parameters from non-isothermal decomposition data; these are outlined in an excellent review by Wall [37]. These can loosely be divided into: integral methods, differential methods, and difference-differential methods, each method having its own advantages and disadvantages.

Integral methods obtain Arrhenius values through direct integration of the rate expression. These methods, are the most straight forward, but generally require *a priori* knowledge of the order of reaction. Differential methods suffer from loss of accuracy due to the amplification in data scatter due to numerical differentiation, and at times it may be impossible to use this approach with empirical data [37]. Difference-differential methods employ finite difference relations which are applied to data that is collected at various heating rates. This analysis suffers many of the same limitations as differential methods. All share the following key assumptions: that the Ea, so determined, is kinetically meaningful in a chemical sense, and more seriously, that the Ea and the pre-exponential term are constant over the entire temperature domain of the decomposition. (This temperature range is commonly over 200 °C.)

These methods, in addition, assume that Ea is constant with respect to the various heating rates employed. Some methods assume first order decomposition while others determine the order parametrically. All require a thermally thin sample, i.e. thermal gradients within the sample are small. Cognizant of "data scatter" associated with differential methods, an integral approach was selected in the following work.

If the sample heating rate, $\beta(T) \equiv dT/dt$, is used in Eqn. (2-3), and an Arrhenius type dependence is assumed for the rate constant, k, this relation becomes:

$$\frac{d\alpha}{dT} = \frac{A}{\beta(T)} e^{-E/RT} f(1-\alpha) \qquad (2-4)$$

which is the basic differential rate expression for a material decomposing under a programmed temperature rise. The corresponding integral expression is given in Eqn. (2-5).

$$\int_0^{\alpha} \frac{d\alpha}{f(1-\alpha)} = \int_0^{T} \frac{A}{\beta(T)} e^{-E/RT} dT \qquad (2-5)$$

If we assume in the first analysis, for low heating rate cases, that $f(1-\alpha) \equiv (1-\alpha)^n$, and that E, A, and n are constant over the entire range of decomposition (which is not necessarily true), and impose a linear heating program (β = constant), then Eqn. (2-5) becomes:

$$F_n(\alpha) = \int_0^{\alpha} \frac{d\alpha}{(1-\alpha)^n} = \frac{A}{\beta} \int_0^{T} e^{-E/RT}\, dT = \frac{A}{\beta}\, \Phi(T) \qquad (2\text{-}6)$$

The left-hand-side of this equation evaluates easily to $F_1(\alpha)$ or $F_n(\alpha)$ where,

$$F_1(\alpha) = -\ln(1-\alpha) \qquad (2\text{-}7a)$$

$$F_n(\alpha) = \left[\frac{1-(1-\alpha)^{1-n}}{(1-n)}\right] \qquad (2\text{-}7b)$$

depending whether or not n = 1. The right-hand-side of Eqn. 2-6, however, has no closed form solution. The literature is replete with approximations to this integral. Coats and Redfern [35] have evaluated this integral by making the substitution, u = E/RT and expanding the result in an asymptotic series [38] to yield,

$$\Phi(T.) = -\frac{E}{R}\int_{u}^{\infty} e^{-u}\,u^{-2}\,du = -\frac{E}{R}\left[\frac{e^{-u}}{u}\sum_{n=0}^{\infty}\frac{(-1)^{n}\,(2)_{n}}{u^{n+1}}\right] \qquad (2\text{-}8)$$

If the independent variable, u, is large (which is usually the case in solids pyrolysis), it is sufficient to neglect terms of order $O(1/u^{3})$ and higher; through this procedure one may obtain three Equations, 2-9a, b, and c, for the zero, first, and n'th order cases respectively. Here Γ is the "Coats and Redfern Ordinate" or the ordinate in the reduced coordinate system.

$$\Gamma_{0} = \ln\left[\frac{\alpha}{T^{2}}\right] = \ln\left[\frac{AR}{\beta E}\left\{1 - \frac{2RT}{E}\right\}\right] - \frac{E}{RT} \qquad (2\text{-}9a)$$

$$\Gamma_{1} = \ln\left[\ln\frac{(1-\alpha)}{T^{2}}\right] = \ln\left[\frac{AR}{\beta E}\left\{1 - \frac{2RT}{E}\right\}\right] - \frac{E}{RT} \qquad (2\text{-}9b)$$

$$\Gamma_{n} = \ln\left[\frac{1-(1-\alpha)^{1-n}}{T^{2}(1-n)}\right] = \ln\left[\frac{AR}{\beta E}\left\{1 - \frac{2RT}{E}\right\}\right] - \frac{E}{RT} \qquad (2\text{-}9c)$$

Unfortunately, as with all integral methods, evaluation of the Arrhenius parameters requires a priori knowledge of n, the order of reaction. Many schemes have been devised to circumvent this problem where the order of reaction is determined parametrically [39,40,41].

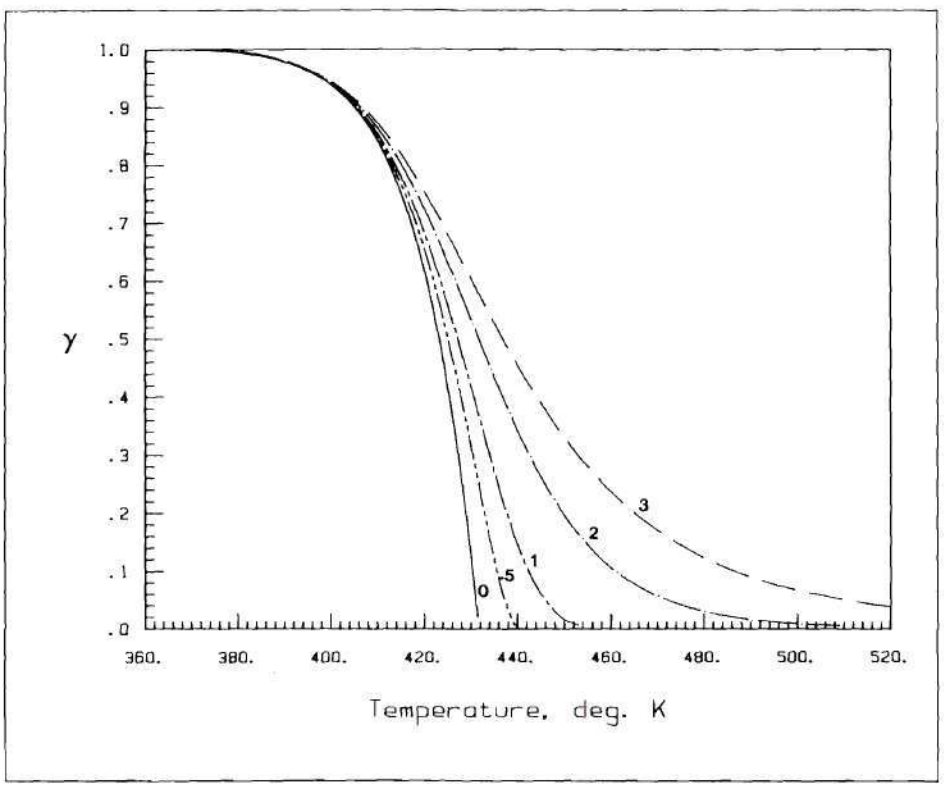

Fig. 2-3a. Solutions to the Differential Form of Eqn. 2-6.

Table 2-2. Fourth Order Runge-Kutta Solution Parameters to Eqn 2-6.

Parameters	Initial Conditions
Ea = 28,000.00 calories/mole	T_o = 370.00 °K
A = 6.00 x 10^{+11} s^{-1}	α_o = 0.0 : τ_o = 1.0
R = 1.987 calories/ mole / °K	
n : 0; ½; 1; 2; 3	
β : 0.05 °K/s	

To illustrate one resolution to this dilemma, the differential form of Eqn. 2-6 has been solved numerically using a fourth order Runge-Kutta method; the solution curves for various reaction orders are shown in Fig 2-3a and the solution parameters are given in Table 2-2. The corresponding differential curves are given in Figure 2-3b.

It has been observed [37] that, in the limit, as α approaches zero, reactions of all orders follow zero order behavior, Fig. 2-3c. This can be exploited to determine Arrhenius parameters during the early stages of reaction without prior knowledge or assumption of the reaction order. Therefore, by equation (2-9a), a plot in the "reduced coordinates" of $\Gamma \equiv \ln(\alpha/T^2)$ versus $1/T$, should produce a straight line with a slope of $-E/R$, since $(1-2RT/E)$ is essentially constant and equal to unity. The pre-exponential may be obtained from the intercept, I, and the relation $A = (\beta E/R)e^{I}$. Applying this procedure to the theoretical data of

Figure 2-3a produced the curves shown in Figure 2-3d. Table 2-3 contains the tabulated Arrhenius data so obtained.

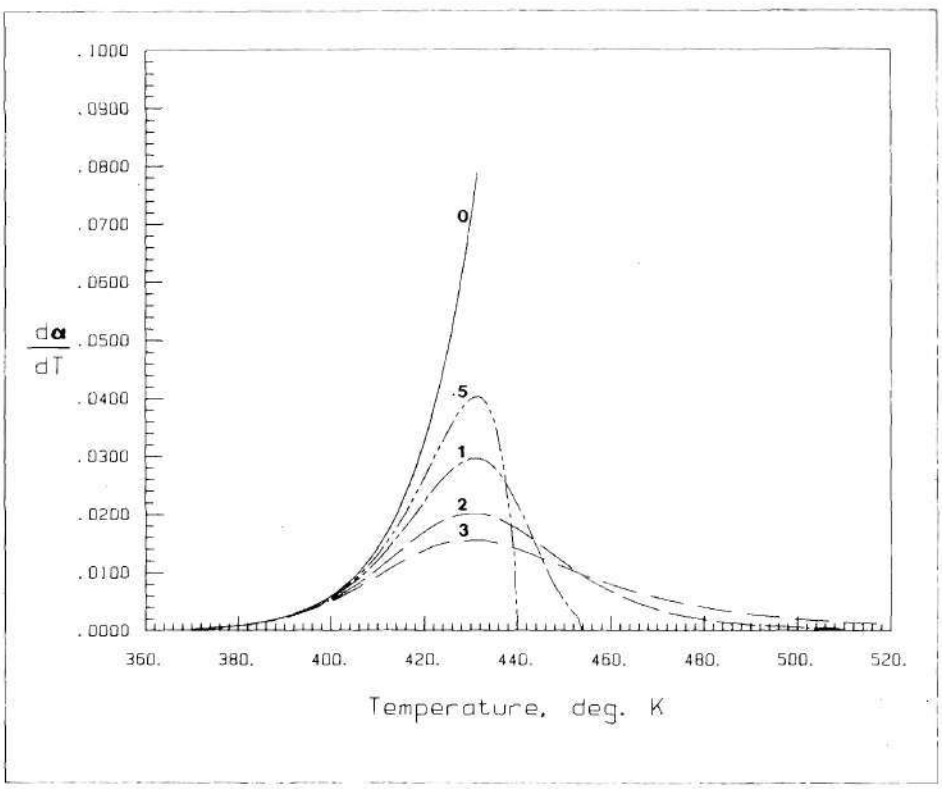

Fig. 2-3b. Differential Curves for Parameters in Tbl. 2-2.

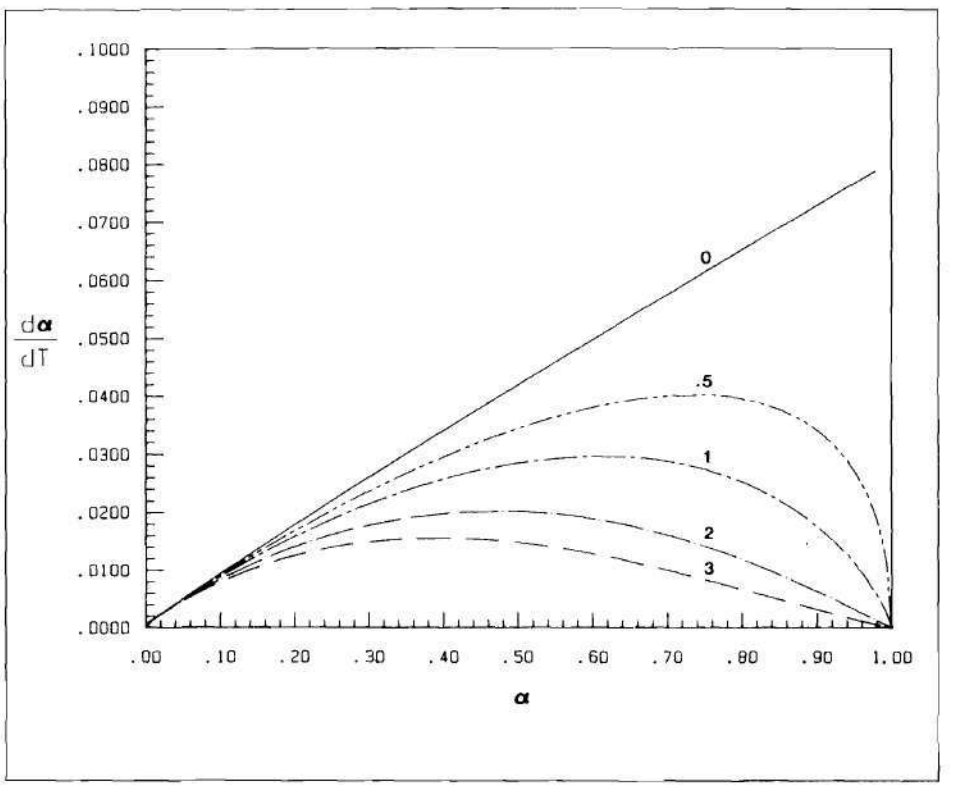

Fig. 2-3c. Rate vs. Extent of Reaction.

Table 2-3. Calculated Arrhenius Data by a Zero Order Analysis - $0.10 < \alpha < 0.30$.

Actual Order	Calculated Values Assuming Zero Order		
	Ea cal/mole	A $\times 10^{-11}$ s^{-1}	Correlation Coefficient
0	30,160	85.9	.9991
½	29,489	35.6	.9986
1	28,830	14.7	.9976
2	27,459	2.49	.9961
3	26,186	0.438	.9937

It apparent that for $\alpha < 0.30$, the data is virtually independent of order. Analyzing the early stages of decomposition frees the experimenter from the necessity of a priori assumptions as to order. In fact, "although there are some special cases for which a theoretical order has real significance, n must be looked upon as a purely empirical parameter, sometimes useful in curve fitting. [37]" Global reaction order can be a complex function of sample geometry, heating rate, etc., and depends largely on experimental method. Moreover, analyzing the first 30% of the reaction, has the added advantage of narrowing the temperature range over which the Arrhenius parameters are determine, and the temperature range over which they are assumed constant. The foregoing is the theoretical basis for the data reduction method which was applied to the TGA

and VTGA data produced in this work; the exact details of the analysis procedure will be explained in Chapter IV.

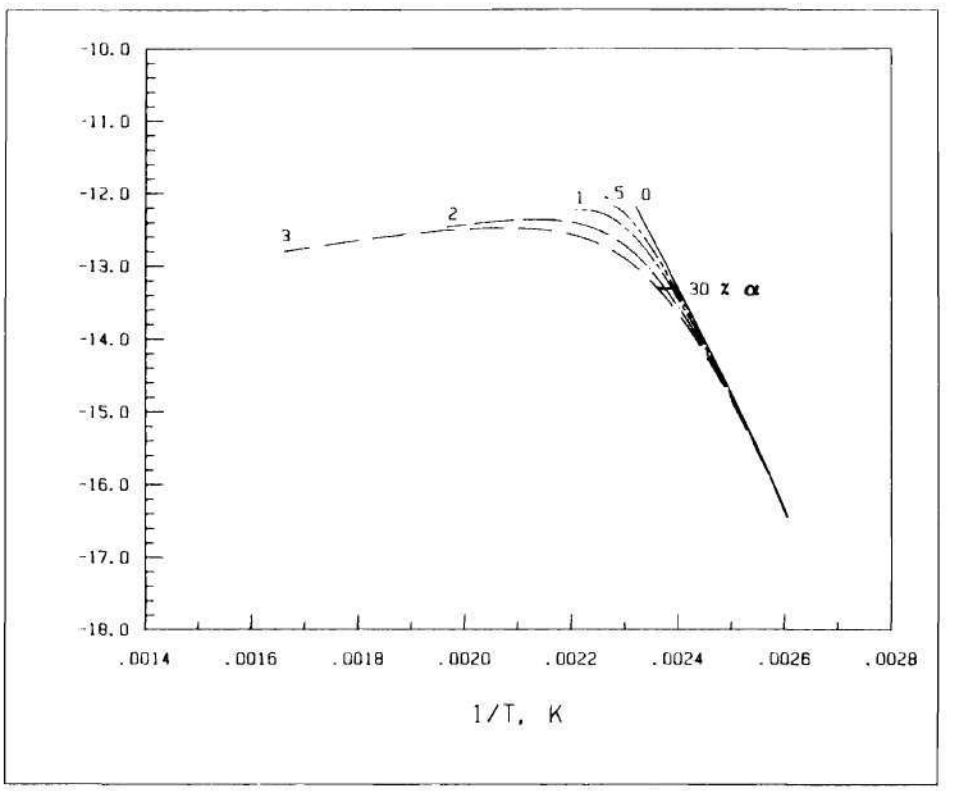

Fig 2-3d. Γ_o vs 1/T

CHAPTER III

INSTRUMENTATION - DESIGN AND CALIBRATION

3.1 The Instrument

Recent years have seen an ever increasing level of sophistication in the design of thermal analysis equipment [42]. These improvements have resulted in instruments which are capable of more accurate mass and thermal measurements, improved temperature control and automatic calibration, as well as units with the ability of attaining higher and lower ultimate temperatures. While these enhancements have facilitated the investigation of polymer stability and other low rate phenomena, they have done little to improve the understanding of polymer combustion. This is mainly due to the inability of such devices to heat samples at rates much above 1 °C/s without significant thermal lags between the sample and its environment. In thermogravimetric analyses, for example, the usual mass measuring device is the double-arm micro-balance; it has too much thermal and mechanical inertia to provide the necessary response at more ambitious heating rates. Factors such as buoyancy, condensation of pyrolysis products on the cooler parts of the balance, and the influence of the pyrolysis-product vapor on mass deter-

minations, all combine to interfere with the most sensitive measurements. Moreover, in conventional TGA systems, the thermocouple is rarely in contact with the sample, and is therefore unable to detect endothermal and exothermal transitions which normally accompany pyrolysis. In definitive work, these thermal deviations within the sample must be minimized by placing the sample in contact with a good heat sink, or they must be accounted for in the data analyses. The ability to overcome such limitations is incompatible with the design of present thermal analysis equipment; this necessitates the development of new techniques which are more suited to operation at higher heating rates.

Therefore, in order to quantitatively evaluate polymers at increased heating rates, a new type TGA was constructed; this prototype instrument, unlike conventional TGA's, uses vibration for mass determination. Moreover, in this new design the sample is in intimate contact with the thermocouple. A considerable portion of present work was devoted to the development of this apparatus and to the evaluation of this method with respect to rapid pyrolysis.

The principal features of the apparatus are illustrated in Figs. 3-1 through 3-3. The main components are mounted on triangular "optical benches" which have been bolted to a half-inch steel plate equipped with leveling legs; the whole assembly is placed on a table fitted with anti-vibration pads.

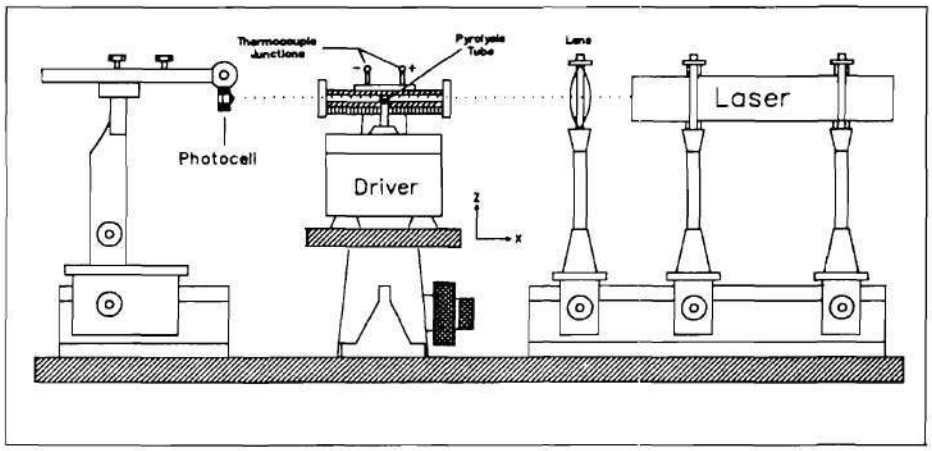

Fig. 3-1. Front View of VTGA Apparatus.

The focal point of the apparatus is a cantilevered quartz tube which has been clamped to a central mount fashioned from a microscope stage and support. A ferromagnetic metal strip with an imbedded fine-wire thermocouple (1 mil) is cemented (2000 °F ceramic cement) in the tip of the quartz tube. The positive lead of the thermocouple is routed through the center of the tube; the negative lead is routed along the outside of the tube to prevent shorting of the leads. These leads are soldered to the base of the thermocouple "pick-ups". The shaft of the vibration exciter is brought into contact with the tube by means of the stage z-axis vernier adjustment.

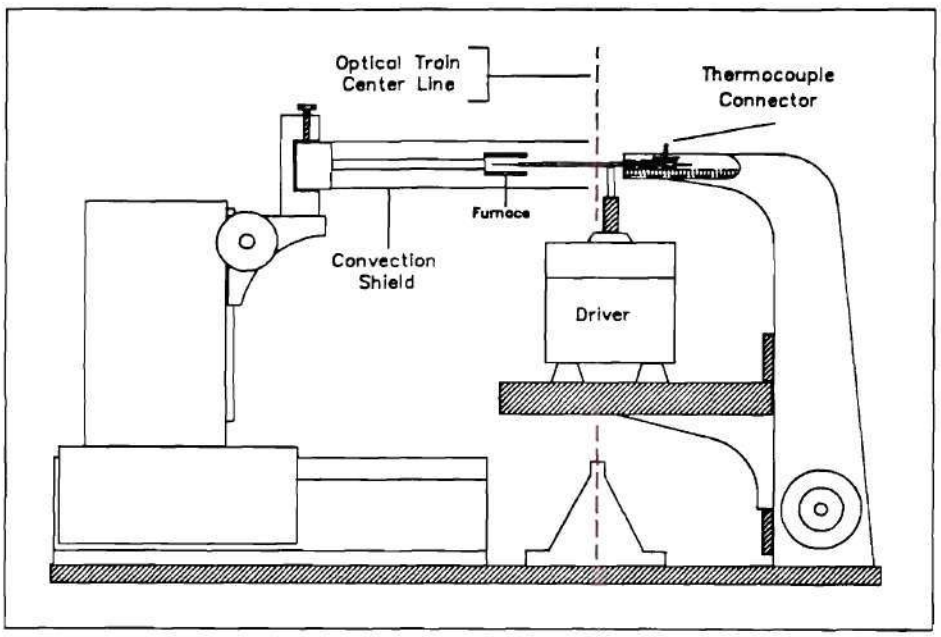

Fig. 3-2 Side View VTGA with Linear Furnace.

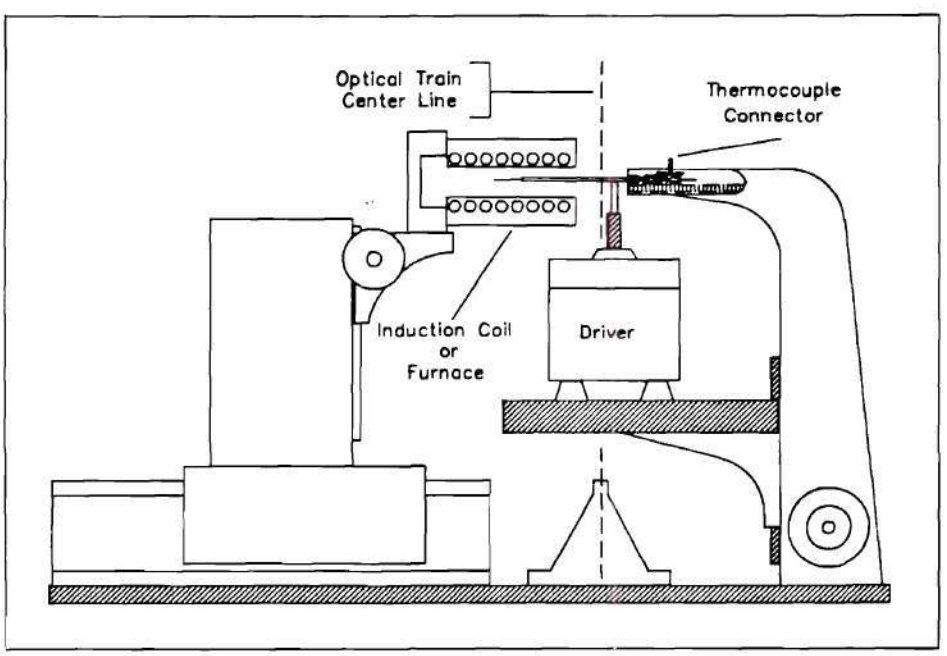

Fig. 3-3 Side View VTGA with Induction Furnace.

Side views of the apparatus are shown in Figs. 3-2 and 3-3. In the former illustration, the instrument is configured with a low heating rate linearly programmed furnace, while the later drawing shows the instrument configured with an induction furnace. The point of contact of the vibration exciter with the quartz "pyrolysis tube" is adjusted using the x-y stage verniers. Likewise, the furnace mount is configured with a vernier adjustments for positioning in the z-direction and may incrementally positioned and locked in other directions. The instrument can be functionally divided in to three main sub-systems: mass determination, sample heating and temperature measurement, and data acquisition.

3.2 Apparatus

3.2.1 Mass Measurement

The problems associated with making a continuous mass measurement of a sample during rapid heating have been pointed out by Kohn [19]. He states, that:

> . . . there are great practical difficulties in making an experimental device to continuously determine the specimen weight during { rapid pyrolysis }. Restrictions are set, on one hand, by the time needed to determine the thermal equilibrium of the weighing device, and on the other, by the difficulty of calculating or of experimentally ascertaining the weight corrections, made necessary by the variation in the Archimedean pressure due to a density decrease in the gaseous atmosphere of the furnace and by the pressure caused by the gas emission accompanying pyrolysis.

Mindful of these difficulties, Th. Gast and H. Jakobs [43,44] have used vibration to make mass measurements of materials subjected to rapid temperature increases. In their work a platinum ribbon was mounted under tension between two fixed supports. Samples were coated on this ribbon, which was then heated by the passage of an electric current. Temperature measurements were made by simultaneously using this ribbon as a platinum resistance thermometer. A continuous mass measurement was made possible by fashioning an electrodynamic feedback-loop; however, no description of the feedback loop is given, nor, is there any mention of how the frequency of the vibrating ribbon is determined. Their measurements included mass and heat capacity of the samples; no attempt was made to extract kinetic data. On the whole, the description of the details of their apparatus and their method are somewhat sparse. While their approach is very interesting with respect to the present work, it was felt that it would be difficult to maintain constant tension in the ribbon during heating, this problem, which was not discussed by the authors, is pivotal to the success of the measurement. After some deliberation, a method using a vibrating cantilevered quartz tube was selected as best suited to the present work.

The mass measurement scheme of the present method derives from the fact that the natural frequency of vibration of a cantilevered tube is inversely proportional to the

linear density of the tube, Eqn. 3-1.

$$\Theta = \left[\frac{EI}{\mu L^4} \right]^{\frac{1}{2}} \qquad (3\text{-}1)$$

If a mass is coated on the end of a cantilevered tube, the period of oscillation is directly proportional to the instantaneous loading.

The basis of the system depends upon an electrodynamic feedback loop, a block diagram of which is shown in Fig. 3-4. The essential features of this feedback system are: a 1 mW laser; a lens, to diffuse the laser beam; the quartz tube; a photodiode; some ancillary circuitry; an amplifier; a power supply; and a vibration exciter. The photodiode is positioned in such a way that the shadow of the tube partially obscures the active part of this device. Transverse motion of the tube causes more and then less of the diode to be obscured. This results in a sinusoidal output from the photodiode, rather than a square-wave which would result if the tube "chopped" the light beam. This signal is fed back to the vibration exciter, via some electronics, to close the loop. The purpose of the electronic circuit, shown at the bottom of Fig. 3-4, is to "kill" any DC-offset induced by the DC power supply and to prevent saturation of the loop amplifier. By using the DC-Offset vernier adjustments on

this amplifier, any remaining DC component may be precisely set or eliminated, as necessary; this adjustment is crucial to the fine tuning of the system. The true RMS signal strength going to the vibration exciter is controlled by the vernier gain adjustment also on this amplifier.

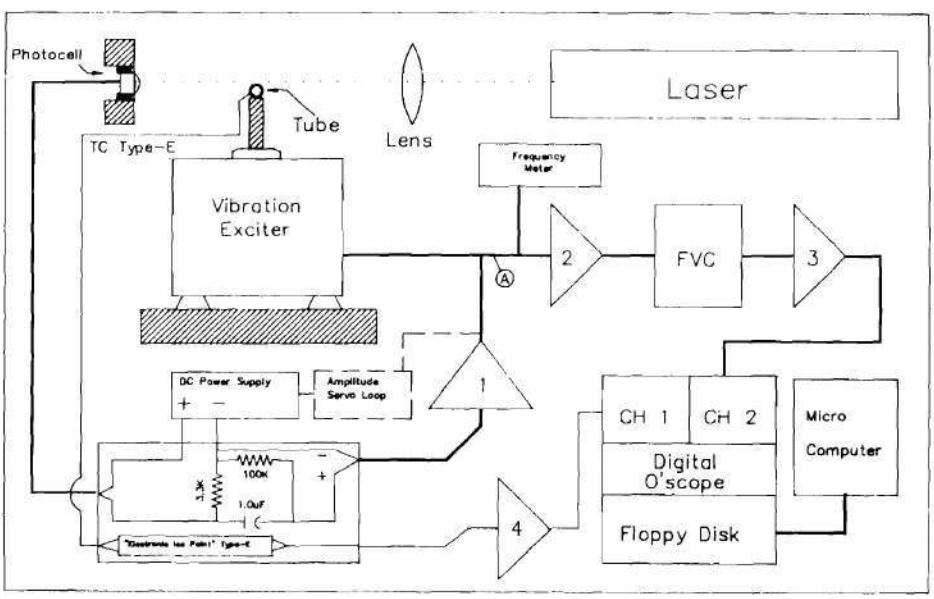

Fig. 3-4. Block Diagram of VTGA.

Any decrease in mass at the end of the tube causes oscillation at a slightly higher frequency thereby producing an analogous change in the output of the photodiode. This causes the tube to be excited at this new natural frequency of the system. Monitoring of the frequency or period, makes a continuous mass measurement possible.

Interestingly enough, the system does not have to be started! If DC power is supplied to the feedback loop, any disturbance or vibration is sufficient to cause the system to start oscillation and to seek its natural frequency. An acoustic analogy may be drawn between the present system and the "feedback" phenomenon common to audio speakers and microphones. In the audio case, the speaker corresponds to the vibration exciter, the microphone to the photodiode, and the transverse oscillation of the tube to the longitudinal oscillations in the air between the speaker and the microphone. In this case, if the density of the medium is changed, as by the introduction of a foreign gas, the system shifts automatically to the new resonance frequency. When properly adjusted, the system will automatically track the variation in mass loading on the tube, the output signal will be a near perfect sinusoidal wave, with zero DC offset, whose period is proportional the instantaneous mass loading. The quality of the signal produced by the oscillation of the composite quartz/metal tube can be seen in the oscillograph shown in the inset of Fig. 3-5. This signal was acquired at location A in Fig. 3-4 under the conditions given in Table 3-1. The almost unimodal character of the oscillation is further illustrated by the Fourier transform of this signal shown in Fig 3-5. This signal, and hence the tube motion, was only virtually unaffected by the magnetic and RF fields generated by the induction heater during rapid

heating. This is primarily due to the large frequency difference between the mechanical oscillations (150 Hertz) and the field oscillations (1.2 MHertz).

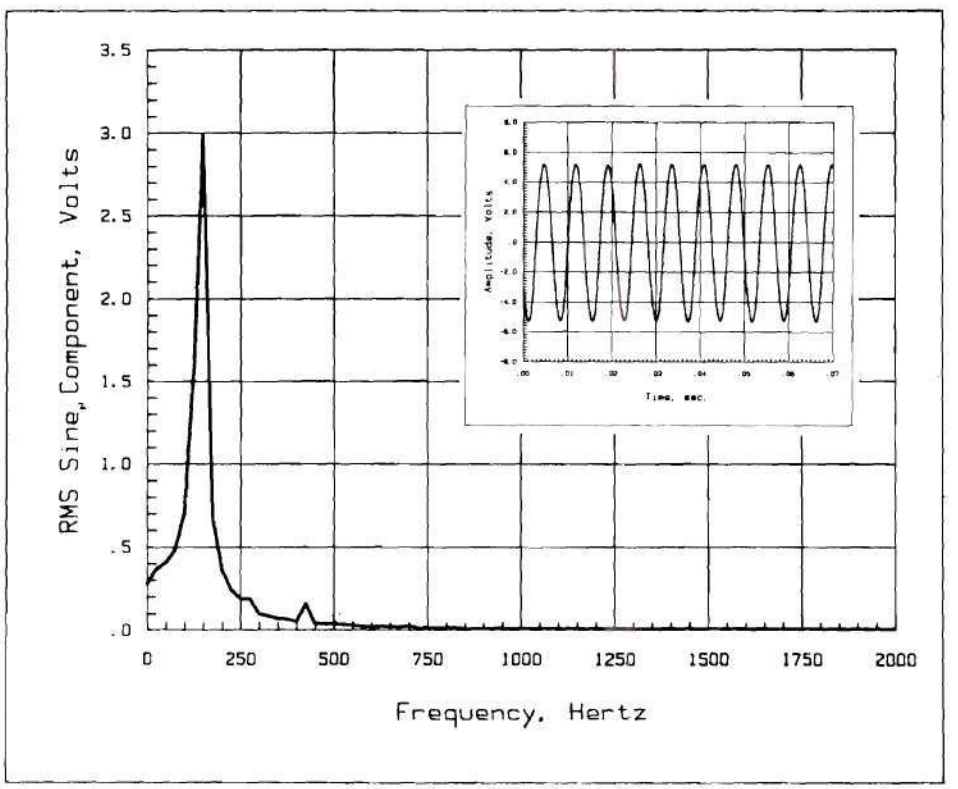

Fig. 3-5. Feedback-loop Signal and Fourier Transform.

Table 3-1. Measured Parameters for Data in Figs. 3-5a and b. #

	Quartz Tube	Metal Tube	Composite Tube
Length +	5.40 cm	0.70 cm	6.1 cm
Outside Diameter *	0.55 mm	0.33 mm	-
Inside Diameter *	0.40 mm	0.178 mm	-
Linear Density +		6.71 mg/cm	-
Youngs Modulus *	3.3×10^{11} dynes/cm^2		
		Flattened Tip	
Weight +		4.19 mg	
Thickness +		101 μm	
Surface Area (one side)+		0.0586 cm^2	

* Effective
\+ Measured
\# The values in this table are typical of those used in this work.
The linear density of the thermocouple wire is essentially negligible.

3.2.2 Thermal Systems

In the low heating rate experiments, samples are heated in a linear furnace, Fig. 3-2. For convenience, and ease of comparison with conventional TGA results, the furnace used in these tests is the very one used in the commercially available TGA-2 made by Perkin-Elmer. The temperature rise is programmed and controlled using the TGA-2 System 7/4 control device.

In the high heating rate experiments, an induction furnace of the type found in Curie point pyrolyzers is used to indirectly heat the samples. Induction heating uses the

magnetic field from a high power radio frequency (RF) coil to induce eddy currents in a ferromagnetic conductor (or heating element). At radio frequencies these induced currents are confined to a small region near the surface of the conductor. The depth of these currents is defined as the skin depth - that depth where the surface magnetic field strength, H_o, drops to 1/e of this value. Ferromagnetic materials are characterized by very small skin depths due to their large relative magnetic permeability, μ_r. The skin depth, δ, is a function of the frequency, θ, of the RF oscillator, and the magnetic permeability, μ. (See Eqn. 3-2). The eddy currents release heat near the surface of the conductor; ninety percent of the heat release takes place in the first skin depth [46]. At radio frequencies, δ, is of the order of 25 μm. The computed skin depths and specifications for the induction heater used in this work

$$\delta = \left[\frac{2\ \phi}{\mu\ \theta} \right]^{\frac{1}{2}} \qquad (3\text{-}2)$$

are given in Table 3-2. These small skin depths permit extremely high surface heating rates up to the Curie point temperature of the ferromagnetic conductor (the ferromagnetic tip on a the quartz tubes). Proper selection of the tube geometry and the RF field parameters causes the system

to heat ballistically to, and stabilize at the Curie

Table 3-2. Calculated Skin Depths for Ferromagnetic Materials

H_o = 382 Oe
μ_o = 4π x 10^{-9} V-sec-turn/A-cm
Ω = 1.2 MHertz
μ = $\mu_r \cdot \mu_o$

Material	Curie Pt. °K [56]	μ_r [56]	Resistivity Ohm-cm x 10^6 20 °C	δ μm
Nickel	631	16.5	7.8	31.5
Iron	1043	50	9.71	20.2
304SS	845	≈35	69.5	64.7
Cobalt	1401	21	9.8	31.4

temperature. It has been reported [45] that the surface of a 0.6 mm Fe wire, as measured by a 1 mil thermocouple, goes from 20 °C to 760 °C in about 40 ms (RF oscillator 480 kHz; magnetic field 1170 Oe; power generator 2000W). This translates into an average heating rate of 25,000 °C/sec. The heating rate can be modified by varying the power input to the coil or the coil geometry. Different final temperatures can be obtained by alloying the ferromagnetic heating materials with various paramagnetic metals.

Near the Curie point, μ_r for the heating element drops precipitously from a value of around five-hundred to about unity. This significantly reduces further absorption of energy from the magnetic field and consequently limits further heating. Any temperature decrease due to radiation or conduction causes magnetic permeability to increase and re-initiates heating to the Curie temperature.

Curie point pyrolyzers have been used for years in connection with pyrolysis gas chromatography, and have gained a reputation of very high precision. This is due to very reproducible heating rates which can be obtained. The principal criticism applied to RF induction heating by most authors [46] is that the sample cannot be subjected to a continuous range of temperatures, but only to the discrete Curie temperatures characteristic of the ferromagnetic material. They make the unwarranted assumption that the heating time to the Curie point is essentially instantaneous. In their understandable desire to design an isothermal experiment, they fail to realize the potential of the system in a non-isothermal mode. Also most authors give very little concern to the heating rate at all, and they mistakenly concentrate only on the final temperature. (Even with induction heating, the half-decomposition time of poly(tetrafluoroethylene), one of the most stable polymers is less than the time required to heat the sample to 600 °C [15].) Given this it is not surprising that, there is only

one report of using a Curie point apparatus to make kinetic measurements [46,47] (Mass measurements were not made continuously.)

The elements of the temperature measurement system are also shown in Fig. 3-4. Samples are coated on a flat metallic surface at the end of the pyrolysis tubes. The temperatures of the surface is measured using a type-E thermocouple, which has been embedded in the surface. To insure that the output of the thermocouple corresponds to the published thermocouple tables [48,49], an electronic "ice point" or compensator is included in the output line. The output is amplified (#4, Fig. 3-4) and filtered to increase the S/N ratio. Fabrication of tubes with embedded thermocouples is described in Appendix A. In the finished tube, the thermocouple resides approximately 50 μm below the surface; this is within one "skin depth". There is an additional advantage of using induction heating with type-E thermocouples. Since the thermocouples are ferromagnetic alloys themselves, they are also heated by magnetic field, but at a lower rate. Therefore their response time is increased over that which can be obtained strictly by conduction. In addition, the RF field generated by the induction coil caused only minimal interference on the temperature data line; this high frequency noise was easily eliminated using by low-pass filtering in amplifier #4, Fig. 3-4.

3.2.3 Data Acquisition System

The data acquisition system consists of separate analog data lines for the mass and temperature information as shown in Fig. 3-4; these signals are sent to two separate channels of a digital oscilloscope. The electronic components of the feedback loop and data lines were assembled from available equipment and are far from optimized. As a result, undesirable signal characteristics arising from incompatibilities were eliminated by filtering of the data lines and the use of differential inputs at the oscilloscope, Fig. 3-6. These measures limit the response of the system and introduce a "time constant" in the data lines.

Thus this prototype instrument is limited in its overall time response; this of course could be corrected in a more ambitious electronic design. The digital oscilloscope samples data at a preset rate which can be varied from 200 s/point up to a maximum of 0.5 μs/point (2 MHertz). A maximum of sixteen-thousand data points can be acquired during a test with an accuracy of 12 bits in preselected ranges of ±100 mV to ±40 mV. The data from individual tests are stored on a floppy disk on the oscilloscope disk drive and are later transferred to a microcomputer through an RS-232 serial port; the necessary data transfer software was written [Program 1, Appendix B] to link the oscilloscope and the computer. Raw data, in the form of Volts vs. time, is stored on the computer's disks for subsequent data

reduction.

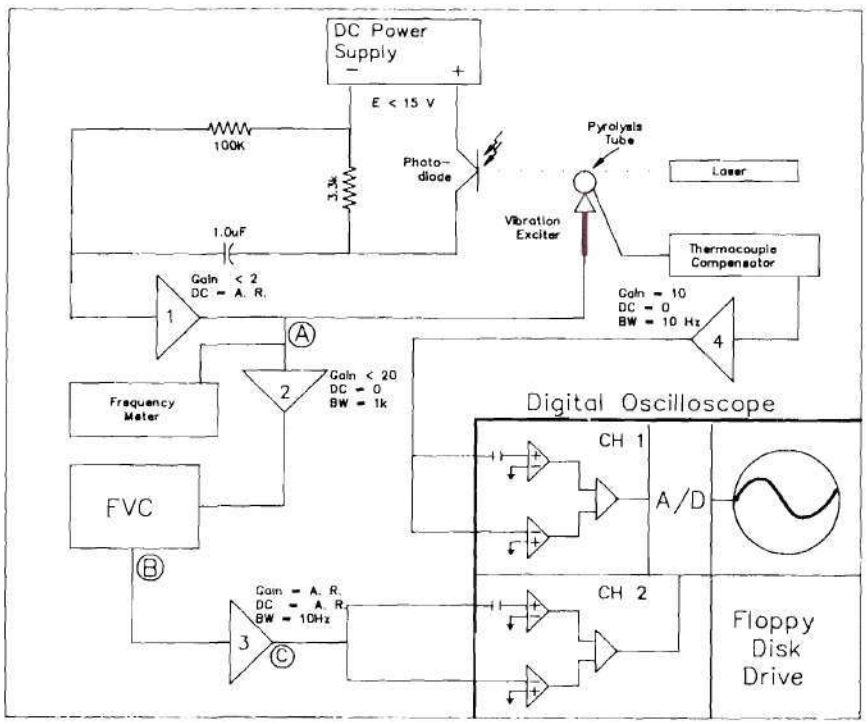

Fig. 3-6 Electronic Block Diagram-Schematic - VTGA.

3.3 Calibration

3.3.1 Mass Calibration

Prior to each calibration of the mass measurement system, the positions of the vibration exciter and the photodiode are mechanically adjusted to produce maximum signal amplitude at location A in Fig. 3-6. The DC power

supply is adjusted such that the amplitude of oscillation of the tube is approximately 1 mm. The input and output DC-offsets of amplifier #1, which has previously been zeroed, are adjusted to give maximum signal at location A with a zero DC offset. The emf to the loop is again adjusted to return the amplitude of the pyrolysis tube to 1 mm. The peak-to-peak voltage of the sinusoidal wave at circuit location A is normally about 0.5 Volts and has a frequency less than 300 Hertz depending upon the geometry of the pyrolysis tube. The purpose of amplifier #2 in the data line is to boost the signal strength sufficiently to drive the Frequency-to-Voltage (FVC) converter. This amplifier is nominally set to: DC offset = 0; gain = 20; and bandpass < 1000 Hertz. The signal from this amplifier is fed to the FVC whose zero has been appropriately adjusted. This DC signal is sent to amplifier #3 whose purpose is to increase the sensitivity of the output to frequency changes. This amplifier is set to: DC offset = A.R.; variable gain ≈ 10; and a bandwidth of 10 Hertz to "kill" any 60 cycle noise. Since the frequencies of interest are outside of the optimum performance range of the FVC, substantial AC noise corresponding to the signal frequency leaks through. This is removed by splitting the signal and using the differential input capability of the digital oscilloscope. Due to the crude electronics in the data line, the differential input is critical to the success of the measurement.

The net effect of this circuitry is to produce positive DC level change at the scope for a corresponding increase in the mechanical frequency of the pyrolysis tube; the polarity of this change can be reversed by reversing the polarity of the coupling at the scope. Therefore, as material pyrolyzes from the end of vibrating tube, the frequency of the tube will increase and produce an increase in the DC level at the scope, Fig. 2-2

The mass calibration is performed quasi-dynamically. This is done by applying known masses to the end of the cantilevered tubes, supplying DC power to the mass feedback-loop, and recording the period of oscillation along with the amplified output of the FVC. "shrink tubing" of the kind used in the electronics industry provides convenient reference masses. Small lengths are cut and placed around the at center of the flat heating element. Heat from a hot-air-gun is applied to insure good adhesion of this 0.5 mm PVC tubing. Care is taken to avoid excessive heating which would inhibit later removal. Power is supplied to the mass measurement system and the period of oscillation is noted along with the FVC output. The applied mass is carefully removed and weighed on a micro-balance to the nearest hundredth of a milligram. The required calibration curve is generated by repeating this procedure for applied loadings ranging from zero to 2.5 mg.

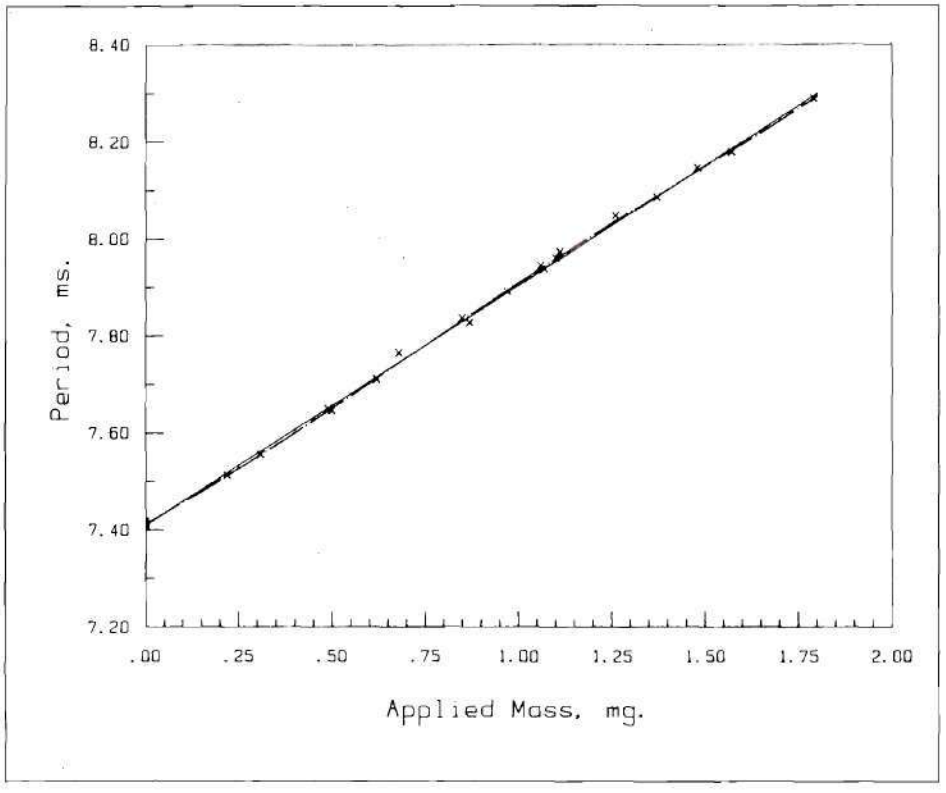

Fig 3-7a. Period of Oscillation vs. Applied Mass.

Representative calibration curves are given in Figs. 3-7a and 3-7b. A straight line, and for comparison a fifth order polynomial have been fit to this data. For all intents and purposes the calibration is linear. With properly designed electronics it could be made exactly linear. This is an important realization. The implication is that no calibration is necessary. Since we are not interested in the absolute mass, but only the relative change - α, the fraction decomposed.

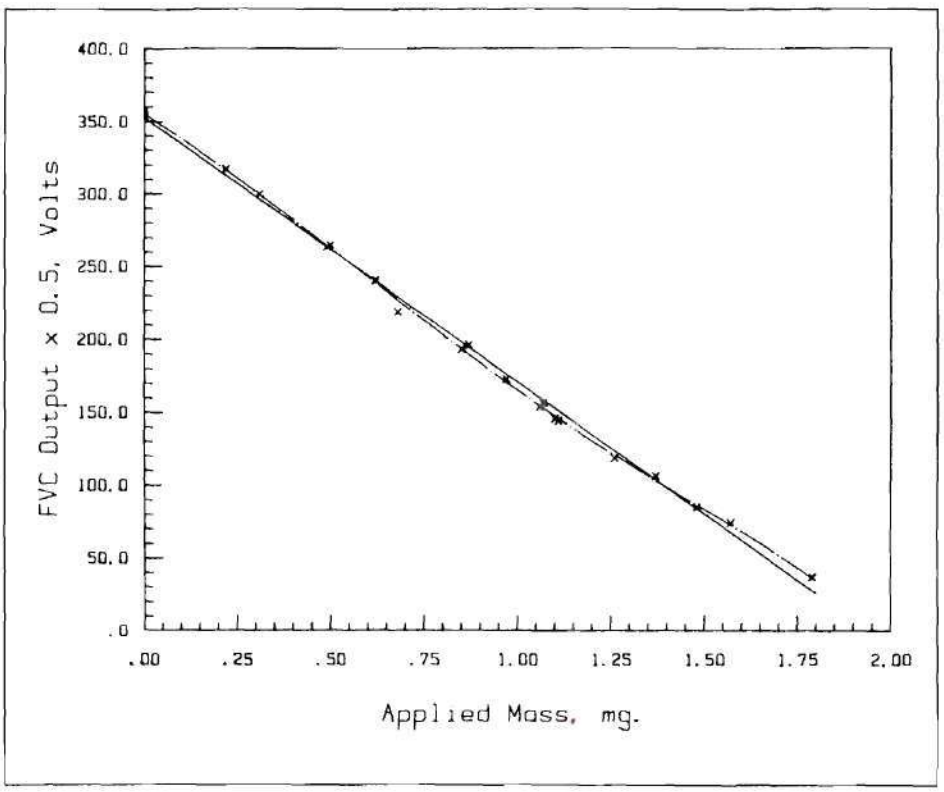

Fig. 3-7b. Amplified FVC Output vs. Mass.

Therefore, the change in period is directly proportional to the change in mass. This simplifies the measurements considerably. If this were not the case, it would be necessary to generate calibration curves for each new tube mounted, as well as curves for various length tubes.

3.3.2 Temperature Calibration

The pyrolysis tube tip contains a type-E thermocouple which has been fashioned according to the procedure outlined in Appendix A. This type of thermocouple was selected due to its large Seebeck coefficient and also because the type-E

materials are ferromagnetic alloys. The output is referenced to a battery powered electronic Type-E "ice-point" or compensator. This provides an output from which temperatures can be interpolated directly from the Type-E thermocouple tables. Interpolation is facilitated through the use of a ninth degree polynomial [48,49] which can accurately interpolate the table to within 0.5 °C. The output is in turn sent to amplifier #4, Fig. 3-4, which has been previously zeroed and configured: DC offset = 0; gain = 10; and bandwidth = 10 Hertz which strips any AC noise. The thermocouple is checked using the linear-furnace which contains an independent type-K thermocouple. This procedure is carried out at several temperatures bracketing the range of interest. This is done mainly to check for shorting of the thermocouple leads. Temperatures are compared at several points spanning the range of interest.

CHAPTER IV

EXPERIMENTAL METHODS AND PROCEDURES

4.1 Low Heating Rate Measurements

A series of pyrolysis measurements were carried out on HTPB and PBAN - polymers which are commonly used as binders in solid propellants. These materials were evaluated on both the TGA and VTGA at low heating rates; this was done, not so much to determine low rate kinetic constants, which may be found in the literature, but mainly to compare the performance of the two techniques. Due to the lack of detailed information on the physical/chemical nature of the polymer samples, it becomes necessary to perform both of these tests on identical samples in order to make a reasonable comparison of the two methods.

4.1.1 Thermogavimetric Analyses

All thermogravimetric analyses were performed on a Perkin-Elmer TGA-2 analyzer equipped with a system 7/4 controller. A diagram of the experimental layout is shown in Fig. 4-1. The main benefit derived from using the System 7/4 controller is that it permits an automatic temperature calibration under the direction of an internal microprocessor. The controller also allows the operator run samples

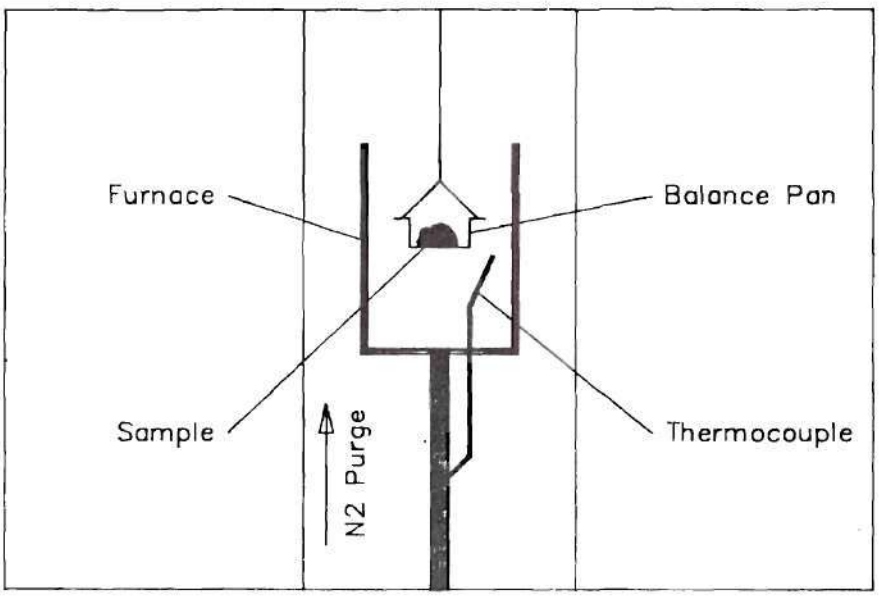

Fig. 4-1 Thermogravimetric Analyzer.

using linear heating programs at rates from 0 to 3.3 °C/s. During automatic calibration, the program temperature and the "apparent temperature" (the measured furnace temperature) are constrained to agree precisely at three predefined temperatures (300 °C, 450 °C and 600 °C were used in this work.) This "apparent temperature" is really the temperature somewhere in the furnace and is not necessarily identical to the temperature in the sample pan. The temperatures in the sample pan were determined using Curie point standards. Small samples of ferromagnetic alloys were placed in the sample pan, the apparatus sealed, and operated under a

Nitrogen purge. A magnet was mounted slightly below furnace/sample pan; the magnetic force on the sample produces an apparent weight increase in the sample. When the furnace temperature approaches the Curie points of the materials in the pan, an apparent weight loss occurs, since at their respective Curie temperatures the materials become paramagnetic. Fig. 4-2 shows the result of this procedure.

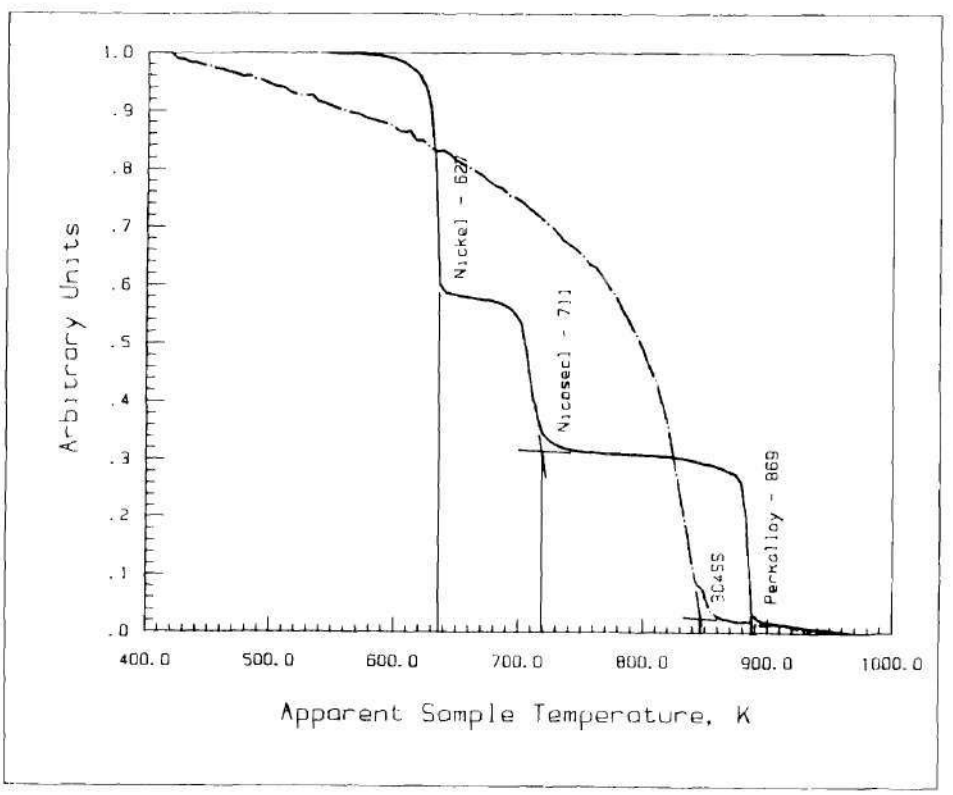

Fig. 4-2. Curie-Point Temperature Calibration Curves

The curve for 304 Stainless Steel, the material in the tips of the VTGA tubes, is also shown, and has a Curie tempera-

ture of 827 °K. This experiment should be repeated for each heating rate of interest, since the discrepancy between the apparent temperature and the true sample temperature becomes greater at higher heating rate. The temperatures in the TGA plots of Chapter V reflect corrections made by this procedure.

The maximum heating rate obtainable with this unit is 3.33 °C/s, but, to guarantee thermal equilibration between the sample, the sample pan, and the furnace, it is best to use heating rates on the order of 0.05 °C/s in practice.

The microbalance was calibrated, using weights of known mass, prior to each set of tests. A digital oscilloscope was used to acquire both mass and temperature data, rather than the usual strip-chart recorder. The mass data-line was amplified one-hundred times to permit good sensitivity for samples sizes of less than one milligram. Acquired data is stored on a floppy disk and is later transferred to microcomputer for analysis.

Two separate TGA analyses were performed on each of the polymers. These differed mainly in the sample preparation. In the first set, sample were cut from the solid polymer; these were "conditioned" in the TGA at 110 °C for several minutes to remove any moisture. Sample sizes were about 1.0 mg. The samples were subjected to a programmed linear temperature rise as is typical in TGA analyses. These results can be compared directly with those found in the

literature. Mindful of the somewhat different sample geometry and environment found in the VTGA apparatus, a second set of tests were performed to facilitate comparison of TGA data with VTGA data. In the VTGA tests, samples dissolved in a solvent, are "painted" on the small pre-oxidized metal strip at the end of the quartz tube; this procedure results in very thin samples. In a similar fashion, samples in the second set of TGA tests, were dissolved in the identical solvent, and coated on the same type of pre-oxidized metal strip. The strip plus the sample were then placed in the TGA pan. The metal strip was included to keep any catalytic effects due to the metal constant. What could not be nullified was the different convective environments to which samples were subjected in the two methods.

The polymeric samples were obtained commercially, the source and the details of which may be found in Appendix A. All test were conducted in a nitrogen atmosphere, and sufficient time was allow for the sample chamber to purge of entrapped air prior to commencing the test.

4.1.2 VTGA Analyses

These tests were performed in the apparatus described in Chapter III. Samples dissolved in appropriate solvents are "painted" on pre-oxidized metal strip. Care is taken to avoid any uneven coatings and to insure sample weight is identical from run-to-run. To determine sample weight, power is applied to the feedback loop, and the period

measured. Run-to-run sample weight is judged to be identical, if after allowing sufficient time for solvent evaporation, the period of oscillation is identical to the previous test. By comparing the periods of oscillation of the "loaded" and "unloaded" quartz tubes with calibration curves, like the one in Fig. 3-7a, estimates of initial sample weights can be made. Sample weights for most VTGA test were under 0.5 mg; the sample thickness is calculated estimated to be approximately 40 μm. This calculation was based upon the measured tip area, which is given in Table 3-1. The linear furnace, which has been preheated to 110 °C, is positioned around the sample and the sample is conditioned until all solvent is removed. This is indicated when the DC-level in the mass data-line (test point C in Fig. 3-6) becomes constant. The furnace mount is equipped with a graduated scale to permit identical positioning of the furnace from test-to-test. The system is "tuned" to achieve the optimum sinusoidal waveform at test point A by adjusting the DC-offset and gain controls on the feedback loop amplifier, amplifier #4. A plexiglass chamber is placed over the apparatus, and the entire enclosure is purged with nitrogen. The nitrogen purge gas is manually cut-off just prior to the onset of sample decomposition to prevent the gas flow from interfering with the measurements. As in the TGA test, the furnace is under linear programmed control by the TGA System 7/4 controller.

At the conclusion of the test the temperature is raised sufficiently, to remove any sample residue which remains, although it is sometimes difficult to remove carbonaceous deposits. This procedure is repeated for subsequent analyses; the same quartz tube and metal sample supports are reused in these tests. These tubes are surprisingly durable and can be reused on numerous samples; with care, thermocouple junction failure normally occurs before mechanical failure of the tube.

4.2 High-Heating-Rate Measurements

The high heating rate measurements used the Fischer Curie point pyrolyzer to rapidly heat the metal support on which the samples were coated. Procedures in these measurements were identical to those in the low rate VTGA tests except with regard to sample heating and the time required for solvent removal from the sample. Very little control over the heating rate was possible with the Curie point pyrolyzer used in this work. This is the principal drawback to the present instrument design. The heating rate is a strong function of the position of the induction coil with respect to the sample and it is not possible to precisely predict the actual value *a priori*. The coil used in this work was larger than the one supplied by the instrument manufacturer; the ID of the redesigned coil was 0.50 inches. This had more room for tube vibration. Heating rates

obtained with this device varied form about 30 °C/s to about 60 °C/s. Figure 4-2 contains an oscillograph showing both the mass and temperature data.

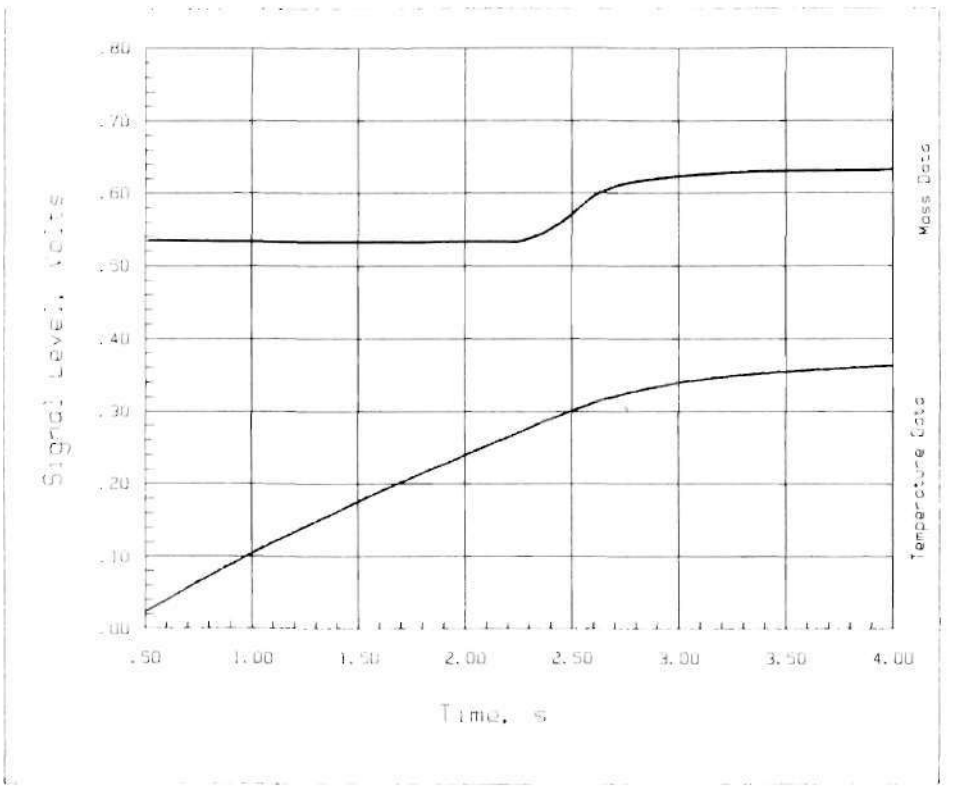

Fig. 4-3 High-Heating-Rate VTGA Output.

As can be seen, sample decomposition takes place near the Curie temperature of the 304SS; the sample was positioned by trial-and-error with respect to the induction coil in an attempt to avoid decomposition in the non-linear region near the Curie temperature. This was a laborious process.

Unfortunately, the Curie point pyrolyzers which are

commercially available have been designed to be used in connection with Gas Chromatography; they offer no way to "throttle" the heating rate, and pyrolysis time is limited to about 9 seconds. In addition, the only tube material readily available for construction of the "heating element" was 304SS steel, thus limiting the ultimate temperature which could be attained. These constraints all combined to seriously limit control over heating rates. In future work these constraints could be designed out of the system.

4.3 Data Analysis Procedures

4.3.1 TGA Data Analysis. Mass and temperature data acquired on the Oscilloscope is transferred to the microcomputer using Program 1, Appendix B; it is stored on disk in the form of Voltage vs. time in two separate files. This data is consolidated and scaled using Program 2. Program 4 reduces this scaled data by the algorithm outlined in Chapter II. Arrhenius parameters are extracted from this data by application of Program 5.

4.3.2 VTGA Data Analysis The Data analysis procedures used here are identical to those used in analyzing the TGA experiments, with the exception that raw data files are consolidated using Program 3, Appendix B, in place of Program 2, due to the different data scaling required in the TGA and VTGA data. A thermogram from such an analysis of HTPB is shown in Fig. 4-4. This figure contains four

separate decomposition curves run under identical conditions; precision is seen to be excellent.

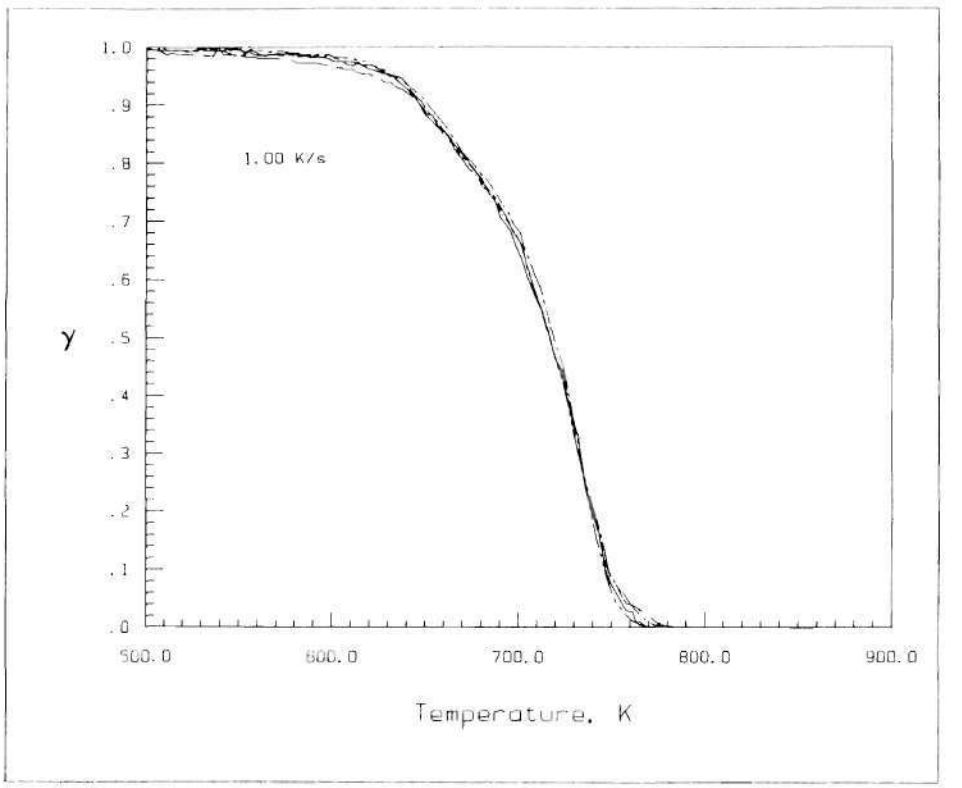

Fig. 4-4 Low-Heating-Rate VTGA Thermogram of HTPB

CHAPTER V

RESULTS AND DISCUSSION

5.1 Baseline Data

In order to obtain baseline data and to test the computational algorithms, the decomposition kinetics of PBAN and HTPB were measured in the TGA and computed. Thermograms for PBAN and HTPB are shown in Figures 5-1a and 5-1b, respectively, and the calculated kinetic parameters are given in Tables 5-1a and 5-1b. Global Arrhenius parameters for these polymers have been computed for $0.10 \leq \alpha \leq 0.30$; Arrhenius parameters have also been computed for $0.10 \leq \alpha \leq 0.90$ to facilitate comparison of the data with the literature. The thermograms shown in these figures are for heating rates varying from 0.05 °K/s to 3.3 °K/s (3 °K/min. to 200 °K/min.) as is indicated in the upper left-hand corner of each figure.

Several observations can be made concerning this data. Firstly, as usual, the decomposition shifts to higher temperatures as the heating rates are increased. (See Eqn. 2-4). Secondly, this shift is proportionally less at higher heating rates. For example, the difference in heating rate between curves a and b in both of these figures is 0.033

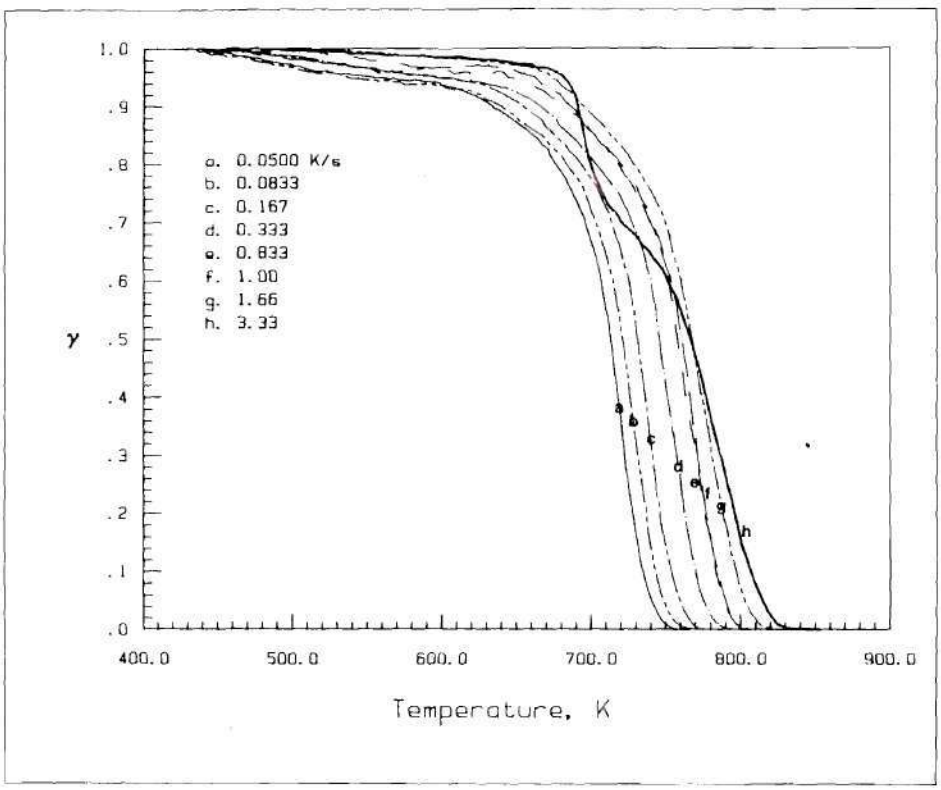

Fig. 5-1a. TGA Thermograms of PBAN - Bulk Sample.

°C/s, whereas, the difference in heating rate between curves g and h is around 1.67 °C/s. - over fifty times greater. Yet the shift in temperature is about the same. Thirdly, precision of the data appears to be quite good, and corresponding kinetic values in Tables 5-1a and 5-1b are in reasonable agreement with values from the literature, Table 5-1c, making some allowance for the expected polymer-to-polymer variability. Lastly, at heating rates of 3.33 °C/s, the bold lines in Figs. 5-1a and 5-1b, both PBAN and HTPB exhibit anomalies which could be interpreted as evidence of two

Table 5-1a. TGA Kinetic Results for PBAN - Bulk Sample

Ea : cal/mole
A : sec-1
β : °K/s
T : °K

Item	ID	Material	Ea	A	n	β	$\alpha_o - \alpha_f$	T Range	Analysis	Source
							0.1≤α≤0.3			
1	240186-10	PBAN	11875	1.175E+0	0	0.0500	0.083-0.28	623-694	CR	TGA
2	240186-09	PBAN	11269	1.096E+0	0	0.0833	0.081-0.28	626-701	CR	TGA
3	240186-08	PBAN	13556	1.141E+1	0	0.1667	0.082-0.28	643-711	CR	TGA
4	240186-11	PBAN	13932	2.547E+1	0	0.3333	0.081-0.30	653-723	CR	TGA
5	240186-03	PBAN	17499	7.268E+1	0	0.8333	0.091-0.29	682-738	CR	TGA
6	240186-02	PBAN	15235	1.568E+2	0	1.0000	0.085-0.29	673-739	CR	TGA
7	240186-05	PBAN	17719	1.392E+3	0	1.6667	0.084-0.29	689-749	CR	TGA
8	240186-07	PBAN	-	-	-	3.3333	-		-	-
							0.1≤α≤0.3			
9	240186-10	PBAN	16545	5.629E+1	0	0.0500	0.083-0.88	623-733	CR	TGA
10	240186-09	PBAN	15969	5.269E+1	0	0.0833	0.081-0.89	626-743	CR	TGA
11	240186-08	PBAN	17715	3.231E+2	0	0.1667	0.082-0.86	643-750	CR	TGA
12	240186-11	PBAN	17309	2.547E+1	0	0.3333	0.081-0.86	653-766	CR	TGA
13	240186-03	PBAN	20174	5.507E+3	0	0.8333	0.091-0.86	682-781	CR	TGA
14	240186-02	PBAN	19473	4.041E+3	0	1.0000	0.085-0.86	673-789	CR	TGA
15	240186-05	PBAN	21225	1.926E+4	0	1.6667	0.084-0.29	689-794	CR	TGA
16	240186-07	PBAN	-	-	-	3.3333	-		-	-

competing chemical processes, which only become distinct at the higher heating rates. This would perhaps be more apparent if the derivative of these curve were shown.

Closer scrutiny suggests that the anomalies in the higher heating rate curves are in reality physical processes related to the geometry of the sample - most probably due to entrapment and escape of decomposition products or low

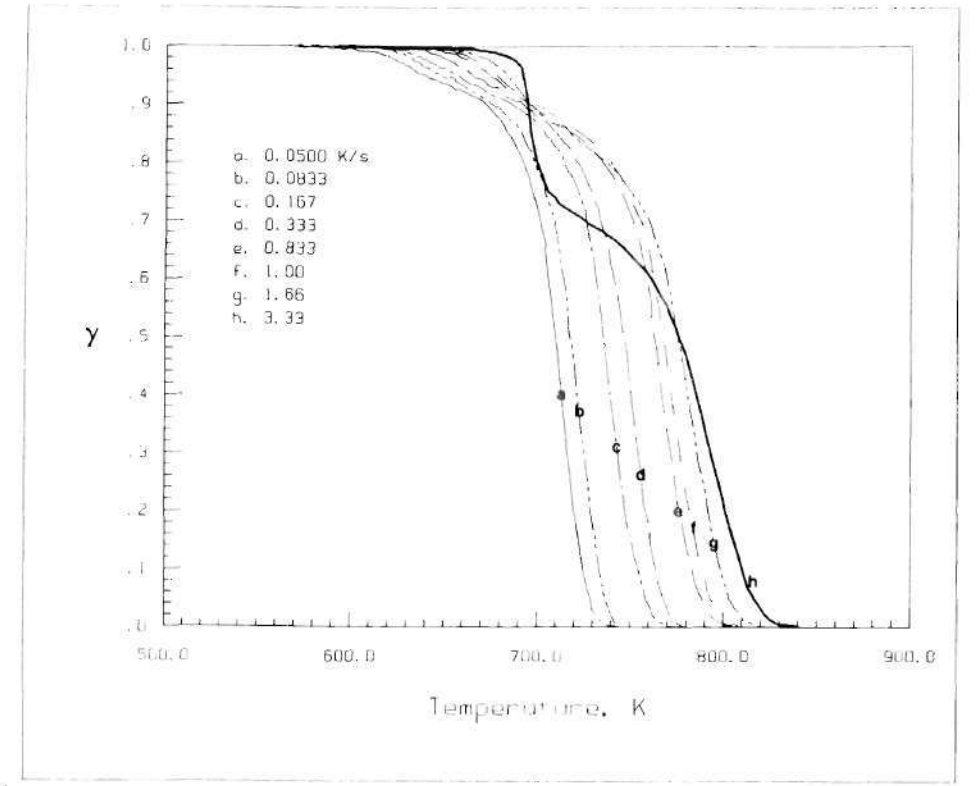

Fig. 5-1b. TGA Thermograms of HTPB - Bulk Sample.

molecular weight material in the interior of the sample. This conclusion was arrived at by repeating these test with samples in the form of thin films.

Figures 5-2a and 5-2b contain this data. The samples were deposited on small strips of pre-oxidized stainless steel in similar fashion to the VTGA sample preparation described in Chapter IV. This procedure also facilitates the comparison of the TGA data with the VTGA data. The corresponding kinetic data for these curves may be found in Tables 5-2a and 5-2b. It can be seen that no such anomalies

Table 5-1b. TGA Kinetic Results for HTPB - Bulk Sample

Ea : cal/mole
A : sec-1
β : °K-sec-1
T : °K

Item	ID	Material	Ea	A	n	β	$\alpha_o - \alpha_f$	T Range	Analysis	Source
							0.1≤α≤0.3			
1	290186-09	HTPB	32188	5.534E+6	0	0.0500	0.10 -0.28	672-700	CR	TGA
2	290186-08	HTPB	29657	1.093E+6	0	0.0833	0.10 -0.30	675-708	CR	TGA
3	290186-06	HTPB	23729	1.649E+4	0	0.1667	0.10 -0.28	687-725	CR	TGA
4	290186-01	HTPB	21938	7.432E+3	0	0.3333	0.10 -0.28	692-732	CR	TGA
5	290186-02	HTPB	16102	1.952E+2	0	0.8333	0.10 -0.29	696-750	CR	TGA
6	290186-03	HTPB	16328	2.571E+2	0	1.0000	0.10 -0.29	698-753	CR	TGA
7	290186-04	HTPB	13624	4.891E+1	0	1.6667	0.10 -0.30	697-759	CR	TGA
8	290186-05	HTPB	-	-	-	3.3333	-	-	-	-
							0.1≤α≤0.3			
9	290186-09	HTPB	40770	3.794E+9	0	0.0500	0.10 -0.87	672-723	CR	TGA
10	290186-08	HTPB	37584	4.437E+8	0	0.0833	0.10 -0.87	675-732	CR	TGA
11	290186-06	HTPB	33732	2.908E+7	0	0.1667	0.10 -0.88	687-752	CR	TGA
12	290186-01	HTPB	30354	3.889E+6	0	0.3333	0.10 -0.89	692-763	CR	TGA
13	290186-02	HTPB	24851	1.289E+5	0	0.8333	0.10 -0.89	696-782	CR	TGA
14	290186-03	HTPB	24749	1.2974+3	0	1.0000	0.10 -0.90	698-788	CR	TGA
15	290186-04	HTPB	19845	6.273E+3	0	1.6667	0.10 -0.87	697-796	CR	TGA
16	290186-05	HTPB	-	-	-	3.3333	-		-	-

exist in the thin film data! This suggests that this phenomenon is a function of sample geometry; most probably, at higher heating rates, trapped vapors in the interior of the sample can not diffuse to the surface with sufficient rapidity. Gases apparently escape all at once when the pressure within the sample rises to a sufficient level. The rate of decomposition becomes diffusion limited, at least in

Table 5-1c. Literature Values of Kinetic Constants

Ea : cal/mole
A : sec-1
β : °K-sec-1
T : °K

Item	ID	Material	Ea	A	n	β	αo - αf	T Range	Analysis	Source
1	-	HTPB	23228	3.85E+3	0	0.0167	0 - 1	-	CR	TGA[50,Tbl 5]
2	-	HTPB	26775	8.22E+4	0	0.0333	0 - 1	-	CR	TGA[50,Tbl 5]
3	-	HTPB	26132	9.11E+4	0	0.0833	0 - 1	-	CR	TGA[50,Tbl 5]
4	-	HTPB	28917	1.03E+6	0	0.1667	0 - 1	-	CR	TGA[50,Tbl 5]
5	-	HTPB	25632	1.39E+5	0	0.3333	0 - 1	-	CR	TGA[50,Tbl 5]
6	-	HTPB	22419	2.54E+4	0	0.8333	0 - 1	-	CR	TGA[50,Tbl 5]
7	-	HTPB	19516	7.44E+3	0	1.6667	0 - 1	-	CR	TGA[50,Tbl 5]
8	-	CTPB	28000	3.4 E+5			0 - 1	-		DSC[52,Tbl 1]

the early stages. Thus the TGA is unable to adequately represent the thermal decomposition kinetics of these polymers even at rates as low as 3.33 °C/s when a bulk sample is employed.

It can also be seen that the decomposition temperatures of the samples in these figures and those in figures 5-1a and b are virtually identical. It should be mentioned in passing that it is doubtful if the temperature of the sample and the furnace are in equilibrium at heating rates much above 0.5 °C/s. This is why, in the most accurate work, TGA analyses are normally run at heating rates below this value.

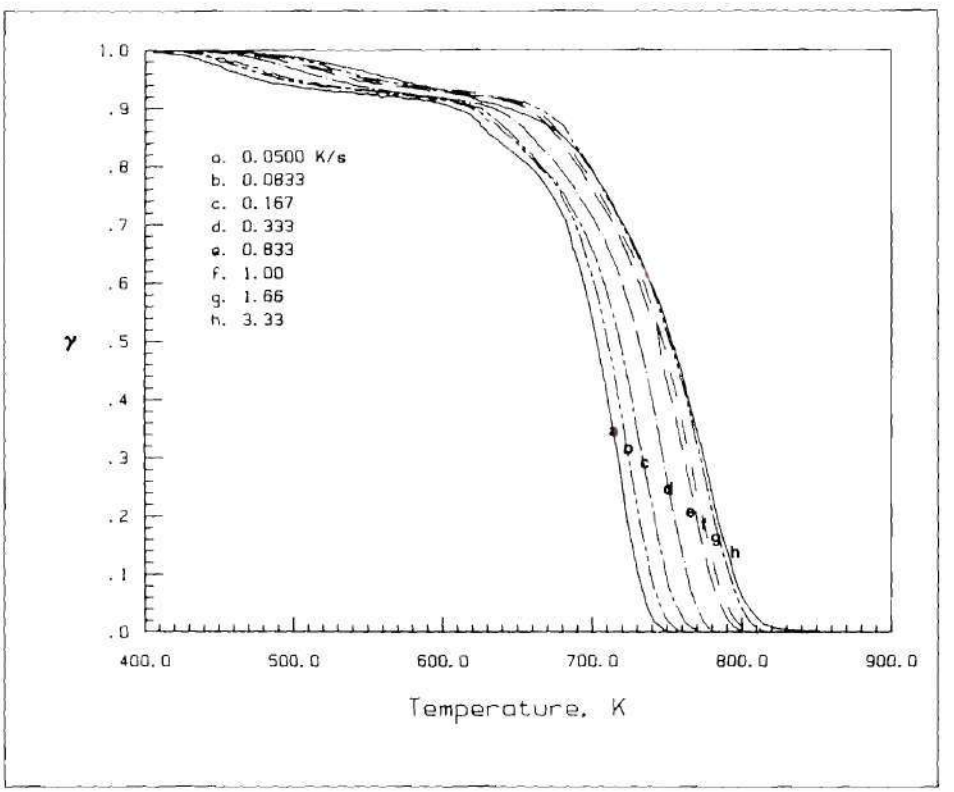

Fig. 5-2a. TGA Thermograms PBAN - Thin Films.

Table 5-2a. TGA Kinetic Results for PBAN - Thin Film.

Ea : cal/mole
A : sec-1
β : °K-sec-1
T : °K

Item	ID	Material	Ea	A	n	β	$\alpha_o - \alpha_f$	T Range	Analysis	Source
							0.1≤α≤0.3			
1	160186-10	PBAN	9087	1.613E-1	0	0.0500	0.10 -0.29	608-682	CR	TGA
2	160186-09	PBAN	10026	5.242E-1	0	0.0833	0.10 -0.29	619-686	CR	TGA
3	160186-08	PBAN	11062	2.385E+0	0	0.1667	0.10 -0.30	622-692	CR	TGA
4	160186-11	PBAN	11535	5.927E+0	0	0.3333	0.10 -0.29	632-700	CR	TGA
5	160186-03	PBAN	15412	2.488E+2	0	0.8333	0.10 -0.29	657-711	CR	TGA
6	160186-02	PBAN	15911	4.159E+2	0	1.0000	0.10 -0.29	660-714	CR	TGA
7	160186-01	PBAN	15709	3.522E+2	0	1.0000	0.10 -0.29	661-715	CR	TGA
8	160186-05	PBAN	16397	9.219E+2	0	1.6667	0.10 -0.29	662-717	CR	TGA
9	160186-07	PBAN	17009	3.522E+2	0	3.3333	0.10 -0.29	642-718	-	-
							0.1≤α≤0.9			
10	160186-10	PBAN	13060	4.802E+0	0	0.0500	0.10 -0.90	608-730	CR	TGA
11	160186-09	PBAN	13957	1.429E+1	0	0.0833	0.10 -0.90	619-739	CR	TGA
12	160186-08	PBAN	13326	1.593E+1	0	0.1667	0.10 -0.88	622-748	CR	TGA
13	160186-11	PBAN	13552	3.132E+1	0	0.3333	0.10 -0.86	632-763	CR	TGA
14	160186-03	PBAN	15359	2.419E+2	0	0.8333	0.10 -0.86	657-775	CR	TGA
15	160186-02	PBAN	15462	2.972E+2	0	1.0000	0.10 -0.89	660-782	CR	TGA
16	160186-01	PBAN	15674	3.481E+2	0	1.0000	0.10 -0.86	661-778	CR	TGA
17	160186-05	PBAN	15419	4.392E+2	0	1.6667	0.10 -0.87	662-788	CR	TGA
18	160186-07	PBAN	16132	1.178E+2	0	3.3333	0.10 -0.87	642-792	-	-

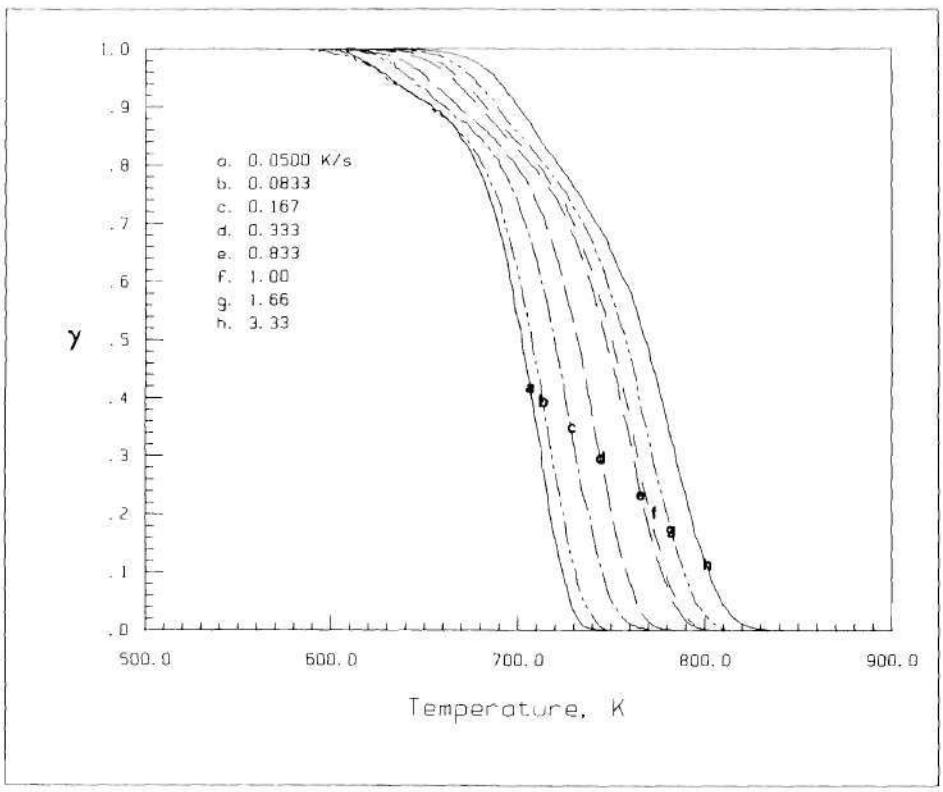

Fig. 5-2b. TGA Thermograms HTPB - Thin Films.

Table 5-2b. TGA Kinetic Results for HTPB - Thin Film.

Ea : cal/mole
A : sec-1
β : °K-sec-1
T : °K

Item	ID	Material	Ea	A	n	β	$\alpha_o - \alpha_f$	T Range	Analysis	Source
							$0.1 \leq \alpha \leq 0.3$			
1	310186-02	HTPB	25418	4.919E+4	0	0.0500	0.10 -0.29	654-688	CR	TGA
2	310186-03	HTPB	20902	2.257E+3	0	0.0833	0.11 -0.29	654-692	CR	TGA
3	310186-01	HTPB	19474	1.1937+3	0	0.1667	0.10 -0.29	661-702	CR	TGA
4	310186-04	HTPB	18313	8.073E+2	0	0.3333	0.10 -0.29	669-714	CR	TGA
5	310186-05	HTPB	18196	1.511E+3	0	0.8333	0.10 -0.29	679-726	CR	TGA
6	310186-07	HTPB	18627	2.356E+3	0	1.0000	0.10 -0.29	683-728	CR	TGA
7	310186-09	HTPB	19773	8.408E+3	0	1.6667	0.10 -0.30	689-734	CR	TGA
8	310186-10	HTPB	23117	1.643E+5	0	3.3333	0.10 -0.30	700-741	CR	TGA
							$0.1 \leq \alpha \leq 0.3$			
9	310186-02	HTPB	29385	1.116E+6	0	0.0500	0.10 -0.88	654-722	CR	TGA
10	310186-03	HTPB	26164	1.437E+5	0	0.0833	0.11 -0.90	654-731	CR	TGA
11	310186-01	HTPB	24361	5.452E+4	0	0.1667	0.10 -0.90	661-744	CR	TGA
12	310186-04	HTPB	22820	2.634E+4	0	0.3333	0.10 -0.89	669-757	CR	TGA
13	310186-05	HTPB	20715	1.037E+4	0	0.8333	0.10 -0.90	679-777	CR	TGA
14	310186-07	HTPB	21125	1.573E+4	0	1.0000	0.10 -0.88	683-778	CR	TGA
15	310186-09	HTPB	20428	1.385E+4	0	1.6667	0.10 -0.89	689-787	CR	TGA
16	310186-10	HTPB	20051	1.725E+4	-	3.3333	0.10 -0.90	700-802	CR	TGA

5.2 Low-Heating-Rate VTGA Data

In order to demonstrate that the VTGA was a functional thermogravimetric analyzer, a series of thermal decompositions experiments were performed on PBAN and HTPB at low heating rates; in this work every effort was expended to insure that conditions matched those found in the previous thin-film TGA experiments.

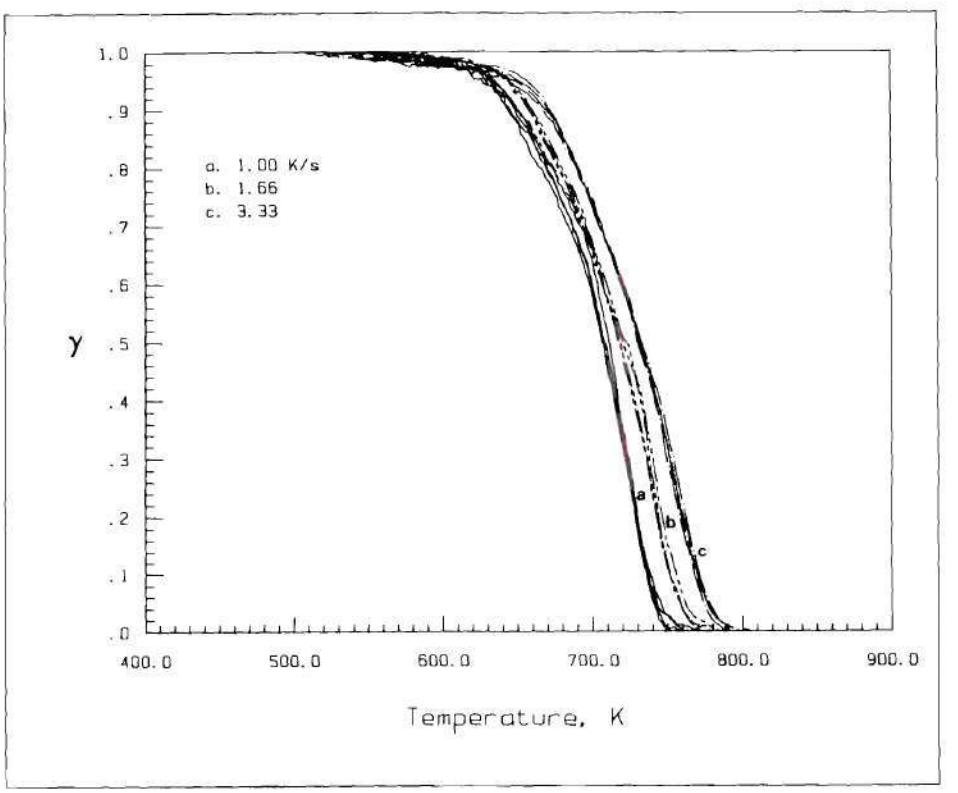

Fig. 5-3a. VTGA Thermograms of PBAN

It must be recognized that low-heating-rate VTGA experiments are similar to, but not identical with, the thin-film TGA tests. Samples in the VTGA are subjected to a

much different convective environment during sample pyrolysis. Data from these experiments is presented in Figs. 5-3a and 5-3b and the corresponding Arrhenius data may be found in Tables 5-3a and 5-3b.

In this low-heating-rate VTGA work, four decomposition experiments were run at each of three heating rates. The curves have the same overall appearance as those found in Figures 5-2 and display the same dependence upon heating rate as found in the earlier TGA work. The precision in these VTGA curves is excellent! Note, however, that the temperature range over which the decompositions occur, at any heating rate, is about 20 °C lower than found in the corresponding TGA data. This was found to be the case in all VTGA experiments in this work. It is believed that this is the result of the different convective environments in the two experiments.

Both PBAN and HTPB polymers decompose <u>via</u> a random depolymerization mechanism, producing products which are both liquids and gases. Providing of course that the decomposition is not diffusion limited, gases formed upon decomposition immediate leave the sample, and consequently produce an immediately weight loss. However, this is not necessarily the case with liquids. Liquids formed during decomposition in the TGA can remain on the sample or in the sample pan and evaporate at some later time.

Table 5-3a. VTGA Kinetic Results for PBAN - Low Rate.

Ea : cal/mole
A : sec-1
ß : °K-sec-1
T : °K

Item	ID	Material	Ea	A	n	ß	$\alpha_o - \alpha_f$	T Range	Analysis	Source
							$0.1 \leq \alpha \leq 0.3$			
1	130286-01	PBAN	19994	1.714E+4	0	1.0000	0.10 -0.29	646-686	CR	TGA
2	130286-02	PBAN	20740	2.825E+4	0	1.0000	0.10 -0.30	650-692	CR	TGA
3	130286-03	PBAN	20928	3.971E+4	0	1.0000	0.10 -0.29	644-682	CR	TGA
4	130286-04	PBAN	21966	8.128E+4	0	1.0000	0.10 -0.30	650-687	CR	TGA
5	130286-05	PBAN	23639	4.035E+5	0	1.6667	0.10 -0.30	658-693	CR	TGA
6	130286-06	PBAN	23732	3.999E+5	0	1.6667	0.10 -0.29	662-695	CR	TGA
7	130286-07	PBAN	24410	7.105E+5	0	1.6667	0.10 -0.29	660-693	CR	TGA
8	130286-08	PBAN	20704	4.384E+4	0	1.6667	0.10 -0.29	652-691	CR	TGA
9	130286-09	PBAN	25875	3.106E+6	0	3.3333	0.10 -0.29	669-706	CR	TGA
10	130286-10	PBAN	26704	5.730E+6	0	3.3333	0.10 -0.30	674-706	CR	TGA
11	130286-11	PBAN	26424	4.762E+6	0	3.3333	0.11 -0.29	673-701	CR	TGA
12	130286-12	PBAN	24705	1.322E+6	0	3.3333	0.10 -0.29	668-701	CR	TGA
							$0.1 \leq \alpha \leq 0.9$			
13	130286-01	PBAN	20239	2.103E+4	0	1.0000	0.10 -0.89	636-735	CR	TGA
14	130286-02	PBAN	21263	4.273E+4	0	1.0000	0.10 -0.89	650-735	CR	TGA
15	130286-03	PBAN	18750	6.967E+3	0	1.0000	0.10 -0.89	644-737	CR	TGA
16	130286-04	PBAN	20123	1.892E+4	0	1.0000	0.10 -0.89	650-736	CR	TGA
17	130286-05	PBAN	19353	1.424E+4	0	1.6667	0.10 -0.88	658-749	CR	TGA
18	130286-06	PBAN	19029	1.039E+4	0	1.6667	0.10 -0.89	662-755	CR	TGA
19	130286-07	PBAN	19826	2.000E+4	0	1.6667	0.10 -0.89	660-750	CR	TGA
20	130286-08	PBAN	17362	3.165E+3	0	1.6667	0.10 -0.88	669-768	CR	TGA
12	130286-09	PBAN	19240	1.926E+4	0	3.3333	0.10 -0.88	669-768	CR	TGA
22	130286-10	PBAN	18487	1.083E+4	0	3.3333	0.11 -0.88	674-769	CR	TGA
23	130286-11	PBAN	18557	1.168E+4	0	3.3333	0.11 -0.89	673-769	CR	TGA
24	130286-12	PBAN	19069	1.781E+4	0	3.3333	0.10 -0.87	668-765	CR	TGA

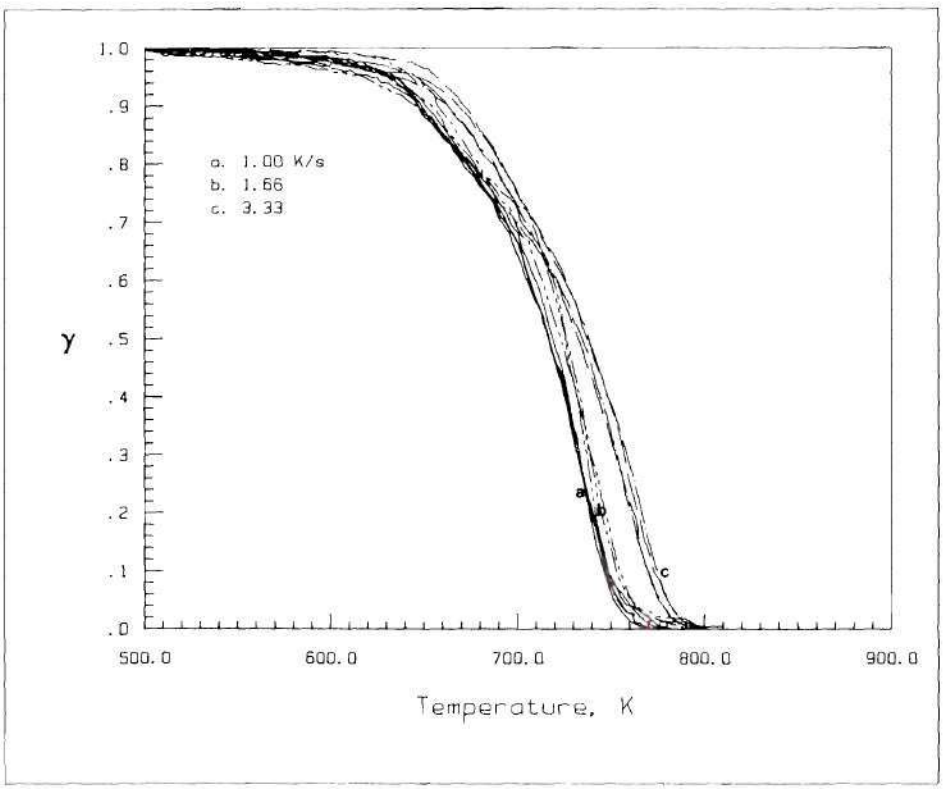

Fig. 5-3b. VTGA Thermograms of HTPB.

Table 5-3b. VTGA Kinetic Results for HTPB - Deposited on 304SS from Toluene

Ea : cal/mole
A : sec-1
β : °K-sec-1
T : °K

Item	ID	Material	Ea	A	n	β	$\alpha_o - \alpha_f$	T Range	Analysis	Source
							0.1≤α≤ 0.3			
1	090286-13	HTPB	18510	4.887E+3	0	1.0000	0.10 -0.30	647-690	CR	VTGA
2	090286-14	HTPB	17703	2.560E+3	0	1.0000	0.11 -0.29	650-692	CR	VTGA
3	090286-15	HTPB	18442	4.342E+3	0	1.0000	0.10 -0.29	652-694	CR	VTGA
4	090286-16	HTPB	17109	1.651E+3	0	1.0000	0.11 -0.29	648-691	CR	VTGA
5	090286-01	HTPB	16901	2.487E+3	0	1.6667	0.10 -0.30	642-690	CR	VTGA
6	090286-02	HTPB	20815	4.822E+4	0	1.6667	0.10 -0.30	650-693	CR	VTGA
7	090286-03	HTPB	18153	6.405E+3	0	1.6667	0.10 -0.30	643-689	CR	VTGA
8	090286-04	HTPB	18337	8.919E+3	0	1.6667	0.10 -0.30	638-683	CR	VTGA
9	090286-05	HTPB	17741	7.340E+3	0	3.3333	0.10 -0.29	652-700	CR	VTGA
10	090286-06	HTPB	18178	1.032E+4	0	3.3333	0.11 -0.28	654-697	CR	VTGA
11	090286-07	HTPB	15573	1.445E+3	0	3.3333	0.10 -0.29	646-698	CR	VTGA
12	090286-08	HTPB	22254	2.263E+5	0	3.3333	0.10 -0.29	662-699	CR	VTGA
							0.1≤α≤0.9			
13	090286-13	HTPB	17922	3.092E+3	0	1.0000	0.10 -0.87	647-744	CR	VTGA
14	090286-14	HTPB	18025	3.333E+3	0	1.0000	0.11 -0.90	650-745	CR	VTGA
15	090286-15	HTPB	18371	4.127E+3	0	1.0000	0.10 -0.87	652-746	CR	VTGA
16	090286-16	HTPB	17198	1.784E+3	0	1.0000	0.11 -0.89	648-746	CR	VTGA
17	090286-01	HTPB	16271	1.511E+3	0	1.6667	0.10 -0.89	642-747	CR	VTGA
18	090286-02	HTPB	17507	3.512E+3	0	1.6667	0.10 -0.88	650-752	CR	VTGA
19	090286-03	HTPB	16060	1.209E+3	0	1.6667	0.10 -0.90	643-754	CR	VTGA
20	090286-04	HTPB	15883	1.207E+3	0	1.6667	0.10 -0.89	638-747	CR	VTGA
12	090286-05	HTPB	15020	8.676E+2	0	3.3333	0.10 -0.89	652-773	CR	VTGA
22	090286-06	HTPB	15716	1.524E+3	0	3.3333	0.11 -0.90	654-770	CR	VTGA
23	090286-07	HTPB	13834	3.663E+2	0	3.3333	0.11 -0.87	646-770	CR	VTGA
24	090286-08	HTPB	15864	1.570E+3	0	3.3333	0.10 -0.88	662-772	CR	VTGA

Thus even though the sample has decomposed, there is no apparent weight loss until the sample is at a higher temperature. In addition, liquids formed can condense on cooler parts of the apparatus and obscure the results; this was actually observed in the decomposition of these polymers, particularly with PBAN. In the VTGA, on the other hand, liquids formed during decomposition would vaporize much more readily, due the much greater convective environment in which the sample pyrolyzes.

In Table 5-3a are the calculated Arrhenius parameters for PBAN obtained with the VTGA. This data shows fair agreement with that obtained in the thin-film TGA work. Global energies of activation are slightly higher than in the TGA work, this may illustrate that evaporation is a significant factor in the TGA decomposition of PBAN. Results for HTPB, Table 5-3b, are in excellent agreement with the thin-film TGA work. Global energies of activation are graphically presented in Figures 5-4a and 5-5b for both the low-heating-rate TGA and VTGA work; data points for the VTGA results in these figures represent the average of four distinct experiments.

Given the precision in the VTGA curves and the ability to measure reasonable values of Arrhenius parameters for these polymers, the claim is made that this device is indeed a functioning thermogravimetric analyzer possessing some distinct advantages over the conventional methods. These

advantages include: small sample size, ≈0.5 mg; samples are thin films in contact with a good heat sink, minimizing thermal irregularities with in the sample; sample temperatures are measured directly; condensation on the cooler parts of the instrument would not significantly affect results; results are independent of buoyancy and vapor pressure effects in the sample pan, and elevated heating rates are possible.

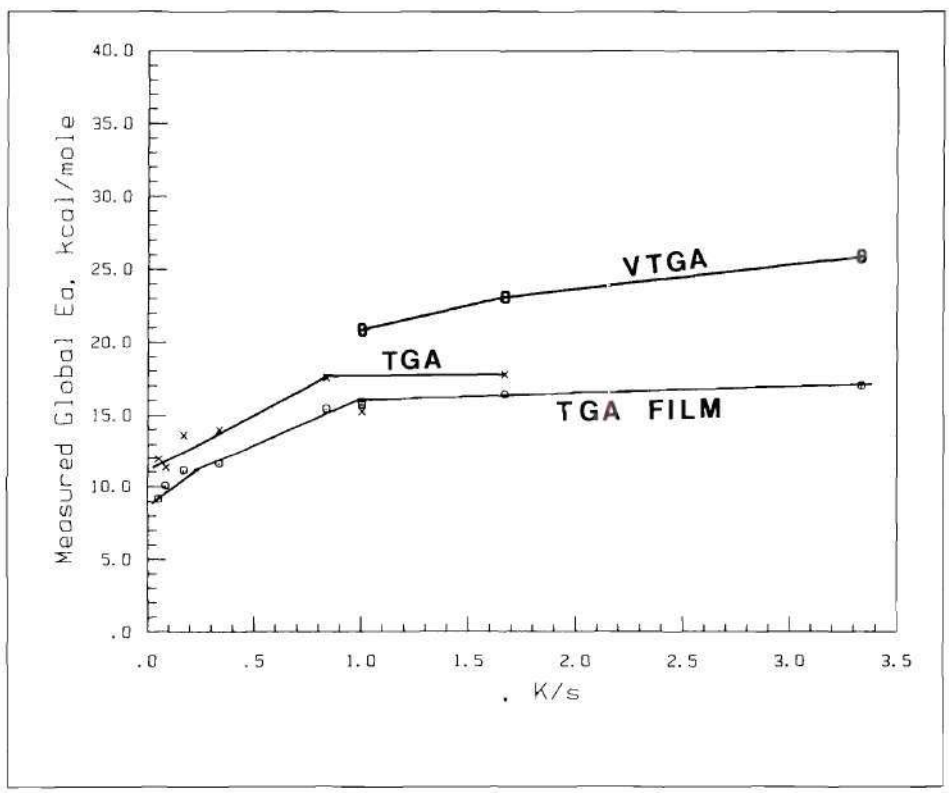

Fig. 5-4a. Low-Heating-Rate Global Ea's for PBAN.

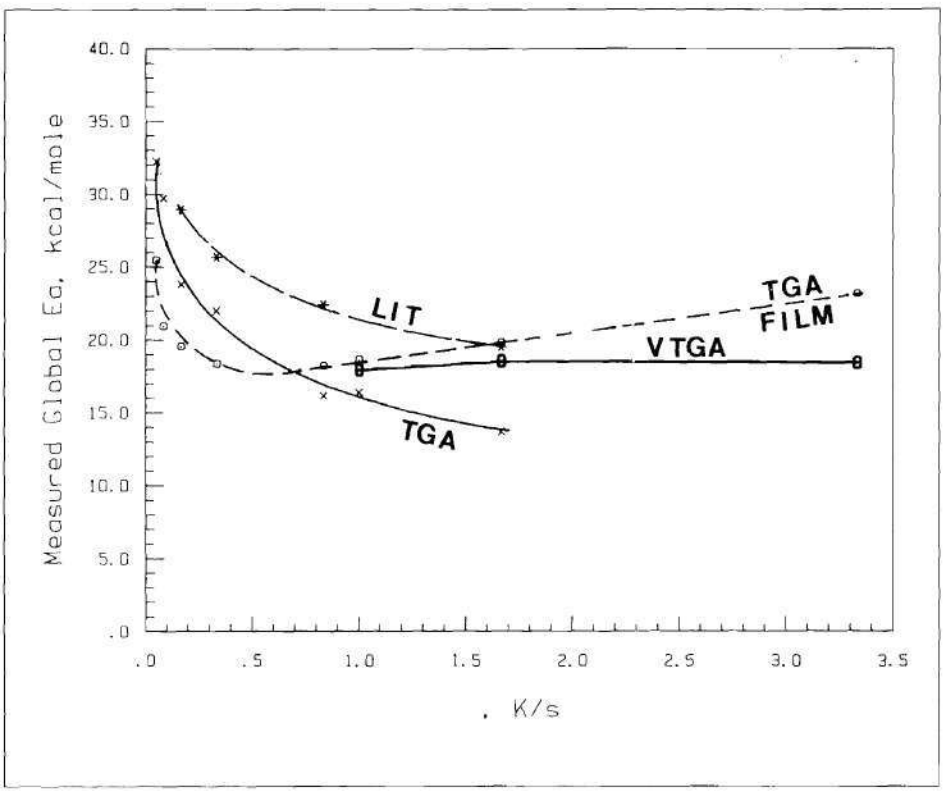

Fig. 5-4b. Low-Heating-Rate Global Ea's for HTPB.

5.3 High-Heating-Rate Results

5.3.1 PBAN

A series of pyrolysis experiments were conducted on PBAN at increased heating rates. Heating rates varied from around 20 °K/s to 60 °K/s. It is worth mentioning again that very little control over the heating rate was possible with the induction heating unit used in this work, and the upper temperature limit was restricted to values below about

830 °K. The upper bound on the temperature was mainly imposed by the availability of materials for heating element fabrication. (The only available ferromagnetic fine gauge tubing available at the time was 304 stainless steel.)

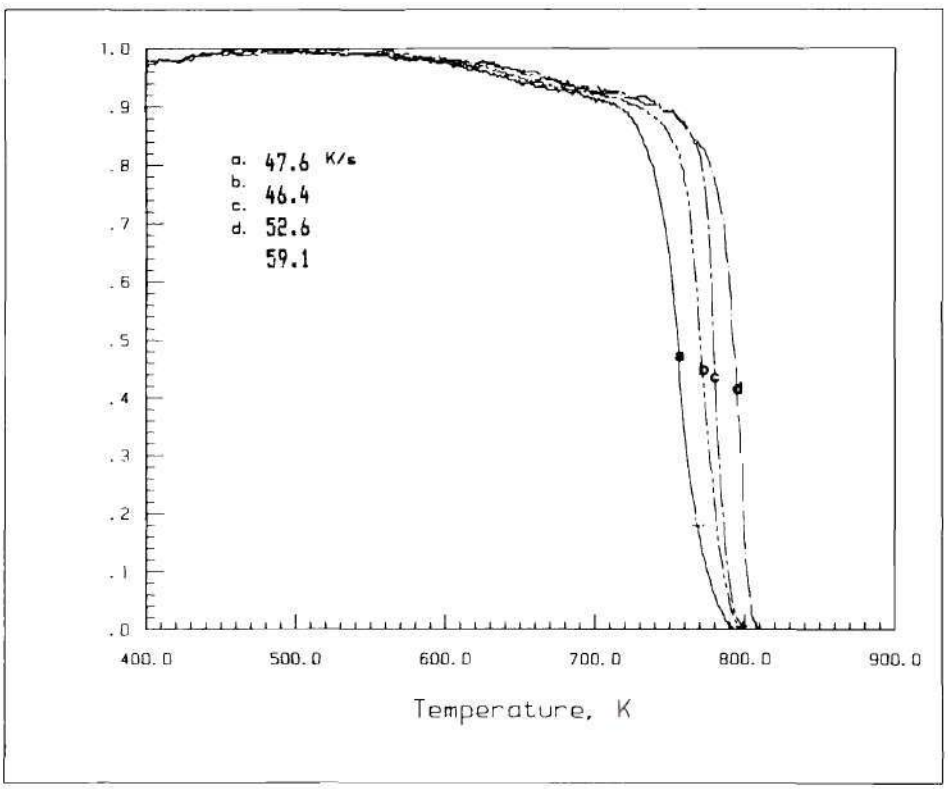

Fig. 5-5. VTGA Thermograms of PBAN - High-Heating-Rate.

Figure 5-5 contains typical results for the decomposition of PBAN. Sample sizes were between 0.25 mg and 0.50 mg which of course were applied as a thin film to both sides of the strip - about 0.125 mg to 0.25 mg per side. Heating rates are over an order of magnitude greater than those presented in the previous section.

Comparing the data in this figure with that of Figs. 5-2a and 5-3a, several differences are apparent. The temperature range of the decomposition has shifted to slightly higher values, and this range has become narrower. This implies a higher rate of decomposition as can be seen by the steepness of the curves. This translation to higher

Table 5-4. VTGA Kinetic Results for PBAN - High Rate.

Ea : cal/mole
A : sec-1
β : °K-sec-1
T : °K

Item	ID	Material	Ea	A	n	β	αo - αf	T Range	Analysis	Source
							0.1≤α≤ 0.3			
1	190286-10	PBAN	33366	2.457E+9	0	47.6	0.10 -0.29	714-745	CR	VTGA
2	190286-09	PBAN	26496	1.055E+7	0	46.4	0.10 -0.30	728-763	CR	VTGA
3	190286-13	PBAN	25013	3.040E+6	0	52.6	0.10 -0.29	740-775	CR	VTGA
4	190286-11	PBAN	24072	9.447E+6	0	59.1	0.10 -0.28	743-784	CR	VTGA

temperatures is more pronounced in the early stages of the pyrolysis, and pyrolysis at these higher heating rates occurs over a much narrower temperature range. The kinetic constants for PBAN are presented in Table 5-4. The global Ea's for PBAN presented in the previous section were about 25 kcal/mole with A's of about 10^{15}; the values presented in

Table 5-5 are for all intents and purposes the same. This coupled with the similar shaped pyrolysis curves would suggest that about the same physical/chemical processes are occurring at these elevated heating rates as are occurring at the lower rates.

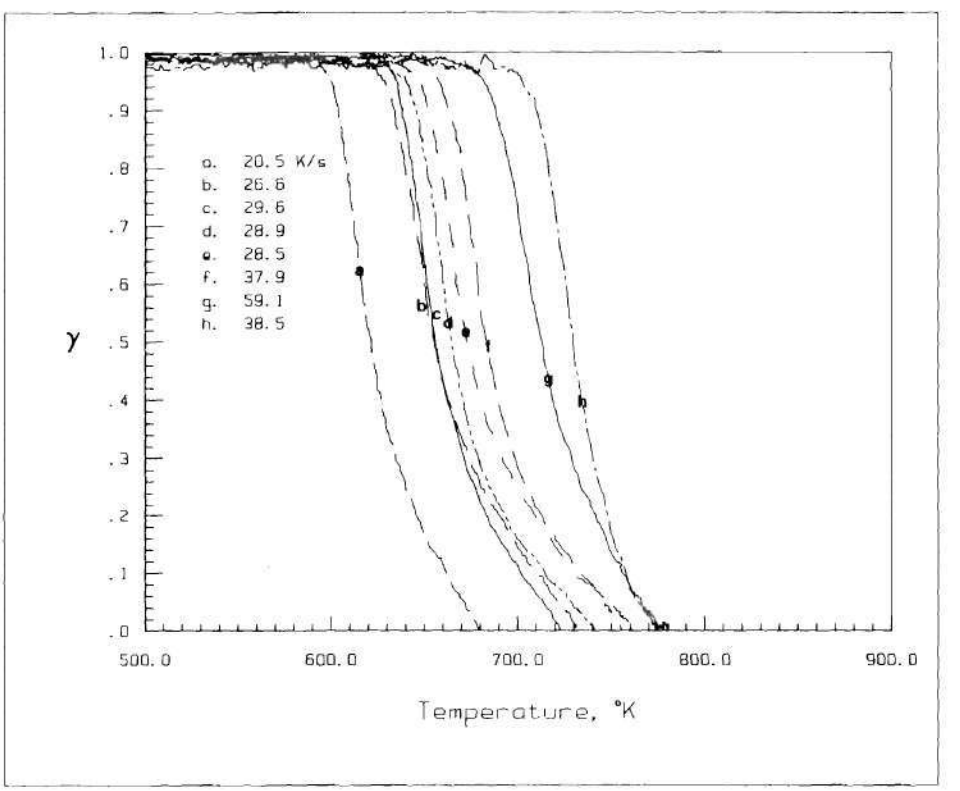

Fig. 5-6. VTGA Thermogram of HTPB - High-Heating-Rate.

5.3.2 HTPB.

Fig. 5-6 contains the results of the high heating rate experiments on HTPB. As with PBAN, sample sizes are between 0.25 mg and 0.50mg. These were deposited on the pre-oxidized heating element from a solution of the polymer in Toluene. There are very obvious differences between thermograms in this figure and those found in figures 5-2b and 5-3b. Not only are the overall shapes different, but the decomposition has shifted to slightly lower temperatures. Comparing these curves with those in Fig. 5-3b shows that with the exception of curve a the onset of the decomposition is at about the

Table 5-5. VTGA Kinetic Results for HTPB - High Heating Rate.

Ea : cal/mole
A : sec-1
β : °K-sec-1
T : °K

Item	ID	Material	Ea	A	n	β	$\alpha_o - \alpha_f$	T Range	Analysis	Source
							0.1≤α≤ 0.3			
1	170286-16	HTPB	89601	7.564E+31	0	20.5	0.10 -0.30	604-612	CR	VTGA
2	170286-19	HTPB	69643	2.803E+23	0	26.6	0.10 -0.29	634-645	CR	VTGA
3	190286-02	HTPB	82850	8.321E+27	0	29.6	0.11 -0.30	638-648	CR	VTGA
4	190286-03	HTPB	79153	1.975E+26	0	28.9	0.10 -0.29	645-656	CR	VTGA
5	170286-20	HTPB	78499	5.922E+25	0	28.5	0.11 -0.29	652-662	CR	VTGA
6	170286-17	HTPB	84412	2.483E+27	0	37.9	0.11 -0.30	663-674	CR	VTGA
7	170286-18	HTPB	71930	2.974E+22	0	49.7	0.11 -0.29	689-701	CR	VTGA
8	190286-06	HTPB	98880	1.088E+30	0	38.5	0.11 -0.28	710-720	CR	VTGA

temperature, but the rates are significantly higher.

The lower portion of the curves are much more protracted, possibly, but not necessarily, indicating a shift in the apparent order of the decomposition. (See Fig. 2-3a.) With but one exception there is a trend to higher temperatures as heating rate to the sample is increased. Examination of the calculated kinetic parameters presented in Table 5-6 shows that there has been a dramatic change in the global Arrhenius values. Ea's have increase from below 20 kcal/mole to around 80 kcal/mole. All this would indicate a radical shift in decomposition mechanism. These values are startlingly high compared to the previous results, and to the high-rate data in the literature. In mitigation, it must be remembered that bond energies in HTPB are around 80 kcal/mole; if the global energy of activation is interpreted in terms of the weakest bond in the molecule, then these values do not seem as unrealistic. These larger values could also be explained in terms of the finding of Gontkovskaya, et al. [31], discussed in Chapter I. In this work the authors solved rate expressions with heat transfer for the cases where the decomposition proceeded via several parallel reactions. They showed that an increase in heating rate promotes the course of the reaction along the path with the highest activation energy. Real-time chemical analysis of the decomposition products would be necessary in order to draw any meaningful conclusions as to the details of the processes which are occurring.

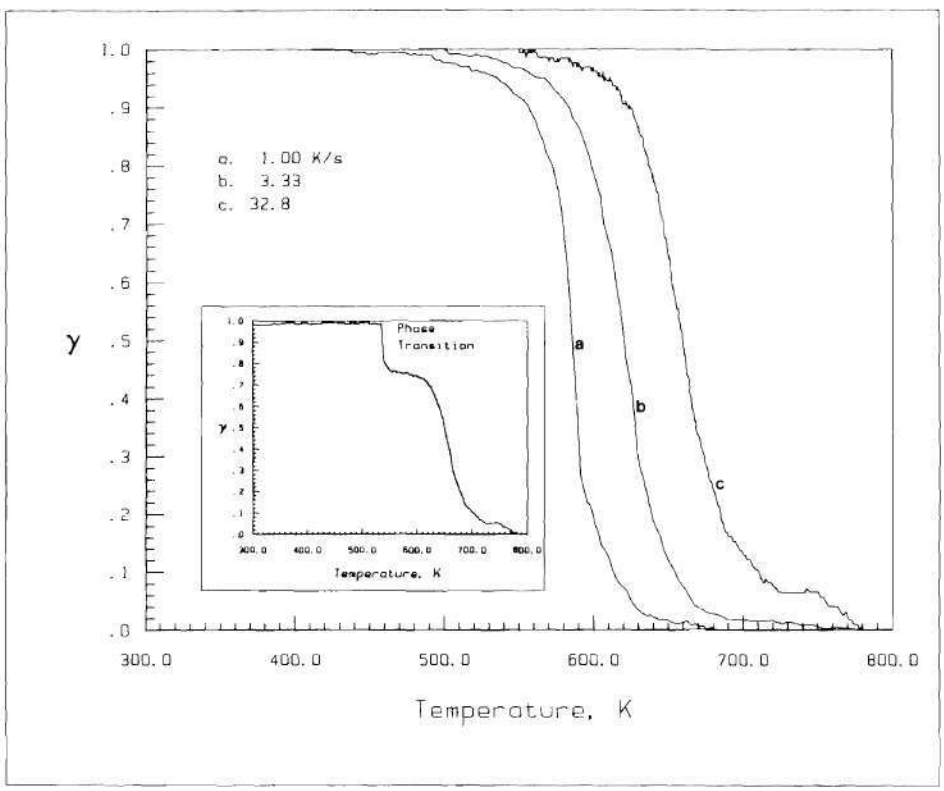

Fig. 5-7a. VTGA Thermogram of AP.

5.3.3 AP

The VTGA was designed to measure pyrolysis data on polymers. It was felt that crystalline materials would not adhere to the heating elements during rapid heating. Several runs were made on ammonium perchlorate to demonstrate this. Surprisingly, it was possible to make kinetic measurements on this material using both the linear furnace and the induction furnace. Sample size was again between 0.25 and 0.50 mg only in this case it was deposited on the metal strip from an acetone solution. Many applications of the solution were required to build up a sufficient quantity of sample. Several pyrolysis curves are shown in Fig 5-7a. Curves a and b were obtained with the linear furnace while curve c was obtained with the induction furnace. The inset in Fig 5-7a shows curve c as it was recorded. The abrupt weight loss at 545 °K corresponds to the temperature of the crystalline phase change in AP; apparently this is sufficiently violent to loosen some of the AP which was affixed to the heating element. Normalizing this pyrolysis curve produces curve c in the main figure. Corresponding kinetic data may be found in Table 5-6. A comparison of this data with the literature values given in the lower portion of the table is shown in Fig. 5-7b. (The numbers in Fig. 5-7b refer to item numbers in Table 5-6.) It is well known that the Ea of AP is strongly dependent upon the temperature of the decomposition, the data in this figure is presented as a

function of temperature, where the box represents the VTGA data in Table 5-6, items 1 through 3.

Table 5-6. VTGA Kinetic Results for AP - Deposited on 304SS from Acetone

Ea : cal/mole
A : sec-1
β : °K-sec-1
T : °K

Item	ID	Material	Ea	A	n	β	αo - αf	T Range	Analysis	Source
							0.1≤α≤ 0.3			
1	130286-13	AP	26168	8.953E+7	0	1.00	0.11 -0.28	558-578	CR	VTGA
2	130286-15	AP	28172	5.506E+8	0	3.3	0.10 -0.25	584-604	CR	VTGA
3	190286-15	AP	36145	7.616E+11	0	32.8	0.10 -0.29	652-694	CR	VTGA
4		AP(90μm)	≈30000*	-	1	0.16-0.3	≈0 - 1	613-683	DSM	TGA[54]
5		AP(90μm)	56000#	-	1	-	≈0 - 1	673-713	DSM	TGA[54]
6		AP	25100	-	1,2	-	0.0 - 0.2	523-573	AE	G [55]
7		AP(80μm)	46700	-	2	-	0 - 1 ?	643-673	CC	G [55]
8		AP(56μm)	35700	-	2	-	0 - 1 ?	643-673	CC	G [55]
9		AP(28μm)	31000	-	2	-	0 - 1 ?	643-673	CC	G [55]
10		AP	33490	8.950E+10	3	-	0 - 1 ?	-	AE	G [55]

* Actual Values for in temperature range were reported as "slightly less than 30 kcal/mole.
\# Pre-decomposed on DSC to investigate high temperature region.

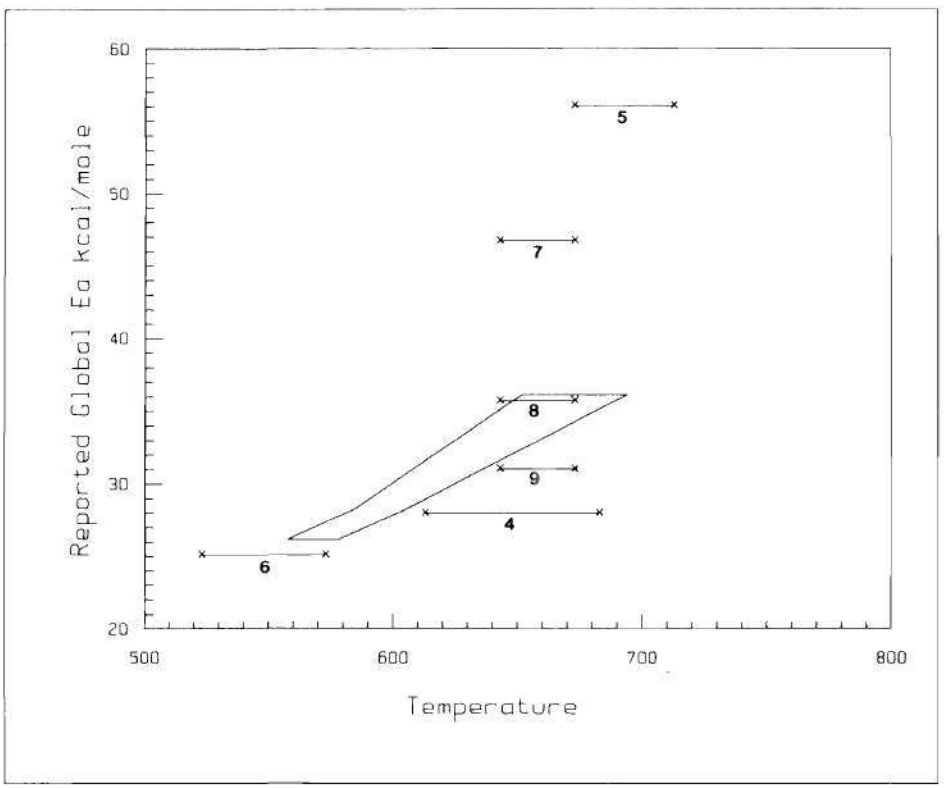

Fig. 5-7b. VTGA and Literature Results for AP.

CHAPTER VI

CONCLUDING REMARKS AND SUGGESTIONS

6.1 General Remarks

In the previous chapter it was demonstrated that it is possible to make a mass measurement of a sample during rapid pyrolysis at heating rates up to 60 °C/s. Pyrolysis curves so obtained, agreed well with curves obtained using a conventional TGA. The precision demonstrated in Figs. 5-3a and 5-3b is excellent. Kinetic values are in reasonable agreement with the TGA and the literature. With a better inductive heating unit and data-line frequency response, it should be possible to attain rates of several hundreds of degrees per second. Nevertheless, given the serious limitations in the current induction heater, results obtained at the these higher heating rates are fairly good - at least reasonable. Moreover, the work demonstrates that using vibration to make sensitive mass measurements is feasible. As far as is known to the author, this is the first device which will make continuous mass and temperature measurements on sub-milligrams sample at heating rates above about 3.3 °C/s.

6.2 The Method - Advantages and Disadvantages

VTGA apparatus has several advantages over existing TGA equipment. However, in its present form, there are also some glaring design deficiencies which need to be re-worked in order to have a routinely usable instrument at heating rates of 100 °C/s or better. It is believed that by correcting some of the design deficiencies, the most important of which is the high-heating-rate control and frequency of the data-line, the instrument would be capable of routine analyses at heating rates of 100 °C/s. Thermal decomposition experiments at heating rates, which would be relevant to solid propellant combustion, would of course require a new experimental approach using high-energy lasers of 1000 Watts or more to heat the sample.

6.2.1 Advantages

The instrument has several clear advantages for the thermal analysis of polymers over the traditional TGA which uses the double-beam balance. In TGA's, buoyancy and convection can affect the most sensitive mass measurements; this would be particularly true of energetic materials which give considerable off-gassing during decomposition. It has been shown [53] that significant pressures of pyrolysis products exist within the weighing pan during decomposition. Moreover, condensation of pyrolysis products on the cooler parts of the balance mechanism can effect overall results. This would be a minor concern in the VTGA. Rapid-off

gassing would still affect the motion of the tube to some degree, but, this would occur only at the highest rates.

Conventional TGA's, suffer from problems in the accuracy with which they can measure temperature. The sample is not in contact with the heat source nor is it in contact with the thermocouple. This results in considerable thermal inertia and limits heating rates to very low values. Moreover, due to exo- and endo-thermal processes taking place within the sample, the actual sample temperature may be significantly different than the indicated temperature; this has been shown to be critical in the analysis of results [31]. Since the samples in the VTGA are thin films, this is not expected to be as great a problem; these films are in intimate contact with the heat source and the thermocouple. This heating element/thermocouple is a good heat sink - thermal gradients across the sample will not be as significant. Thin film samples also reduce the problem of diffusion of subsurface gaseous products to the exterior. The relative importance of each these limitations are pointed out in Ref. [53].

6.2.2 Deficiencies

The present design of the apparatus is far from optimum. Improvements can be made to the laser, and signal conditioning and data lines; major improvements need to be made to the heater control system.

The Laser. Low mW lasers, like the one used in the

VTGA frequency detection system, are mainly used for alignment of optical systems, with the result that the quality of the emitted light is often poor. It may contain considerable 60 cycle noise, particularly if a low quality power supply is used. The photocell can not differentiate between noise in the light source and the signal generated by the oscillation of the tube. The presence of noise requires oscillation of the tubes at amplitudes greater than 1 mm. To a certain extent it impacts on the sensitivity of the measurement; also, the higher the amplitude the more pronounced is convection in the area of the sample. By switching to a higher quality laser during this work, it was possible to determine the period of oscillation to another decimal place. Presumably, better quality lasers would further improve results.

Signal Conditioning and Data Acquisition. Time resolution of the apparatus could be improved by going to higher frequencies, shortening the tube is of course the simplest way of doing this. As the sample volatilizes, the amplitude decreases, and frequency increases. At times, the amplitude decreases sufficiently, such that the S/N ratio in the feedback loop is high enough to cause the motion of the tube to stop. For this and other reasons it is desirable to maintain the amplitude constant during the test. This indicates the need for a servo-loop as indicated by the dashed box in Fig. 3-4. This servo-system would increase

the emf to the main feedback-loop when a decrease in RMS voltage was detected in the circuit. It would function in much the same way as does a radio which maintains constant volume as the automobile travels into areas of varying signal strength.

The FVC currently used, operates at 0 to 10 volts for an input of 0 to 10000 Hertz; thus, at 160 Hertz, we are operating on the outer limits of its performance range. This necessitates the use of extensive filtering of the signal and the use of a differential input at the scope, Fig 3-6; both of these seriously limit the frequency response of the mass data-line. It would be much more desirable to replace this with a frequency to voltage converter operating at 0 -10 Volts over 0 -1000 Hertz, or better still, a zero crossing detector/counter combination.

Heater Control. The principal limitation of the VTGA is in heating rate control at high heating rates and the ultimate temperature attainable. Improvement to the heating rate control would require the construction of an induction heating unit which permitted a variable power output to the induction coil and longer heating times. (The one used in this work was limited to 9 s.) A temperature-heating rate servo-loop to linearize and control the heating rate would go a long way to improve the results. In subsequent work in this area, small ferromagnetic tubes should be manufactured so that heating-element/thermocouple combinations can be

fabricated which are capable attaining higher temperatures.

6.3 Suggested Work.

6.3.1 Experimental

A very interesting experiment would be the modification of Baer's and Hedge's rapid pyrolysis experiment [10] to include the feedback-loop/mass measuring system used in present work. Their experiment is briefly described in Chapter I. Baer was able to rapidly heat thin films of polymer which were mounted on a thin metal strip which also served as a heating element. This heating element was fixed between two supports and heating was accomplished by passing a strong electric current through the strip. Mass measurements were made discontinuously by "quenching" the sample with a cold blast of air and weighing the strip. Sample temperatures were measured using an infrared radiometer "looking" at the back side of the heating element rather than at the sample itself; this eliminates the problem of radiation absorption by pyrolysis products. Radiometers are available with 8 μs response times, a significant improvement over the thermocouple (3 ms). (A similar radiometric temperature measurement scheme could be used with the present quartz tube arrangement.) If Baer's 25 μm thick heating element were mounted in such a way that it could vibrate, introduction of the feedback-loop system used in the present work would make a continuous mass measurement

possible. Moreover, with this arrangement it should be possible to obtain higher frequencies of vibration than with a cantilevered tube, and hence, obtain better time resolution. The frequency of vibration would depend upon the tension in the vibrating metal ribbon. The tension of course would have to be kept constant; this difficulty has apparently been overcome by Gast and Jokobs [43,44]. Such an arrangement could effectively be implemented at pressure. And heating rates up to several hundreds of °C/s would not be unreasonable with such an arrangement.

6.3.2 Theoretical.

In the linear pyrolysis experiments reviewed in Chapter I, reported values for global energies of activation for HTPB and PBAN are between 10 and 17 kcal/mole. The bond energies for the weakest bonds in these molecules are, however, closer to 80 kcal/mole. The relatively low values for Ea have been attributed to evaporation being the rate limiting step at the higher heating rates. (It was pointed out in Chapter I that evaporation could be expressed in terms of an Arrhenius type expression, Eqn. 1-9.) This argument has also been used by Chaiken [27] to explain the shift to lower values of Ea when PMMA is decomposed at higher heat fluxes. It would be interesting to determine if this shift to lower values has a plausible theoretical foundation.

In Chapter I, the work of Gontkovskaya, et al. [30,32]

was described wherein they analyzed the kinetics of decomposition with heat transfer for a material decomposing via two parallel reactions. Numerical solutions to the differential equations showed that higher heating rates promoted the process with the higher activation energy! This result would seem to be at odds with the explanation of Chaiken and others.

In related papers they analyze and numerically solve the case of sequential reactions. [32,33] In a similar fashion, the decomposition/vaporization of a polymer can be described as a sequential processes, Eqn. 6-1:

$$P \xrightarrow{k_1} n_1 \xrightarrow{k_2} n_2 \qquad (6\text{-}1)$$

where, n1 is the condensed phase decomposition product of the polymer, P, and n2 is the product of vaporization of n1. k_1 and k_2 are the rate constants for the decomposition and vaporization, respectively. The following equations would describe the process:

$$\frac{dp_1}{dt} = - A_1 e^{- E_1/RT} p_1 \qquad (6\text{-}2)$$

$$\frac{d\eta_1}{dt} = - R_2 + A_1 e^{-E_1/RT} p_1 \qquad (6\text{-}3)$$

$$c\rho \frac{dT}{dt} = Q_1 A_1 e^{-E_1/RT} p_1 + R_2 \Delta H_v - \alpha \frac{S}{V} (T - T_s) \qquad (6\text{-}4)$$

with the initial conditions,

$$\beta = dT/dt, \qquad T = T_s = T_i, \qquad p_1 = 1, \quad \eta_1 = 0 \qquad (6\text{-}5)$$

where R_2 is the rate of vaporization of n1, given by the non-dimensional form of Eqn. 1-9. It would be interesting to see if the numerical solution to this set of differential equations, for plausible values of the various parameters, would yield situations where vaporization would be the rate limiting condition. Reasonable values for some parameters may be found in [12] and [15].

6.4 Conclusions

1. Global Arrhenius parameters are in general not constants and must be empirically determined - this is particularly true for complex substances such as polymers.

2. Arrhenius parameters used in kinetic and combustion models must be empirically determined under conditions

similar to those over which the model is to be used and considered valid.

3. Global kinetic parameters can be strong functions of the experimental conditions, for example, heating rate, pressure, and temperature; calculations which determine Arrhenius parameters from experimental data, should make this determination over as narrow a range in these condition as is possible.

4. In order to obtain the maximum benefit from high-heat-flux experiments, numerical techniques for the smoothing of thermal analysis data, and for the integration of the rate expression over finite limits, need to be developed.

5. An algorithm which uses only the early stages of decomposition for determination of Arrhenius parameters necessarily requires fewer assumptions as to the details of the decomposition; no assumption as to reaction order is necessary.

6. Global reaction order is an empirical parameter dependent upon the details of the experiment.

7. Construction of a thermogravimetric analyzer which uses vibration (VTGA) to measure small changes mass of thin polymer films is feasible. Moreover, it is possible to construct such a device where the sample is in contact with the thermocouple. Such a device is not impaired by effects such as buoyancy, condensation of products, and to a certain

extent, sample off-gassing.

8. The VTGA developed in this work is capable of measuring the decomposition kinetics of thin polymer films, at heating rates up to 3.33 °C/s, with a precision and accuracy at least as good, and probably better, than a conventional TGA.

9. The present VTGA design can measure decomposition kinetics of polymer films at heating rates in the range of 20 - 60 °C/s. ; major redesign of the induction heater and FVC will be necessary to precisely and accurately represent the high-high-heat flux kinetics of polymers at varied and reproducible heating rates. Such a redesign should provide for programmable heating rates - not necessarily linear. Redesign should permit operation at heating rates in excess of 100 °C/s.

10. Over the small variations in mass used in the VTGA, the calibration is essentially linear; this greatly simplifies the use of this device.

11. The TGA could not successfully determine kinetic constants for bulk samples of HTPB and PBAN at heating rates 3.3 °C/s. At heating rates above this value it is likely that the decomposition in bulk samples is diffusion controlled. It is also doubtful that thermal equilibrium exists in the TGA test cell even at this low rate.

12. Data indicates that PBAN is likely to decompose via the same mechanism at heating rates of 0.5 °C/s - 3.3

°C/s as it does at heating rates of 40 - 60 °C.

13. Data indicates that there is a change the controlling mechanism or the path in the decomposition of HTPB when heating rates are changed from values around 1 °C/s to values of about 40 °C/s.

14. It is possible to determine kinetic parameters of crystalline materials in a VTGA-type apparatus.

APPENDIX A

EQUIPMENT, INSTRUMENTATION, AND MATERIALS

Equipment and Instrumentation.

Item.

1. IBM-Personal Computer

Manufacturer: IBM Corporation

Configuration: 515K Ram Total; two 360K Floppy disk drives; Quadboard II Expansion Board, w/ two Serial Ports, Clock, 256K Ram; Amdek 300A Monitor; Hercules Color Card w/Parrallel Port; HP 7470A Digital Plotter; Okidata 92P Printer.

2. Nicolet 4094 Digital Osciloscope

Manufacturer: Nicolet Instrument Corporation
5225-2 Verona Road
Madison, WI 53711

Configuration: Model 4562 two-channel plug-in, up to two MHertz sampling rate both channels; single Floppy Diskette Drive; RS-232 Computer Interface.

3. Vibration Exciter (Mini-Shaker), Type 4810

Manufacturer: Brel & Kjaer
DK-2850 Naerum, Denmark

Specifications: Force rating 10 Newton Sine Peak; Frequency range 10 Hz to 18 kHz; Max. bare table acceleration 56g; First axial resonance above 18 kHz.; Max. displacement 6 mm.

4. Neff Model 122 DC Amplifier

Manufacturer: NEFF Instrument Corporation

1088 East Hamilton Road
Duarte, California 91010

a. Configuration: without bandpass filter.

b. Configuration: with bandpass filter.

5. DC Power Supplies

Manufacturer: Hewlett-Packard Co.
1501 Page Mill Road
Palo Alto, CA 94304

a. Specifications: HP 6215A, 0 - 30V, 0 -500 mA.

b. Specifications: HP 6228B Dual Power Supply, 0 - 50 V, 0 - 1 A.

c. Specifications: HP Harrison 6204B, 0 - 4 V, 0 - .3 A; 0 - 20 V, 0 - .6 A

6. Laser

Manufacturer: Uniphase, Inc.

Configuration: Model 1101
Max-Power 1 mW, Beam Diameter 0.63 mm
Power Supply, External Type, Model 1201-1

7. Optical Bench and Mounts

Manufacturer: Ealing Corporation
Pleasant Street
South Natic, Mass. 01760

a. Specifications: Model 22-6894, 1 meter.

b. Specifications: Model 22-6837, 1/4 meter.

8. Curie Point Pyrolyzer

Manufacturer: Fischer
5309 Meckenheim/b. Bonn
Insustriepark Kottenforst

Specifications: Model 0310, 1.2 MHertz, 2000 W output, 382 Oe. coil Field Strength.

9. Electronic Compensator ("Ice Point")

Manufacturer: Omega Engineering
One Omega Drive
Box 4047
Stamford, CT 06907

Specifications: Model LXCJ-E, Type-E(Chromel-Constantan).

Configuration: Self-Powered by Battery

10. Electronic Digital Balance

Manufacturer: Mettler Instrument Corporation
Box 71
Hightstown, NJ 08502

Specifications: Model AE-160, Range 0 - 162g,
Reproducibility S.D. .1 mg., Linearity +/-
.2 mg., Readability .1 mg.

11. Thermocouples

Manufacturer: Omega Engineering
One Omega Drive
Box 4047
Stamford, CT 06907

Specifications: Type E, Chromel SPCH-001, Constantan
SPCR-001

12. Thermogravimetric Analyzer

Manufacturer: Perkin-Elmer Corp.
Instrument Division
Norwalk, Connecticut 06856
203-762-1000

Specifications: TGA-2 and System 7/4 Controler
Maximum Programmable Heating Rate 200°C/min
Temperature Range: Ambient - 1040°C

13. Frequency Meter

Manufacturer: John Fluke Mfc. Co Inc.
P. O. Box 43210
Mountain Lake Terr., WA 98043
206-744-2211

Specifications: Model 1900A Multi-Counter

14. Photodiode Support

Manufacturer: Brinkman Instruments Inc.
Cantiague Road
Westbury, NY 11590
516-334-7500

Specifications: Model RP-IV Micro-manipulator

15. Photodiode.

Manufacturer: TRW, Inc.

Specifications: Photo-transistor, TRW-OP802W

16. Frequency-to-Voltage Converter

Manufacturer: In-House Built Unit

Specifications: Unit designed around Teledyne-Philbrick 4710 low drift 100kHz F/V Converter. Output set to yield 0-10 Volts for 0-1kc.

Supplier: Teledyne-Philbrick

Materials

Item.

1. Quarts Tubes

Manufacturer: Vitro Dynamics Inc.
114 Beach Street
Rockaway, New Jersey 07866

Specifications: Convenience Vials.

2. Steel Tubbing

Manufacturer: Small Parts Inc.
6901 N.E. Third Avenue
P.O. Box 381736
Miami, Florida 33238-1736
305-715-0856

Specifications: 304 Stainless Steel, Hypodermic Tubbing
304 Stainless Steel, Thin Wall Tubing

3. Polymers

Manufacturer: Scientific Polymer Products, Inc.
6265 Dean Parkway
Ontario, N. Y. 14519
716-265-0413

Specifications: PBAN
Acrylonitrile/butadiene Copolymer
Acrylonitrile Content 21%
Average Mooney Viscosity 55
Density 0.95
Soluble in MEK, Toluene, THF

HTPB
Polybutadiene, cis and trans
9% Vinyl 1.2
Nominal M.W. 200,000
Nominal M.N. 96,000
Density 0.90
Tg - 95°
Solubility Parameter 8.38
n_{D20} = 1.5178
Soluble in THF, aliphatic, cycloaliphatic, and aromatic hydrocarbons.

Preparations and Fabrications

1. Composite Pyrolysis Tubes

The quartz pyrolysis tubes are actually composite tubes formed by cementing a metal tube of smaller outside diameter to the end of the quartz tube. This metal tip serves several purposes: it mainly functions as a support upon which to coat the polymer samples, however, it also provides a convenient point of attachment for thermocouple leads, and is consequently an excellent medium for heat transfer between the sample and the thermocouple. In cases where induction heating is employed, it can also function as a heating element - the metal is ferromagnetic and is fabricated from 304 stainless steel tubing.

To construct one of these pyrolysis tubes, a 3 cm length of stainless steel tubing is cut from tubing stock with a typical O.D. of 0.013 inches and an I.D. of 0.007 inches. Cutting is performed using a hand grinder equipped with a very thin grinding wheel; this is used so as not to collapse the tube ends. These ends are polished with the grinder, if necessary, to remove sharp edges and to insure that the tube is open at both ends. One lead of one-mil thermocouple wire is inserted through the tube (a hypodermic cleaning wire is often helpful to drag the wire through the tube). In a similar fashion, the second lead is also inserted. The respective leads are marked with tape for later identification, and the leads are cut leaving about six inches of both leads extending from this tube section. The tube is placed between two pieces of hardened tool-steel; about a millimeter of the tube on the side with the long thermocouple leads is allowed to protrude outside. This is the serve as a "stem" which will later be inserted into the quartz tube. The edges of these tool-steel pieces have been sanded to a rounded edge so as not to cut the stainless steel tube section. This assembly is placed in a 30,000 lb. press and pressed for a short time. The resulting piece, when removed, resembles a spatula blade with the thermocouple leads extending from the stem. The flattened end of the "spatula" is trimmed the desired length. The "stem" inserted into the end of a quartz tube of slightly larger I. D. routing one lead of the thermocouple through the center of the quartz tube. The stem is cemented in place using a 2000 °F ceramic cement; the remaining lead is spirally wound around the outside of the tube and secured at the opposite end with a small piece of shrink tubing. The thermocouple is checked for continuity and the entire assembly is mounted in the experimental apparatus and the thermocouple leads are soldered in place. Where ferromagnetism is not important

lighter metal tubing, such as aluminum could be used.

Note: One of the most difficult tasks of the project was to find a method to make these metal tips complete with thermocouples. Several other methods were attempted but with out success. For example, ferromagnetic materials were chemically deposited on a gold substrate on the tip of the quartz tube. The gold was sputtered coated on the tip. The materials so formed, did not heat well in the induction heater and thermocouples could not be readily applied. Welding the thermocouples proved difficult and welds would not hold. Clearly if a method can be found to apply low weight ferromagnetic materials to quartz tubes or ribbons, and thermocouples could be attached or temperatures measured with a radiometer, the sensitivity of the method would be greatly enhanced. A large penalty is paid in sensitivity by the necessity of using the rather heavy (about 7 mg) stainless steel tube for the heating elements.

APPENDIX B

COMPUTER PROGRAMS

Program 1. This program, written in MS-BASIC, transfers data from memory of a Nicolet 4094 Digital Oscilloscope to an IBM-PC/XT/AT; temporary files and data are stored on Drive C:. Data transmission rate is 9600 BAUD via an RS-232 interface; data transmission requires the use of a nul-modem since both the oscilloscope and the computer are configured as data terminal equipment. Data is stored in an ASCII file in two columns - time and volts.

```
2 '****************** IBM-PC - NICOLET DATA TRANSFER PROGRAM ********************
3 '*****************************************************************************
4 '**   Author: Robert J. Powers, Aerospace Engineering Dept., Georgia Tech
5 '
6 '******************************** MAIN PROGRAM ********************************
7 '** CONFIGURATION, IBM-PC : RS-232C PORT SET UP A COM PORT 1
8 '** CONFIGURATION, NICOLET: RS- 232C ADDRESS 30 (ASCII CHARACTER N);
9 '**                        DATA TRANSMISSION RATE 9600 BAUD
10 '
15 DIM TIT$(4),N$(11),W(8,4)
20 OPT = 0
40 CLS :LOCATE 1,25
50 COLOR 0,7
60 PRINT "IBM-PC - Nicolet";
70 COLOR 7,0
80 PRINT " Data Transfer Program"
90 PRINT:LOCATE 3,37:PRINT "Version 1.00":PRINT
100 PRINT "
110 PRINT "
120 PRINT "                1. Initialize Data Transfer (C)(B)
130 PRINT "
140 PRINT "                2. Nicolet Disk Storage and Retrieval (R)(S)(U)
150 PRINT "
160 PRINT "                3. Display Waveform Data in Nicolet Memory (W)
170 PRINT "
200 PRINT "                4. Transfer Data in Nicolet Memory to PC (D)(N)
210 PRINT "
220 PRINT "                5. Add Title to Waveforms in Nicolet Memory (T)
230 PRINT "
```

```
240 PRINT "      ╔═══════════════════ 6. Exit to System ═══════════════════════════════╗"
250 PRINT "      ╚═══════════════════════════════════════════════════════════════════╝"
260 PRINT "
270 LOCATE 24,1
280 INPUT "Select Option: ",OPT
290 CLS
300 IF OPT = 1 THEN GOSUB 350
310 IF OPT = 2 THEN GOSUB 560
320 IF OPT = 3 THEN GOSUB 2000
325 IF OPT = 4 THEN GOSUB 5000
330 IF OPT = 5 THEN GOSUB 1590
335 IF OPT = 6 THEN SYSTEM
336 LOCATE 24,1:PRINT "                                                    ";
340 GOTO 20
345 END
346 '
347 '
348 '
350 '************************ INITIALIZATION SUBROUTINE ************************
360 '***************************************************************************
410 CLS
420 OPEN "COM1:9600,N,8,1,LF" AS #1
425 CTRLA$ = CHR$(1)
430 PRINT #1, CTRLA$;"N";
460 PRINT #1,"C,4,2,13,10"
480 CLOSE #1
482 OPEN "COM1:9600,N,8,1,LF" AS #1
484 PRINT #1,"B"
486 INPUT #1,E$
488 CLOSE #1
490 E = VAL(E$)
500 IF E <>0 GOTO 530
510 PRINT "                              Initialization Successfull !"
515 LOCATE 24,1:INPUT "Press Return to Continue",DUM
520 GOTO 550
530 PRINT "                 Initialization Error Detected !  Error Code = ";
540 PRINT E$
545 LOCATE 24,1:INPUT "Press Return to Continue",DUM
550 RETURN
560 '********************* NICOLET DISK ACCESS SUBROUTINE **********************
565 '***************************************************************************
570 CLS
580 LOCATE 1,30
590 COLOR 0,7
600 PRINT " Nicolet Disk Access "
610 COLOR 7,0
620 PRINT "                                                                    "
630 PRINT "          ╔═══════════════════════╦═══════════════════════════╗     "
640 PRINT "          ║  Memory Section #     ║  Memory Section           ║     "
650 PRINT "          ╠═══════════════════════╬═══════════════════════════╣     "
660 PRINT "          ║           0           ║  All                      ║     "
          ║           1           ║  Q1                       ║
```

```
670 PRINT "              ╔═══════════════════════════════════════════╗"
680 PRINT "              ║              2                  Q2        ║"
690 PRINT "              ║              3                  Q3        ║"
700 PRINT "              ║              4                  Q4        ║"
710 PRINT "              ║              5                  H1        ║"
720 PRINT "              ║              6                  H2        ║"
730 LOCATE 14,56: PRINT "              ╚═══════════════════════════════════════════╝";:LOCATE 14,13
740 LINE INPUT; "Select Mode (R = Recall, S = Store, E = End): "; MODE$
750 IF MODE$ = "R" THEN GOTO 780
760 IF MODE$ = "S" THEN GOTO 960
770 IF MODE$ = "E" THEN GOTO 1290 ELSE GOTO 730
780 OPEN "COM1:9600,N,8,1,LF" AS #1
790 LOCATE 14,61
800 COLOR 16,7
810 PRINT " RECALL "
820 COLOR 7,0
830 LOCATE 24,1
840 INPUT; "Enter -- Track #, Memory Section:  ", RN,MS
850 N$ = STR$(RN)
860 S$ = STR$(MS)
870 R$ = "R" + "," + "0" + "," + N$ + "," + S$
880 PRINT #1,R$
890 LINE INPUT #1,E$
900 CLOSE #1
910 LOCATE 24,1
920 PRINT "                                          ";:LOCATE 24,1
930 LINE INPUT; "More ? "; DUM$
940 IF DUM$ = "y" OR DUM$ = "Y" OR DUM$ = "YES" OR DUM$ = "yes" THEN GOTO 730
950 GOTO 1290
960 OPEN "COM1:9600,N,8,1,LF" AS #1
970 LOCATE 14,61
980 COLOR 16,7
990 PRINT " STORE "
1000 COLOR 7,0
1010 LOCATE 24,1
1020 INPUT; "Enter -- Memory Section, Track Number #:  ",MS,TN
1030 N$ = STR$(TN)
1040 S$ = STR$(MS)
1050 R$ = "S,0,"+N$+","+S$
1060 PRINT #1,R$
1070 INPUT #1,E$
1080 CLOSE #1
1090 IF E$ = "02" THEN 1100 ELSE GOTO 1250
1100 LOCATE 24,1
1110 PRINT "                                          ";
1120 LOCATE 24,1
1130 BEEP
1140 PRINT "Track";:PRINT N$;:PRINT " is write protected!";
1150 LINE INPUT;"  Unprotect and Retry (Y or N)? ",DUM$
1160 IF DUM$ = "y" OR DUM$ = "Y" THEN GOTO 1170 ELSE GOTO 1250
1170 OPEN "COM1:9600,N,8,1,LF" AS #1
```

```
1180 PRINT #1,"U,0,"+N$+S$
1190 INPUT #1,E$
1200 PRINT #1,R$
1210 INPUT #1,E$
1220 CLOSE #1
1230 GOTO 1090
1240 LOCATE 24,1
1250 LOCATE 24,1:PRINT "                                                                    ";
     :LOCATE 24,1
1260 LINE INPUT; "More ? ";DUM$
1270 IF DUM$ = "y" OR DUM$ = "Y" OR DUM$ = "YES" OR DUM$ = "yes" THEN GOTO 730 ELSE GOTO 1290
1280 IF DUM$ = "y" OR DUM$ = "Y" THEN GOTO 1170 ELSE GOTO 1250
1290 RETURN
1300 '********************** WAVEFORM DATA SUBROUTINE ***************************
1305 '*******************************************************************************
1307 FOR I = 1 TO 8
1309 FOR J = 1 TO 4
1310 W(I,J) = 0
1312 NEXT J
1315 NEXT I
1320 OPEN "COM1:9600,N,8,1,LF" AS #1
1330 PRINT #1,"W"
1340 INPUT #1,E$
1350 INPUT #1,W1
1360 FOR J = 1 TO W1
1370 FOR I = 1 TO 8
1380 INPUT #1,W(I,J)
1390 NEXT I
1400 NEXT J
1410 CLOSE #1
1420 LOCATE 2,1
1430 PRINT "   ╔═══════════════════════════════════════════════════════════════════╗"
1440 PRINT "   ║     Waveform Number                                               ║"
1450 PRINT "   ║     Extra Data                                                    ║"
1460 PRINT "   ║     Number of Data Points                                         ║"
1470 PRINT "   ║     Normalization Set Number                                      ║"
1480 PRINT "   ║     Normalization Step                                            ║"
1490 PRINT "   ║     Channel Number                                                ║"
1500 PRINT "   ║     Retain Reference Status                                       ║"
1510 PRINT "   ║     Title Number                                                  ║"
1520 PRINT "   ╚═══════════════════════════════════════════════════════════════════╝"
1530 FOR I = 1 TO 8
1540 LOCATE I+2,43
1545 COLOR 15,0
1550 PRINT USING "#######";W(I,1);W(I,2);W(I,3);W(I,4)
1555 COLOR 7,0
1560 NEXT I
1570 RETURN
1580 '********************** DISPLAY TITLING SUBROUTINE ************************
1585 '*******************************************************************************
1590 CLS
```

```
1600 LOCATE 1,32
1610 COLOR 0,7
1620 PRINT "Display Titling"
1630 COLOR 7,0
1640 PRINT
1650 PRINT "
1660 PRINT "
1670 PRINT "
1680 PRINT "
1690 PRINT "
1700 PRINT "
1710 PRINT "
1720 PRINT "
1730 LOCATE 14,30
1740 PRINT "┌─┐"
1750 LOCATE 15,30
1760 PRINT "                                    ";
1770 LOCATE 17,30
1780 PRINT "                                    ";
1790 LOCATE 15,13
1800 INPUT "Enter -- Title #: ",TN
1810 LOCATE 17,13
1820 PRINT "Enter -- Title  : "
1830 LOCATE 16,30
1840 PRINT "┌──────────────────────────────┐"
1850 LOCATE 17,32
1860 INPUT "",T$
1870 OPEN "COM1:9600,N,8,1,LF" AS #1
1880 D$ = STR$(TN)
1890 PRINT #1, "T,1,"+MID$(D$,2,1)
1900 INPUT #1,E
1910 PRINT #1, USING "\                              \";T$
1920 INPUT #1,E
1930 CLOSE #1
1940 LOCATE 24,14
1950 PRINT "             ";
1960 LOCATE 24,1
1970 LINE INPUT ;"More Titles ? ";DUM$
1980 IF DUM$ = "y" OR DUM$ = "Y" OR DUM$ = "YES" OR DUM$ = "yes" THEN GOTO 1730
1990 RETURN
2000 LOCATE 1,23
2010 COLOR 0,7
2020 PRINT " Data for Waveforms Currently in Memory "
2030 COLOR 7,0
2040 LOCATE 5,1
2050 GOSUB 1300
2060 LOCATE 24,1
2070 INPUT "Press Return to Continue",DUM
2080 RETURN
5000 '************************ DATA TRANSFER SUBROUTINE ************************
5010 '**************************************************************************
```

Title #	Memory Section
1	Q1,H1,ALL
2	Q2,H2
3	Q3
4	Q4

```
5020 '
5030 '****************************************** DISPLAY CURRENT WAVEFORM DATA
5040 CLS
5050 LOCATE 1,35
5060 COLOR 0,15
5070 PRINT " Data Transfer "
5080 LOCATE 1,1
5090 COLOR 7,0
5100 GOSUB 1300
5110 LOCATE 2,7
5120 COLOR 0,7
5130 PRINT " Current Waveform Data "
5140 COLOR 7,0
5150 OPEN "COM1:9600,N,8,1,LF" AS #1
5160 FOR I = 1 TO 4
5170 I$ = STR$(I)
5180 PRINT #1,"T,0," + I$
5190 INPUT #1,E$
5200 INPUT #1,TIT$(I)
5210 NEXT I
5220 CLOSE #1
5230 LOCATE 12,1
5240 PRINT "
5250 PRINT "
5260 PRINT "
5270 PRINT "
5280 PRINT "
5290 PRINT "
5292 LOCATE 18,1
5293 PRINT "
5294 PRINT "
5295 PRINT "
5296 PRINT "
5300 LOCATE 12,6:COLOR 0,7:PRINT " Title # ";
5310 LOCATE 12,26: PRINT " Titles ": COLOR 7,0
5320 FOR I = 1 TO 4
5330 LOCATE 12 + I,8
5340 TIT$(I) = LEFT$(TIT$(I),32)
5350 PRINT " ";:PRINT I;: PRINT ".  ";:COLOR 15,0:PRINT TIT$(I):COLOR 7,0
5360 NEXT I
5370 LOCATE 12,57:PRINT "═══════════"
5375 LOCATE 13,52:PRINT "Waveform #:  "
5376 LOCATE 13,66:PRINT "Org:       "
5380 LOCATE 14,52:PRINT "Start:";:PRINT "        End:      "
5390 LOCATE 15,52: PRINT "Step:              "
5400 LOCATE 16,52:PRINT "Total Pts:        "
5405 LOCATE 18,10:COLOR 0,7:PRINT " Transfer Status ":COLOR 7,0
5406 LOCATE 19,10:PRINT "Status:";:LOCATE 19,32:PRINT "#:";:LOCATE 19,38:PRINT "To: "
     ;:LOCATE 19,55:PRINT "Origin: "
5407 LOCATE 20,10:PRINT "Start: ";:LOCATE 20,25:PRINT "End: ";:LOCATE 20,40:PRINT "Step: ";
     :LOCATE 20,55:PRINT "Total Pts: "
```

```
5410 '********************************************** SETUP FOR DATA TRANSFER
5420 OPEN "COM1:9600,N,8,1,LF" AS #1
5430 LOCATE 24,1
5440 LINE INPUT; "Select Option (T = Transfer; E = Exit): ", DUM$
5450 IF DUM$ = "T" OR DUM$ = "t" THEN GOTO 5460 ELSE CLOSE:RETURN
5460 LOCATE 24,1:PRINT "                                                                    ";
5470 LOCATE 24,1: LINE INPUT; "Enter -- Target File Name: ", FILE$
5480 FILENAME$ = "C:TEMP.RAW"
5490 TARGET$ = FILE$
5500 LOCATE 24,1:PRINT "                                                          ";
5510 LOCATE 12,57: COLOR 0,7:PRINT "To: "+TARGET$:COLOR 7,0
5520 LOCATE 24,1:INPUT; "Enter -- Waveform #: ",NUM
5521 LOCATE 13,63:COLOR 15,0:PRINT NUM:COLOR 7,0
5525 LOCATE 24,1:PRINT "                                                            ";
5526 LOCATE 24,1: LINE INPUT; "Select Origin (N = Normal; R = Reset): ",ORIG$
5528 IF ORIG$ = "R" OR ORIG$ = "r" THEN NUMERICS$ = "Reset" ELSE NUMERICS$ = "Normal"
5529 LOCATE 13,71:PRINT "      ":LOCATE 13,71:COLOR 15,0:PRINT NUMERICS$:COLOR 7,0
5530 '********************************************** RETRIEVE NORMALIZATION DATA
5540 SET$ = STR$( W(4,NUM) )
5550 PRINT #1, "N," + SET$
5560 INPUT #1,E$
5570 FOR I = 1 TO 11
5580 INPUT #1,N$(I)
5600 NEXT I
5610 INPUT #1,E$
5620 '************************************ CALCULATE NORMALIZATION PARAMETERS
5630 VNORM  = VAL( N$(5) )
5640 HNORM  = VAL( N$(6) )
5650 VZERO  = VAL( N$(7) )
5660 HZERU  = VAL( N$(8) )
5670 HZERL  = VAL( N$(9) )
5680 RVZERO = VAL( N$(10))
5690 RHZERO = VAL( N$(11))
5700 HZERT  = ( HZERU * 65536! ) + HZERL
5710 '********************************************** SPECIFY DATA TRANSFER LIMITS
5720 LOCATE 24,1:PRINT "                                                          ";
5730 LOCATE 24,1:LINE INPUT; "Enter -- Starting Point # (C = Cursor Position): ",SRT$
5740 IF SRT$ = "c" OR SRT$ = "C" THEN 5750 ELSE 5840
5750 LOCATE 24,1:PRINT "                                                           ";
5760 PRINT #1, "M,14"
5770 INPUT #1,E
5780 INPUT #1,E
5790 INPUT #1,VPOS
5800 INPUT #1,E
5810 VPOS = VPOS - 49664!
5820 SRT = VPOS/(15872/W(3,NUM))
5825 SRT = INT(SRT)
5830 GOTO 5850
5840 SRT = VAL(SRT$)
5845 SRT = INT(SRT)
5850 LOCATE 14,58:COLOR 15,0:PRINT SRT:COLOR 7,0
```

```
5860 LOCATE 24,1:PRINT "                                                                    ";
5870 LOCATE 24,1:LINE INPUT; "Enter -- End Point (C = Cursor Position): ",ENDS$
5880 IF ENDS$ = "C" OR ENDS$ = "c" THEN 5890 ELSE 5980
5890 LOCATE 24,1:PRINT "                                                                    ";
5900 PRINT #1, "M,14"
5910 INPUT #1,E
5920 INPUT #1,E
5930 INPUT #1,VPOS
5940 INPUT #1,E
5950 VPOS = VPOS - 49664!
5960 ENDS = VPOS / (15872 / W(3,NUM))
5965 ENDS = INT(ENDS)
5970 GOTO 5990
5980 ENDS = VAL(ENDS$)
5985 ENDS = INT(ENDS)
5990 LOCATE 14,70:COLOR 15,0:PRINT ENDS;:COLOR 7,0
6000 LOCATE 24,1:PRINT "                                                                    ";
6010 LOCATE 24,1:INPUT; "Enter -- Step Size: ",STP
6011 LOCATE 15,57:COLOR 15,0:PRINT STP:COLOR 7,0
6012 TOT = INT(((ENDS - SRT) / STP)+1)
6014 LOCATE 16,62:COLOR 15,0:PRINT TOT:COLOR 7,0
6020 LOCATE 24,1:PRINT "                                                                    ";
6030 LOCATE 24,1
6040 LINE INPUT; "Enter -- A to Abort; C/R to Continue: "; DUM$
6050 IF DUM$ = "a" OR DUM$ = "A" THEN :CLOSE:GOTO 5370
6054 COLOR 23,0
6055 LOCATE 19,18:PRINT "Transfering "
6058 COLOR 7,0:LOCATE 19,34:PRINT "  ":LOCATE 19,34:COLOR 15,0:PRINT NUM:COLOR 7,0
6059 LOCATE 19,42:PRINT "           "
6070 LOCATE 19,42:COLOR 15,0:PRINT TARGET$:LOCATE 19,63:PRINT "      ":LOCATE 19,63
     :PRINT NUMERICS$
6076 LOCATE 20,16:PRINT "       ":LOCATE 20,16: PRINT SRT
6077 LOCATE 20,29:PRINT "       ":LOCATE 20,29: PRINT ENDS
6078 LOCATE 20,45:PRINT "       ":LOCATE 20,45: PRINT STP
6079 LOCATE 20,65:PRINT "       ":LOCATE 20,65: PRINT TOT
6080 COLOR 7,0
6082 '********************************************** PREPARE FOR DATA TRANSFER
6090 XOFF$ = CHR$(19): XON$=CHR$(17)
6100 OPEN FILENAME$ FOR OUTPUT AS 2
6110 WN$ = STR$(NUM)
6120 ST$ = STR$(SRT)
6130 TPTS$ = STR$(TOT)
6140 SEP$ = STR$(STP)
6150 '************************************* SEND STRING TO BEGIN DATA TRANSFER
6160 PRINT #1,"D,0," + WN$ +","+ ST$ +","+ TPTS$ +","+SEP$
6170 INPUT #1,E
6180 '******************************************** XOFF/XON HANDSHAKING ROUTINE
6190 WHILE NOT EOF(1)
6200 COUNT = 0
6210 WHILE LOC(1) < 20  AND COUNT < 10
6220 COUNT = COUNT + 1
```

```
6230 WEND
6240 PRINT #1,XOFF$
6250 WHILE NOT EOF(1)
6260 D$ = INPUT$(LOC(1),#1)
6370 PRINT #2,D$;
6380 WEND
6390 PRINT #1,XON$
6400 WEND
6410 CLOSE #2
6420 '************************************************** NORMALIZATION ROUTIN
6425 OPEN FILENAME$ FOR INPUT AS 2
7000 OPEN TARGET$ FOR OUTPUT AS 3
7060 POINTNUM = SRT
7070 FOR I = 1 TO TOT
7080 INPUT #2,D$
7090 D = VAL(D$)
7094 IF NUMERICS$ = "Reset" THEN GOTO 7115
7100 TIME =  ( POINTNUM -  HZERT) * HNORM
7110 VOLTAGE = (D - VZERO) * VNORM
7114 GOTO 7120
7115 TIME = ( POINTNUM - RHZERO) * HNORM
7116 VOLTAGE = ( D - RVZERO ) * VNORM
7120 PRINT #3, USING "##.####^^^^";TIME;
7130 PRINT #3, "   ";
7140 PRINT #3, USING "##.####^^^^";VOLTAGE
7150 POINTNUM = POINTNUM + STP
7160 NEXT I
7170 CLOSE #3
7180 CLOSE #2:LOCATE 24,1:PRINT "                                                                    ";
7190 KILL FILENAME$
7200 CLOSE #1
7210 LOCATE 19,18:COLOR 15,0:PRINT "Complete !    ":COLOR 7,0
7220 LOCATE 24,1:LINE INPUT; "More ? ",DUM$
7230 IF DUM$ = "YES" OR DUM$ = "yes" OR DUM$ = "Y" OR DUM$ = "y" THEN LOCATE 19,18
     :COLOR 15,0:PRINT "Previous       ":COLOR 7,0:GOTO 5370
7240 RETURN
```

Program 2. Program 2 consolidates and scales raw TGA data files. The two data files, mass and temperature, transferred using Program 1 are converted into a single file containing mass and temperature data. The program computes α, τ, and $1/T$.

```
      PROGRAM TGA
* *** ************************************************************************
*     This program converts and consolidates raw TGA data, acquired on a     *
*     digital oscilloscope, and produces a file containing mass, fraction    *
*     remaining, or fraction decomposed, as a function of time, or           *
*     temperature.                                          Version 31 Jan 86  *
* *** ************************************************************************

      INTEGER      FLAG, FLAG1
      REAL         MTIME,MASS,MASS0,LMASS,OMALFA
      CHARACTER*14 FNOUT,FNMASS,FNTDEGC
      CHARACTER*14 DUMMY

      CALL CLEAR

      FLAG         = 0
      FLAG1        = 0

      WRITE(*,'(A,//)') ' * TGA:  Nicolet Mass-Temperature Data Conversi
     1on and Consolidation - 31Jan86 *'
      WRITE(*,'(A\)') ' Enter Mass Data File Name: '
      READ(*,'(A)') FNMASS
      WRITE(*,'(A\)') ' Enter Mass Scale Factor: '
      READ(*,*) SFMASS
      WRITE(*,'(A\)') ' Enter Temperature Data File Name: '
      READ(*,'(A)') FNTDEGC
      WRITE(*,'(A\)') ' Enter Temperature Scale Factor: '
      READ(*,*) SFTEMP
      WRITE(*,'(A\)') ' Enter Output  File Name: '
      READ(*,'(A)') FNOUT


      OPEN(3,FILE=FNOUT, STATUS = 'NEW' )
   50 OPEN(1,FILE=FNMASS,STATUS = 'OLD')
      OPEN(2,FILE=FNTDEGC,STATUS = 'OLD')


  100 READ(1,*,END=200) MTIME,MASS
      READ(2,*) TTIME,TDEGC

      MASS         = MASS * SFMASS
      TDEGC        = TDEGC * 1.E+3

      IF(TTIME .NE. MTIME) THEN
```

```
      WRITE(*,'(A)') ' WARNING *** TIME MISSMATCH  '
      ENDIF

      IF (FLAG  .EQ. 0) THEN
      MASS0       = MASS
      FLAG        = 1
      ENDIF

      IF(FLAG1 .EQ. 1) THEN
      ALFA        = (MASS0 - MASS) / (TOTAL)
      OMALFA      = 1. - ALFA
      TDEGK       = TDEGC + 273.15
      WRITE(3,105) TTIME,TDEGK,MASS,ALFA,OMALFA
  105 FORMAT(1X,F7.2,3X,F7.2,3X,F9.4,3X,F12.7,3X,F12.7)
      ENDIF

      GOTO 100

  200 IF(FLAG1 .EQ. 0) THEN
      LMASS       = MASS
      TOTAL       = MASS0 - LMASS
      FLAG1       = 1
      CLOSE(1)
      CLOSE(2)
      GOTO 50
      ENDIF

      CLOSE(1)
      CLOSE(2)
      CLOSE(3)

      STOP 'NORMAL Program Termination'

      END
```

Program 3. Program 3 consolidates and scales raw VTGA data files. The two data files, mass and temperature, transferred using Program 1 are converted into a single file containing mass and temperature data. The program computes α, τ, and $1/T$. Voltage readings from the temperature data file are converted to Temperature using a ninth-degree polynomial from Ref. [ ].

```
      PROGRAM VTGA
* *** ************************************************************************
*     This program converts VTGA millivolt readings to fraction decomposed,  *
*     α, and temperature.  The conversions are based on the assumptions that *
*     the VTGA mass calibration is linear and that thermocouple outputs      *
*     correspond to the type-E tables.  R. J. Powers  Version: 9Feb86        *
* *** ************************************************************************

      INTEGER      PTNO, I
      REAL         MTIME,TTIME,TIME,MVOLTS,MTVOLTS,MVOLT0,MVOLT1,ALFA
      REAL         DELTA
      CHARACTER*14 FNOUT,FNMASS,FNTEMP

      CALL CLEAR
      WRITE(*,'(A)') ' * VTGA Mass-Temperature Data Conversion and Conso
     1lidation-9Feb86*'

      WRITE(*,*)
      WRITE(*,*)

* *** Initialization ***
      WRITE(*,'(A\)') ' Enter Mass Data File Name <fname.ext> : '
      READ(*,'(A)') FNMASS
      WRITE(*,'(A\)') ' Enter Temperature Data File Name <fname.ext> : '
      READ(*,'(A)') FNTEMP
      WRITE(*,'(A\)') ' Enter Output  File Name <fname.ext> : '
      READ(*,'(A)') FNOUT
      WRITE(*,'(A\)') ' Enter Thermocouple Amplification Factor: '
      READ(*,*) AMPFACT

      OPEN(3,FILE=FNOUT, STATUS = 'NEW' )
      OPEN(1,FILE=FNMASS,STATUS = 'OLD')
      OPEN(2,FILE=FNTEMP,STATUS = 'OLD')

* *** Find Max-Min Values of the Mass Voltage Values ***
      READ(1,*) MTIME,MVOLTS
      MVOLT0      = MVOLTS
      MVOLT1      = MVOLTS
      I           = 1

   40 READ(1,*,END=50) MTIME, MVOLTS
```

```
      IF( MVOLTS .LT. MVOLT0 ) MVOLT0 = MVOLTS
      IF( MVOLTS .GT. MVOLT1 ) MVOLT1 = MVOLTS
      I           = I + 1
      GOTO 40

* *** Number of Data Points and Mass Voltage Change
  50  PTNO        = I
      DELTA       = MVOLT1 - MVOLT0
      CLOSE(1)
      OPEN(1,FILE=FNMASS,STATUS = 'OLD')

* *** Read Voltages and Convert to Alfa, Gamma, and Temperature
      DO 100     I = 1, PTNO
      READ(1,*) MTIME, MVOLTS
      READ(2,*) TTIME, TVOLTS

      IF(TTIME .NE. MTIME) THEN
      WRITE(*,'(A)') ' WARNING *** TIME MISSMATCH  '
      ELSE
      TIME        = TTIME
      ENDIF

*     Convert vVolt Readings to Alfa, Gamma, And Temperature
      ALFA        = ( MVOLTS -  MVOLT0 ) / DELTA
      GAMMA       = 1.0 - ALFA
      CALL TEMP(TVOLTS,AMPFACT,MTVOLTS,TDEGC)
      TDEGK     = TDEGC + 273.15
* *** Send Output to Data File ***
      WRITE(3,90) TIME,MTVOLTS,TDEGC,TDEGK,MVOLTS,ALFA,GAMMA
   90 FORMAT(1X,F9.2,2X,F9.4,2X,F7.2,2X,F7.2,2X,1PE12.4,2X,0PF10.6,
     1       2X,F10.6)
  100 CONTINUE

      CLOSE(1)
      CLOSE(2)
      CLOSE(3)

      STOP 'NORMAL Program Termination'
      END

      SUBROUTINE TEMP(TEMPVOLTS,AMPFACT,MVOLTS,TDEGC)
* *** ************************************************************************
*     This Subroutine converts VOLTS from a type-E thermocouple and returns   *
*     mVolts (MVOLTS) and temperatrue in Deg. C. (TDEGC); an amplification    *
*     factor (AMPFACT) must also be supplied.                                 *
*****************************************************************************
      REAL MVOLTS
      DIMENSION A(10)

* *** Polynomial Coefficients
      DATA A /0.104967248,17189.45282,-282639.0850,12695339.5,-448703084
```

```
1.6,1.10866D+10,-1.76807D+11,1.71842D+12,-9.19278D+12,2.06132D+13/

 MVOLTS       = (TEMPVOLTS/AMPFACT) * (1.0E+3)
 X            = TEMPVOLTS/AMPFACT

 TDEGC = (A(1) + X*(A(2) + X*(A(3) + X*(A(4) + X*(A(5) + X*(A(6) +
1X *(A(7) + X*(A(8) + X*(A(9) + A(10)*X)))))))))

 RETURN
 END
```

Program 4. This program operates on the output data file of Program 2 or 3 and converts these into "Coats & Redfern coordinates" from which Arrhenius parameters may be extracted using Program 5.

```
      PROGRAM CR
C *** ***************************************************************************
C     The following program reduces TGA data using the algorithm of Coats &  *
C     Redfern. [35,42] Required inputs are Temperature, T, and the fraction  *
C     decomposed, α. Outputs are: data point number, input data, the C&R     *
C     coordinates, and the zero order ordinate.  R. J. Powers Version 28JAN86*
C *** ***************************************************************************

      REAL*8       T,ALFA,ALFA1,ALFA2,COLUMN,X,Y,N,Z
      INTEGER      NN,ACOL,TCOL,NCOL
      CHARACTER*14 FNDATA,FNOUT
      DIMENSION    T(1000),ALFA(1000),COLUMN(12),X(1000),Y(1000),Z(1000)
      DATA         NN /0/

      CALL CLEAR

      WRITE(*,'(A,//)') ' *** Coats and Redfern Kinetic Analysis - 31Jan
     186 *** '
      WRITE(*,'(A\)') ' Enter Input Data File Name:  '
      READ(*,'(A)') FNDATA
      WRITE(*,'(A\)') ' Enter Reaction Order:  '
      READ(*,*) N
      WRITE(*,'(A\)') ' Enter - # columns, T column, alfa column: '
      READ(*,*) NCOL,TCOL,ACOL
      WRITE(*,'(A\)') ' Enter Initial α: '
      READ(*,*) ALFA1
      WRITE(*,'(A\)') ' Enter  Final  α: '
      READ(*,*) ALFA2
      WRITE(*,'(A\)') ' Enter Output File Name:  '
      READ(*,'(A)') FNOUT

      OPEN(3,FILE = FNDATA, STATUS = 'OLD')
      OPEN(4,FILE = FNOUT, STATUS = 'NEW')

      I            = 1
  608 READ(3,*,END = 700) (COLUMN(J), J = 1, NCOL)
      IF (COLUMN(ACOL) .LE. ALFA1 .OR. COLUMN(ACOL) .GE. ALFA2) GOTO 608
      NN           = NN + 1
      ALFA(I)      = COLUMN(ACOL)
      T(I)         = COLUMN(TCOL)
      I            = I + 1
      GOTO 608

  700 CONTINUE
```

```
      IF( N .EQ. 1.D0 ) THEN
      CALL ORDER1( T,ALFA,NN, X,Y,Z )
      ELSE
      CALL ORDERN( T,ALFA,NN,N,  X,Y,Z )
      ENDIF

      WRITE(*,77) NN,ALFA1,ALFA2
   77 FORMAT(1X,/,I4,' Data Points Read between α = ',F6.3,' and α = ',
     1F6.3,/)
      DO 35 I = 1,NN
      WRITE(4,37) I,T(I),ALFA(I),X(I),Y(I),Z(I)
   37 FORMAT(1X,I3,4X,F7.2,4X,F8.3,4X,1PD12.4,4X,1PD12.4,4X,1PD12.4)
   35 CONTINUE

      CLOSE(3)
      CLOSE(4)
      STOP ' NORMAL Program Termination'
      END

      SUBROUTINE ORDER1( T,ALFA,NN, X,Y,Z )
*  *** ************************************************************************
*           Variable List                                                      *
*               X         = First order C&R absissa                          *
*               Y         = First order C&R ordinate                         *
*               Z         = Zero order C&R ordinate                          *
*  *** ************************************************************************
      REAL*8       T,ALFA,X,Y,Z
      DIMENSION    T(1000),ALFA(1000),X(1000),Y(1000),Z(1000)

      DO 10    I = 1,NN
      Y(I)       = DLOG( ( -DLOG(1.D0 - ALFA(I))  ) / (T(I)** 2.D0)  )
      X(I)       = 1.D0 / T(I)
      Z(I)       = DLOG( ALFA(I) / ( T(I)**2.D0 ) )
   10 CONTINUE

      RETURN
      END


      SUBROUTINE ORDERN( T,ALFA,NN,N, X,Y,Z )
*  *** ************************************************************************
*           Variable List                                                      *
*               X         = Nth order C&R absissa                            *
*               Y         = Nth order C&R ordinate                           *
*               Z         = Zero order C&R ordinate                          *
*  *** ************************************************************************
      REAL*8       T,ALFA,X,Y,N,Z
      DIMENSION    T(1000),ALFA(1000),X(1000),Y(1000),Z(1000)
```

```
      DO 10      I = 1,NN
      Y(I)    = DLOG(   ( 1.D0 - ( (1.D0 - ALFA(I)) ** (1.D0 - N) )  )
     1               / (( 1.D0 - N ) * ( T(I) ** 2.D0 ))             )
      X(I)         = 1.D0 / T(I)
      Z(I)         = DLOG( ALFA(I) / ( T(I)**2.D0 ) )
   10 CONTINUE

      RETURN
      END
```

Program 5. This program calculates Arrhenius parameters from the output of Program 4.

```
      PROGRAM CREA
* *** ****************************************************************
*     This program calculates global Arrhenius parameters from C&R    *
*     data by fitting a least squares line to the values.             *
*     Input data are the recriprocal of the temperature and the C&R   *
*     ordinate. Outputs are the global activation energy, pre-        *
*     exponential, and the corrolation coefficient for the fit.       *
*                                                                     *
*     Author: R. J. Powers                        Version:  1 Feb 86 *
* *** ****************************************************************

      REAL*8       COLUMN,X,Y,RATE,E,A,M,B,R,TRUNC,ALPHA1,ALPHA2,A1,A2
      REAL*8       XTEN,XSTART,XEND,YSTART,YEND,LEN,T1,T2
      INTEGER      ACOL,XCOL,YCOL,NCOL,NUM
      CHARACTER*1  REPLY
      CHARACTER*14 FNDATA,FNOUT
      DIMENSION    COLUMN(12),X(500),Y(500)
      CALL CLEAR

      WRITE(*,'(A,//)') ' *** Coats and Redfern: Arrhenius Parameters -
     11Feb86 ***'

      WRITE(*,'(A\)') ' Enter Input Data File Name:  '
      READ(*,'(A)') FNDATA
      WRITE(*,'(A\)') ' Enter Heating Rate (°K/sec):  '
      READ(*,*) RATE
      WRITE(*,'(A\)') ' Enter - # columns, α col, 1/T col(1/°K), C&R ord
     1 col: '
      READ(*,*) NCOL,ACOL,XCOL,YCOL
      WRITE(*,'(A\)') ' Enter Initial α : '
      READ(*,*) ALPHA1
      WRITE(*,'(A\)') ' Enter Final α :  '
      READ(*,*) ALPHA2

      OPEN(3,FILE = FNDATA, STATUS = 'OLD')

      I            = 0
  700 READ(3,*,END=701) (COLUMN(J), J = 1, NCOL)
      IF ( COLUMN(ACOL) .LT. ALPHA1 .OR. COLUMN(ACOL) .GT. ALPHA2 )
     1   GOTO 700

      I            = I + 1
      IF(I .EQ. 1) A1 = COLUMN(ACOL)
      IF(I .EQ. 1) T1 = COLUMN(2)
      X(I)         = COLUMN(XCOL)
      Y(I)         = COLUMN(YCOL)
      A2           = COLUMN(ACOL)
```

```
      T2          = COLUMN(2)
      GOTO 700

  701 NUM         = I
      WRITE(*,38) NUM,A1,A2
   38 FORMAT(1X,/,I3,' Data Points Read between α = ',F7.3,' and α = ',
     1       F7.3)
      WRITE(*,39) T1,T2
   39 FORMAT(1X,  3X,'                          T = ',F7.1,' and T = ',
     1       F7.1,/)
      CALL LINFIT(X,Y,NUM, M,B,R)

      E           = M * (-1.987D0)
      TRUNC       = ( 1.D0 - ( (2.D0 * 1.987 * (1.D0/X(NUM))) / E ) )
      A           = DEXP(B) * RATE * E  / ( 1.987D0 * TRUNC )

      WRITE(*,800) E
  800 FORMAT(1X,'E = ',2PD12.4)
      WRITE(*,810) A
  810 FORMAT(1X,'A = ',1PD12.4)
      WRITE(*,820) R
  820 FORMAT(1X,'R = ',1PD12.4)

      WRITE(*,'(/,A\)') ' Generate This Line (Y/N) ? '
      READ(*,'(A)') REPLY
      IF( REPLY .EQ. 'y' .OR. REPLY .EQ. 'Y' ) THEN
      WRITE(*,'(A\)') ' Enter Output File Name (fname.ext): '
      READ(*,'(A)') FNOUT
      OPEN(5,FILE=FNOUT,STATUS='NEW')

      XTEN        = 0.0D0
      WRITE(*,'(A\)') ' Enter Extension Factor (%): '
      READ(*,*) XTEN

      XTEN        = XTEN /1.0D2
      LEN         = DABS( X(NUM) - X(1))
      XSTART      = DMIN1( X(NUM), X(1) )
      XEND        = DMAX1( X(NUM), X(1) )
      XSTART      = XSTART - ( LEN * XTEN )
      XEND        = XEND   + ( LEN * XTEN )
      YSTART      = B + ( M * XSTART )
      YEND        = B + ( M * XEND   )
      WRITE(5,17) XSTART, YSTART
      WRITE(5,17) XEND,YEND
   17 FORMAT(1X,1PE11.4,5X,E11.4)
      CLOSE(5)
      ENDIF


      CLOSE(3)
      STOP ' NORMAL Termination'
```

```
      END


      SUBROUTINE LINFIT(X,Y,NN, M,B,R)
*  *** ********************************************************************
*     The following subroutine fits the best straight line to a given  *
*     set of "NN" data points. Input data is contained in arrays X and *
*     Y; the outputs are the slope, the Y-intercept, and the           *
*     corrolation coefficient - M,B,R respectively.                    *
*                                                                      *
*          Variable List                                               *
*                                                                      *
*              R         = Corrolation Coefficient                     *
*              B         = Intercept                                   *
*              M         = Slope                                       *
*              SUMX      = Sum of X                                    *
*              SUMY      = Sum of Y                                    *
*              SUMXY     = Sum of X*Y                                  *
*              SUMX2     = Sum of X**2                                 *
*              SUMY2     = Sum of Y**2                                 *
*                                                                      *
*  *** ********************************************************************

      REAL*8 X,Y,M,B,R,DUMY,SUMX,SUMY,SUMX2,SUMY2,SUMXY,A
      INTEGER NN
      DIMENSION X(500),Y(500)

      SUMX      = 0.0D0
      SUMY      = 0.0D0
      SUMXY     = 0.0D0
      SUMX2     = 0.0D0
      SUMY2     = 0.0D0

      DO 100 I  =1,NN
      SUMX      = SUMX + X(I)
      SUMY      = SUMY + Y(I)
      SUMX2     = SUMX2 + ( X(I) * X(I) )
      SUMY2     = SUMY2 + ( Y(I) * Y(I) )
      SUMXY     = SUMXY + ( X(I) * Y(I) )
  100 CONTINUE

      DUMY      = DBLE(NN)
      A         = SUMX2 * DUMY - (SUMX * SUMX)
      B         = (SUMX2 * SUMY - SUMX * SUMXY ) / A
      M         = (SUMXY * DUMY - SUMX*SUMY )/ A
      R         = (B * SUMY + M * SUMXY - SUMY * SUMY /DUMY)/
     1            (SUMY2 - (SUMY * SUMY/DUMY))

      RETURN
      END
```

REFERENCE LIST

1. Hermance, C. F., "A Model of Composite Propellant Combustion Including Surface Heterogeneity and Heat Generation," AIAA J., 4(9), 1966, pp. 1629 - 1637.

2. Glick, R.L., "On the Statistical Analysis of Composite Solid Propellant Combustion," AIAA J., 12(3), 1976, pp. 384-385.

3. Cohen, N. S., Price, C. F., and Strand, L. D., "Analytical Model of the Combustion of Multicomponent Solid Propellant Combustion Based on Multiple Flames," AIAA J., Paper 77-927, July, 1977.

4. Beckstead, M. W., Derr, R. L., and Price, C. F., "A Model of Composite Solid Propellant Combustion Based on Multiple Flames," AIAA J., 8(12), 1970, pp. 2200 - 2207.

5. Flanagan, J. E. and Oberg, C. L., "A Modified Two Stage Flame Model of Steady-State Composite Solid Propellant Combustion," Report 59-017, Rocketdyne Div., Rockewell International Corp., Canoga Park, Calif., Sept 1970.

6. Cohen, N. S., "Review of Composite Burn Rate Modeling," AIAA J., 18(3), 1980, pp. 277 - 293.

7. Lengelle, G., "Thermal Degradation Kinetics and Surface Pyrolysis of Vinyl Polymers," AIAA J., 8(11), 1970, pp. 1989 - 1996.

8. Wilfong, R. E., Penner, S. S., Daniels, F., "An Hypothesis for Propellant Burning," J. Phys. Chem., 54, 1950, pp. 863 - 872.

9. Houser, T. J., "Kinetics of Polymer Pyrolysis from Surface Regression Rates," J. Chem. Phys., Vol. 45, No. 3, 1966, pp. 1031 - 1037.

10. Baer, A. D., Hedges, J. H., Seader, J. D., Jayakar, K. M., Wojcik, L. H., "Polymer Pyrolysis over a Wide Range of Heating Rates," AIAA J., 15(10), 1977, pp. 1398 - 1404.

11. Sabadell, A. J., Wenograd, A. J., and Summerfield, M., "Measurement of Temperature Profiles through Solid Propellant Flames Using Fine Thermocouples," AIAA J., 3(9), 1965, pp. 1580 - 1584.

12. Fenimore, C. P. , and Martin, F. J., "Burning of Polymers", The Mechanisms of Pyrolysis, Oxidation, and Burning of Organic Materials, Nat. Bur. Standards Spec. Pub. 357, 1972, pp. 159 - 170.

13. Williams, F. A., Combustion Theory, Benjamin/Cummings Pub. Co, Menlo Park, 1985.

14. Bouck, L. S., Baer, A. D., and Ryan, N. W., "Pyrolysis and Oxidation of Polymers at High Heating Rates," Fourteenth Symposium (International) on Combustion, The Combustion Institute, Pittsburgh, Pa., 1973, pp. 1139 - 11499.

15. Farre-Ruis, F. and Guichon, G., "On the Conditions of Flash Pyrolysis of Polymers as used in Pyrolysis-Gas Chromatography," Anal. Chem., 40(6), 1968, pp. 998 -1000.

16. Wall, L. A., "Pyrolysis of Polymers," The Mechanisms of Pyrolysis, Oxidation, and Burning of Organic Materials, Nat. Bur. Standards Spec. Pub. 357, 1972, pp. 47 - 60.

17. Madorsky, S. L., Thermal Degradation of Organic Polymers, Interscience, New York, 1964, pp. 293 - 303.

18. Baer, A. D., "Pyrolysis of Polymer Films in Air at High Temperatures and at High Heating Rates," J. of Fire & Flammability, 12(7), 1981, pp. 214 - 228.

19. Kohn, S., "Experimental Techniques of Studying Pyrolysis of High Polymers Subjected to Rapid Heating," (Translation from: La Recherche Aeronautique, 88, 1962),NASA-TT F-11,283, 1967, pp. 1 - 22.

20. Hedges, J. H., Baer, A. D., and Ryan, N. W., "Pyrolysis and Ignition of Polymers under Approximated Fire Conditions," Seventeenth Symposium (International) on Combustion, The Combustion Institute, 1978, pp. 1173 - 1181.

21. Shannon, L. J., and Erickson, J. E., "Thermal Decomposition of Composite Solid Propellant Binders," Sixth ICRPG Combustion Conference, CPIA Publication No. 192, 1969, pp. 519 - 530.

22. McAlevy III, R. F., Lee, S. Y., and Smith, W. H., "Linear Pyrolysis of Polymethylmethacrylate," J. AIAA, Vol. 6, No. 6, 1968, pp. 1137 -1142.

23. Coates, R. L., "Linear Pyrolysis Rate Measurements of Propellant Constituents," J. AIAA, Vol. 3, No. 7, 1965, pp. 1257 - 1261.

24. Mc Alevy III, R. F., and Blazowski, W. S., "The Surface Pyrolysis Boundary Condition for the Combustion of Polymers," The Mechanisms of Pyrolysis, Oxidation, and Burning of Organic Materials, Nat. Bur. Standards Spec. Pubb. 357, 1972, pp. 185 - 192.

25. Cohen, N. S., Fleming, R. W., and Derr, R. L., "Role of Binders in Solid Propellant Combustion," AIAA J., Vol. 12, No. 2, 1974, pp. 212 - 218.

26. Schultz, R. D., and Dekker, A. O., " ," Fifth Symposium (International) on Combustion, Reinhold Pub. Corp., New York, 1955, pp. 260 - 267.

27. Barsh, M. K., Andersen, W. H., Bills, K. W., Moe, B., and Schultz, R. D., "Improved Instrument for the Measurement of Linear Pyrolysis Rates of Solids," Rev. of Sci. Instru., Vol. 29, No. 5, 1958, pp. 392 - 395.

28. Chaiken, R. F., Andersen, W. H., Barsh, M. K., Mishuck, E., Moe, G., and Schultz, R. D., "Kinetics of the Surface Degradation of Polymethylmethacrylate," J. of Chem. Phys., Vol. 32, No. 1, 1960, pp. 141 - 146.

29. Blazowski, W. S., Cole, R. B., and McAlevy III, R. F., "Linear Pyrolysis of Various Polymers Under Combustion Conditions," Fire and Explosion, ( ), pp. 1177 - 1186.

30. Hansel, J. G., and McAlevy III, R. F., "Energetics and Chemical Kinetics of Polystyrene Surface Degradation in Inert and Chemically Reactive Environments," AIAA J., Vol. 4, No. 5, 1966, pp. 841 - 848.

31. Gontkovskaya, V. T., Ozerkovskaya, N. I., Barzykin, V. V., and Pestrikov, S. V., "Special Characteristics of Nonisothermal Processes in Systems with Parallel Reactions with Linear Heating," Fizika Goreniya i Vzryva, Vol. 14, No. 6, 1978, pp. 92 -96, (Translated Plenum Pub. Co. 00010-5082/78/1406-0776)

32. Gontkovskaya, V. T., Ozerkovskaya, N. I., Barzykin, V. V., and Pestrikov, S. V., "Progress of Sequential Reactions Under linear Heating Conditions," Fizika Goreniya i Vzryva, Vol. 16, No. 1, 1980, pp. 63 -68. (Translated Plenum Pub. Co. 0010-5082/80/1601-0058)

33. Gontkovskaya, V. T., Kolpakov, V. A., "Nonisothermal Processes in a System with Serial and Parallel Reactions Under Conditions of Linear Heating," Fizika Gorenia i Vzryva, Vol. 8, No. 3, 1982, pp. 63 - 68. (Translated

Pleenum Pub. Co. 0010-5082/82/1803-0315)

34. Rogers, R. N., "Differential Scanning Calorimetric Determination of Kinetic Constants of Systems that Melt with Decomposition," Thermochemica Acta, 3, 1972, pp. 437 - 447.

35. Coats, A. W. and Redfern, J. P., "Kinetic Parameters from Thermogravimetric Data," Nature, 201(1), 1964, pp. 68 - 69.

36. Tang, T. B., "Kinetic Functions Can Not be Determined from Analysis of Dynamic Data," Thermochimica Acta, 58, 1982, pp. 373 - 377.

37. Flyn, J. H., and Wall, L. A., "General Treatment of the Thermogravimetry of Polymers," J. Research Nat. Bur. Standards - A Physics and Chemistry, 70a(6), 1966, pp. 487 - 523.

38. Rainville, E. D., Special Functions, Macmillan, New York, 1960.

39. Reich, L. and Stivala, S. S., "Kinetic Parameters from Thermogravimetric Curves," Thermochimica Acta, 24, 1978, pp. 9 - 16.

40. Reich, L. and Stivala, S. S., "Computer Determined Kinetic Parameters from TG Curves," Thermochimica Acta, 36, 1980, pp. 103 - 105.

41. House Jr., J. E., "A General Iterative Method for Obtaining Kinetic Parameters from TG Data," Thermochemica Acta, 57, 1982, pp. 47 - 55.

42. Earnst, C. M., "Modern Thermogravimetry," Analytical Chemistry, 56(13), 1984, pp. 4471A - 1486A.

43. Gast, Th. and Jakobs, H., "A Measuring Method for the Simultaneous Observation of Mass and Heat Capacity with the Aid of Vibrations," Proceedings of the Second European Symposium on Thermal Analysis, ed D. Dollimore, Hayyden, London, 1981.

44. Gast, Th. and Jakobs, H., "Gedanken zur Gleichzeitigen Beobachtung von Masse - und Enthalpieanderungen mit Hilfe von Schwingungen," Acta Imeko, 1973, pp. 303 -310.

45. Oertli, Ch., Buhler, Ch., and Simon, W., "Curie Point Pyrolysis Gas Chromatography Using Ferromagnetic Tubes as Sample Supports," Chromatographia, 6(12), 1973, pp. 499 -

502.

46. Lehrle, R. S., "Micropyrolysis Gas-Liquid Chromatography," Laboratory Practice, 17(6), 1967, pp. 696 - 717.

47. Barlow, A., and Lehrle, R. S., Robb, J. C., and Sunderland, D., "PMMA Degradation, Kinetics and Mechanisms in the Temperature Range 340 C to 460 C," Polymer, 8, 1967, pp. 537 - 545.

48. American Society for Testing and Materials, Manual on the Use of Thermocouples in Temperature Measurement, STP 470B, ASTM, Baltimore, 1982.

49. Omega, Temperature Measurement Handbook and Encyclopedia, Omega Engineering Inc., Stamford, CT, 1985, p. T-12.

50. Ninan, K. N. and Krishnan, "Thermal Decomposition Kinetics of Polybutadiene Binders," J. Spacecraft, 19, No. 1, 1982, pp. 92 -94.

51. Price, E. W., "Comment on 'Thermal Decomposition of Polybutadiene Binders'," J. Spacecraft, Vol. 20., No. 3, 1983, p. 320.

52. Strahle, W. C. and Varney, M. M., "Thermal Decomposition Studies of Some Solid Propellant Binders," Combustion & Flame, 16, 1971, pp. 1 - 8.

53. Coats, A. W., and Redfern, A. W., "Thermogravimetric Analysis," Analyst, Vol. 88, 1963, pp. 906 - 924.

54. Waesche, R. H. W., "Research Investigation of the Decomposition of Composite Solid Propellants," United Aircraft Corp. Rept. G910476-24, 1968.

55. Solymosi, F., Structure and Stability of Salts of Halogen Oxyacids in the Solid Phase, John Wiley & Sons, New York, 1977.

56. Buhler Ch. and Simon W., "Curie Point Pyrolysis Gas Chromatography," J. Chromatographic Sci., 8(6), 1970, pp. 323 - 329.

57. Davies, J. and Simpson, P., Induction Heating Handbook, Mc Graw-Hill, Maidenhead, 1979.

58. Simon, W. and Gaiacobbo, H.,, "Thermal Fragmentation and Determination of the Structure of Organic Compounds," Angew. Chem. internat. edit., 4(11), 1965, pp. 938 - 943.

59. Coats, A. W., and Redfern, J. P., "Kinetic Parameters from Thermogravimetric Data II," Polymer Letters, Vol. 3., 1965, pp. 917 - 920.

VITA

Robert J. Powers was born in Brooklyn, New York on the 25th of July, 1947. His secondary schooling was at La Salle Academy in Manhattan, after which he went on to earn a Bachelor of Science degree in Chemistry from the University of Dayton. Upon graduation in 1970, he joined the United States Air Force with whom he served for nine and one-half years. During that time he was attached to the United States Air Force Armament Laboratory, at Eglin AFB, Florida, where he held the positions of R&D Propellant Chemist, and subsequently Acting Chief of the Interior Ballistics Laboratory. He joined the Georgia Institute of Technology in the Fall of 1980 and earned a Master of Science in Aerospace Engineering in the Spring of 1982. He has recently accepted a position as a Principal Scientist with Atlantic Research Corporation of Alexandria, Virginia, where he hopes to pursue a career in rocketry and solid propellant technology. Mr. Powers is currently a chemist in the United States Air Force Reserves where he holds the rank of Major. He is married to Virginia McSherry of Tulsa, Oklahoma, and is the proud father of Erin, and Ryan.